METHANATION

Although a variety of routes and several raw materials are being investigated, it appears that any system for gasification of coal will require additional units for conversion of excess carbon monoxide and hydrogen to achieve heating value equivalent to natural gas.

The magnitude of methanation will vary considerably, depending on the choice of the process in the primary gasification phases. The degree of methanation can vary from a major operation involving conversion of the feed gas containing a minor amount of methane to simple gas composition clean-up.

The future selection of the potential economical gasification process may largely depend on the amount of methanation required to achieve pipeline gas quality. Thus, various catalytic methanation processes must be examined and compared under their optimum design conditions viewing their economic and technical effects on primary gasification phases.

In order to demonstrate the technique involved in the design, simulation, and optimization of the methanation process, three different feeds as listed in Table VII-1 will be considered as approximate gas mixtures.

Although CO concentration as high as 25 per cent can be considered, lacking actual experimental reaction rate data at such a high CO

concentration level, it is not possible to make any reasonable assessment of the process for this case. Besides, in any of the primary gasification phases, it is more than likely that some methane will be produced. The gas compositions listed in Table VII-1 may result from the primary gasification phases, after the adjustment of the composition is made by the water-gas shift reaction and the gas purification.

Since the methanation reaction is a highly exothermic reaction, the heat removal from the reacting gas becomes the major problem in economic optimization. Several types of methanation reactors, such as fixed beds and fluidized beds, have been tested on pilot plant scale.

The fluidized bed operation is found to be difficult because of technical problems involved. The particle elutriation caused by the breaking of catalyst pellets may become severe. Lack of ruggedness of the catalyst and the unavailability of small particle sizes prevent good fluidization of catalysts. Therefore, three types of fixed bed downflow catalytic reactors are considered. They are:

1. The internal heat removal system, or simply, the heat extraction system.
2. The cold shot cooling system, or the cold quench system.
3. The recycle system.

The distinguishing features among the three systems are the manners by which heat is removed and the temperature is controlled in the reactors.

The goal of this study is to economically evaluate their relative technical merits for prospective application in coal gasification

TABLE VII-1 FLOW RATE AND CONCENTRATION
OF FEED AND PRODUCT

	Feed Gas		Product Gas	
	lb. mole/hr.	mole %	lb. mole/hr.	mole %(dry base)
		Low CO Case		
CO	1540	4.5	50	0.2
H_2O	30	0.1	1520	0.0
H_2	5970	17.5	1500	5.1
CO_2	70	0.2	70	0.2
CH_4	25700	75.6	27200	92.1
C_6H_6	0	0.0	0	0.0
N_2	720	2.2	720	2.4
H_2S	-*	0.0	-*	0.0
Total	34030	100.0	31060	100.0
		Intermediate CO Case (Case I)**		
CO	3180	8.0	30	0.1
H_2O	40	0.1	3190	0.0
H_2	11020	27.5	1580	5.2
CO_2	400	1.0	400	1.3
CH_4	24670	61.6	27820	91.0
C_6H_6	0	0.0	0	0.0
N_2	720	1.8	720	2.4
H_2S	-*	0.0	-*	0.0
Total	40030	100.0	33740	100.0
		High CO Case(CaseII)**		
CO	6450	13.4	40	0.1
H_2O	50	0.1	6470	0.0
H_2	20580	42.9	1340	4.7
CO_2	480	1.0	480	1.7
CH_4	19720	41.1	26140	91.0
C_6H_6	0	0.0	0	0.0
N_2	720	1.5	720	2.5
H_2S	-*	0.0	-*	0.0
Total	48000	100.0	35190	100.0
		Super High CO Case (Case III)**		
CO	12420	18.5	40	0.1
H_2O	70	0.1	12450	0.0
H_2	38650	57.5	1520	5.1
CO_2	670	1.0	670	2.2
CH_4	14590	21.7	26970	90.0
C_6H_6	0	0.0	0	0.0
N_2	780	1.2	780	2.6
H_2S	-*	0.0	-*	0.0
Total	67180	100.0	42430	100.0

* Concentration of H_2S is within the tolerance of catalyst.
** The name in parenthesis has been used in other chapters.

processes. To achieve this, it will require all three reactor systems be analyzed from both the technical and economic points of view. Each component information must be integrated by programming it into the computer for simulation. Finally, optimum conditions must be searched by an appropriate technique to arrive at the best economic process and design.

The following specifications and bases are chosen in this study.

1. Production rate is 250 x 10^9 B.t.u./day of pipeline gas.

2. The product gas should have a heating value of more than 950 B.t.u./S.C.F. or the product gas should contain more than 92.1% methane on a dry base. In addition, the concentration of CO must be less than 0.2%.

3. Three different feeds, i.e., low CO case, intermediate CO case, and high CO case, are considered. The temperature of the feed gas is fixed at 100°F for comparison. However, the effect of feed gas temperature will be discussed. The pressure of the feed gas is varied up to 1065 psia.

4. The compositions of feed gases and corresponding product gases are listed in Table VII-1.

Since it is also presently impossible to estimate the costs of the various feed gases which depend largely on the primary gasification phases, only the equipment costs are considered. However, in the optimization study of heat exchangers, in addition to equipment cost, cooling water cost and steam benefit are also considered.

After optimization of the subsystems which involves the primary gasification phases, purification phases and other necessary phases including methanation phases has been completed, the overall plant optimization will be performed. Costs not included in the methanation study will then be taken into consideration in the overall plant optimization study. However, the optimization based on the equipment costs alone at this stage should be sufficient to provide necessary information for the selection of the best system among those considered for methanation.

1. Reaction Kinetics

1.1 Reaction Rate Expressions for Methanation Reaction

The reactions possibly taking place in the methanation process are:

i Methanation Reactions:

$$CO + 3H_2 = CH_4 + H_2O \quad \text{(VII-1)}$$

$$CO_2 + 4H_2 = CH_4 + H_2O \quad \text{(VII-2)}$$

$$2CO + 2H_2 = CH_4 + CO_2 \quad \text{(VII-3)}$$

ii Water-Gas Shift Reaction:

$$CO + H_2O = CO_2 + H_2 \quad \text{(VII-4)}$$

iii Carbon Deposition Reactions:

$$2CO = C + CO_2 \quad \text{(VII-5)}$$

$$CO + H_2 = C + H_2O \quad \text{(VII-6)}$$

$$CH_4 = C + 2H_2 \quad \text{(VII-7)}$$

Although reactions (VII-1) through (VII-4) must take place to a larger or smaller extent regardless of the feed compositions employed, for a high hydrogen concentration feed, only a small amount of CO_2 has been detected experimentally [1]. Therefore, reactions (VII-2) through (VII-4) may be regarded as secondary reactions.

Because carbon deposition reduces the catalyst activity drastically, it is imperative that a range of temperature, pressure and feed compositions within which no carbon deposition takes place must be found. These conditions will become the constraints in the optimization of the processes.

A number of catalysts have been investigated for methanation reactions. The Harshaw catalyst has been found to be more active than nickel-on-alumina and ruthernium catalysts [15]. The formation of a

longer chained hydrocarbon on the Harshaw catalyst has been found to be much less than that from tests with iron and ruthenium catalysts. Also the activity of the Harshaw catalyst has been found to be quite steady and to be quite insensitive against poinsoning. In this study, Harshaw Ni-0104 T having an average diameter of 1/4 inch, is used. This catalyst contains 59% Ni and has a density of 71 lb./ft.^{3}. It has been shown that the catalyst behaves satisfactorily in the temperature range from 550°F to 850°F and the pressure range from 14.7 to 3000 psia without any carbon deposition [15].

A quantitative kinetic rate expression of the methanation reaction on the Harshaw catalyst is very difficult to obtain now because accurate kinetic data are not available. Therefore, it is necessary to simplify the reaction mechanism to consider only reaction (VII-1). The experimental data obtained from I.G.T. [15] using Harshaw catalysts are correlated and are plotted in Figure VII-1. The experimental data were obtained in a flow reactor simulating a complete-mixing flow in a rotating basket packed with catalyst [15]. It is seen from the figure that the rate is affected by the temperature up to approximately 600°F. From 600°F to 850°F, little temperature effect is seen. In this region, it can be probably regarded that the diffusion of gases through the porous catalyst is the rate controlling factor.

The empirical rate equations obtained are:

i. For temperaturesbetween 550°F and 600°F:

$$r_{CH_4} = 120 \exp\left[-\frac{15,660}{R(T+460)}\right] P_{CO}^{0.7} P_{H_2}^{0.3} \qquad \text{(VII-8)}$$

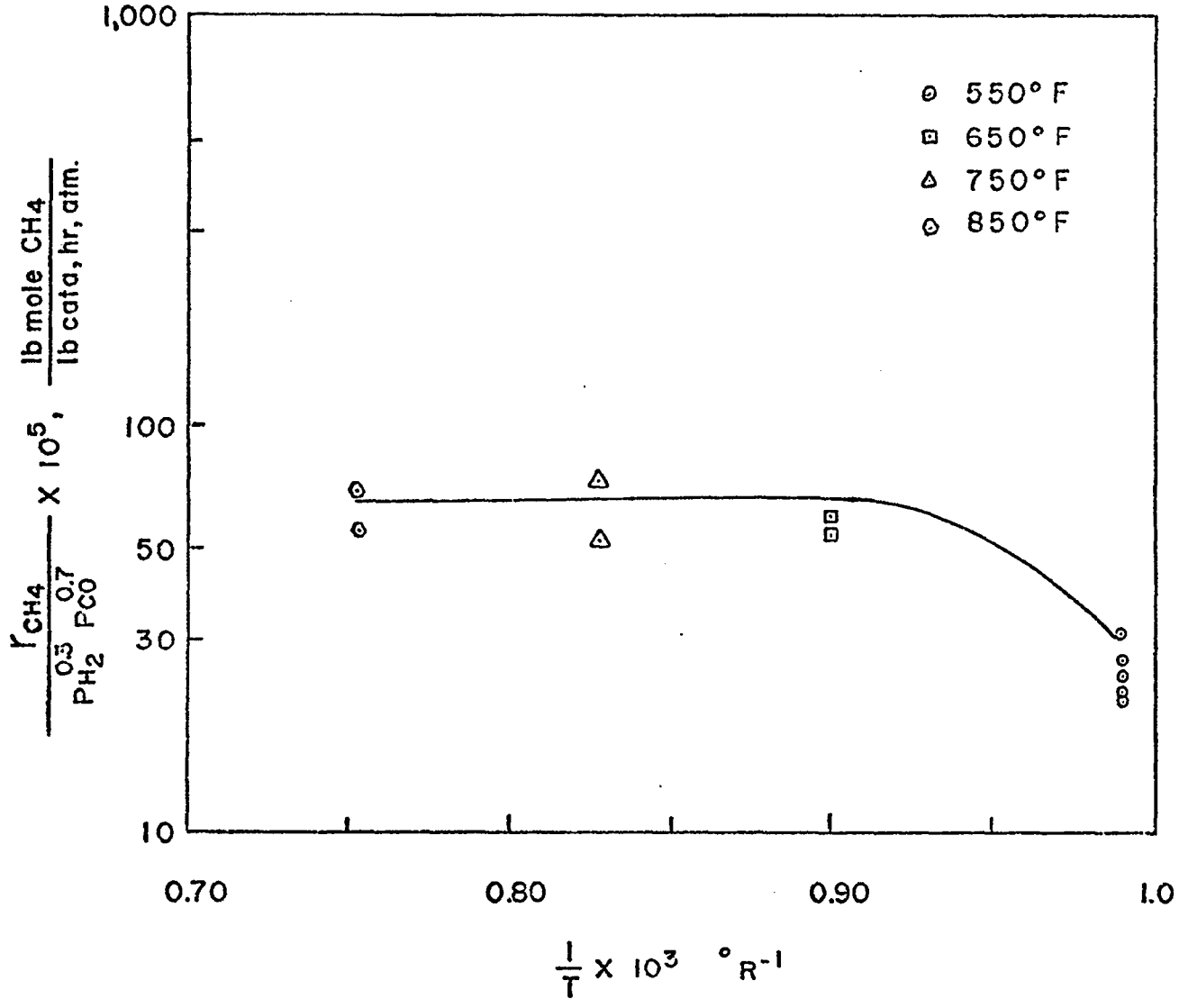

FIGURE VII-1 Analysis Of Kinetic Data In Harshaw Ni-0104T - 1/4" Catalyst.

ii. For temperatures between 600°F and 850°F:

$$r_{CH_4} = 0.0696\ P_{CO}^{0.7}\ P_{H_2}^{0.3} \qquad \text{(VII-9)}$$

where

r_{CH_4} is the rate of methane formation in lb.-moles/(lb.catalyst)(hr.).
T is the temperature in °F.
P_{H_2}, P_{CO} are partial pressures of H_2 and CO in atm., respectively.
R is the gas constant.

The rate equations, Eqs. (VII-8 and (VII-9), may not be precise due to lack of available experimental data and the simplified mechanism assumed. However, it is believed that these equations are adequate for the present optimization purpose in getting a reasonably accurate assessment of the various processes.

It will be demonstrated in a subsequent study that the overall optimum cost of the reactor is not very strongly affected by the kinetic expressions.

The above rate equations have been programmed into the computer subroutine which can be replaced whenever any future refinement of the rate equation based on additional and accurate data becomes available. In the present system of computation, calculation procedure has been developed so that more precise results may be obtained without major changes in the computer program.

1.2 Approach to Equilibrium

Although the above kinetic expressions were obtained from the experimental rate data of the methane forming reactions on the Harshaw catalyst including the runs under equilibrium hindrance, the equations do not provide the reverse reaction term. It would then be necessary

to assure that the rate equations are not applied to conditions too close to the equilibrium.

The equilibrium constant for the methanation reaction expressed as

$$K_{x_1}^* = \frac{(x_{CH_4}^*)(x_{H_2O}^*)}{(x_{CO}^*)(x_{H_2}^*)^3} \qquad \text{(VII-10)}$$

and given by the Bureau of Standards [14], is plotted in Figure VII-2 with the operating pressure as the parameter. Here $x_{CH_4}^*$, $x_{H_2O}^*$, x_{CO}^* and $x_{H_2}^*$ are the equilibrium mole fraction of methane, water, carbon monoxide, and hydrogen, respectively. As shown in the figure the equilibrium constant, $K_{x_1}^*$, is affected by the pressure and very strongly by the temperature. The equilibrium constant for the water gas shift reaction expressed as

$$K_{x_2}^* = \frac{(x_{CO_2}^*)(x_{H_2}^*)}{(x_{CO}^*)(x_{H_2O}^*)} \qquad \text{(VII-11)}$$

is also given by the Bureau of Standards [14] and is plotted in Figure VII-2. $K_{x_2}^*$ is only slightly affected by the temperature and not affected at all by the pressure. The extent of approach to the equilibrium for the methane reaction can be evaluated by computing the mass action law ratio of the product gases, K_{x_1}, defined as

$$K_{x_1} = \frac{(x_{CH_4})(x_{H_2O})}{(x_{CO})(x_{H_2})^3} \qquad \text{(VII-12)}$$

and are tabulated in Table VII-2based on the product gas compositions for the three different feeds considered. It is decided arbitrarily to maintain $K_{x_1} \leq K_{x_1}^*/10$ at all timesto assure the negligible

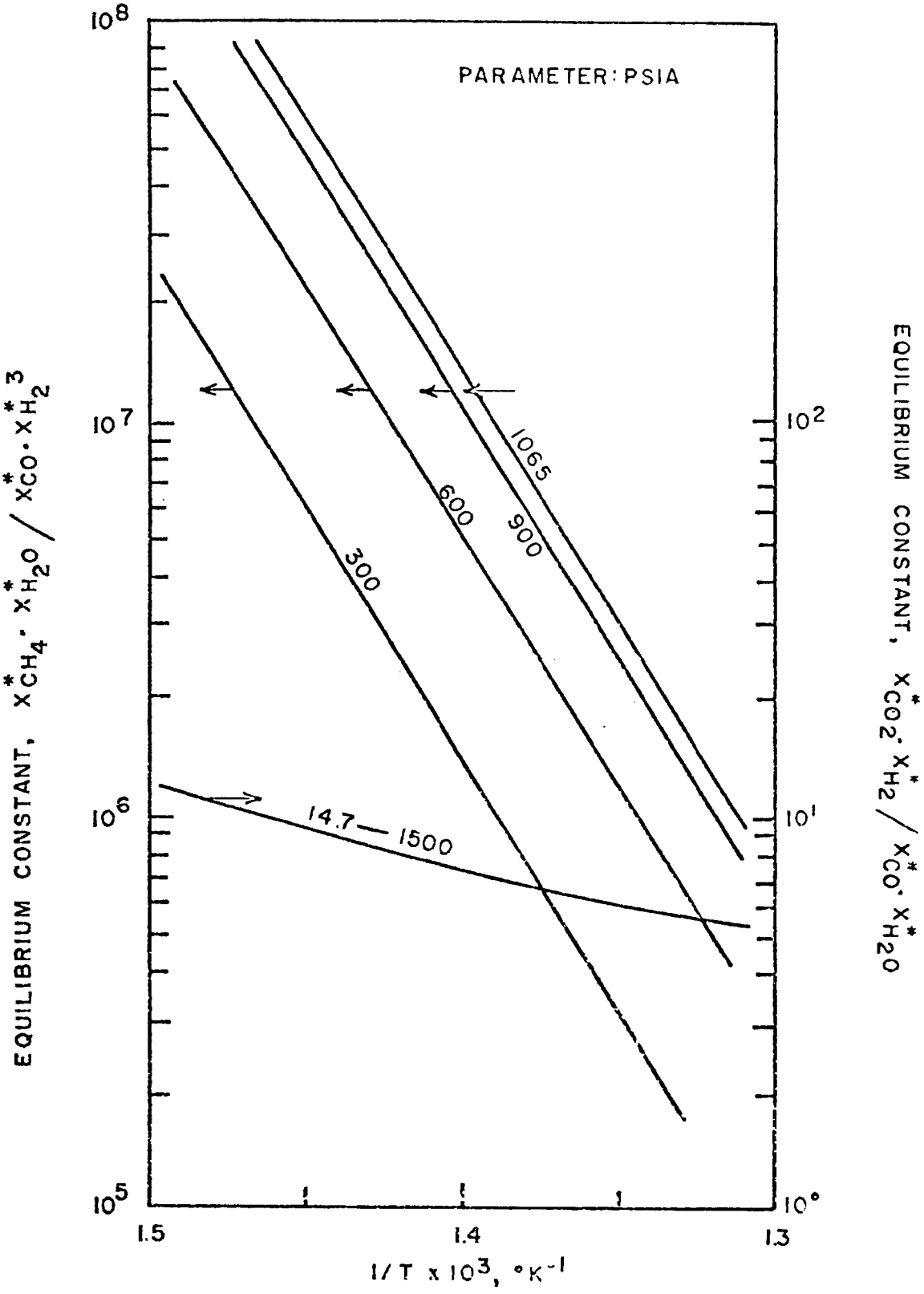

FIGURE VII-2 - Effect Of Temperature On Equilibrium Constants For Reactions $CO+3H_2 \rightarrow CH_4+H_2O$ And $CO+H_2O \rightarrow CO_2+H_2$

reverse reaction. This corresponds to the exit gas temperatures of 850°F, 850°F and 810°F for the low CO case, the intermediate CO case and the high CO case, respectively, when the operating pressure is approximately 1020 psia. Whenever the above criterion is exceeded in the reactor, the temperature of the reactor is lowered to the point where the above condition is again satisfied. Such provision is necessary for the high CO case particularly near the exit of the reactor.

TABLE VII-2 MASS ACTION LAW'S RATIO BASED ON PRODUCT GAS COMPOSITIONS FOR DIFFERENT FEEDS

$$K_{x_1} = \frac{x_{CH_4} \cdot x_{H_2O}}{x_{CO} \cdot x_{H_2}^3} \qquad K_{x_2} = \frac{x_{CO_2} \cdot x_{H_2}}{x_{CO} \cdot x_{H_2O}}$$

	K_{x_1}	K_{x_2}
Low CO Case	2.54×10^5	1.435
Intermediate CO Case	7.94×10^5	1.40
High CO Case	2.40×10^6	0.865

I.3 Mass and Heat Transfer Within Catalyst Bed

Since the methanation reaction is highly exothermic and quite rapid, it will be necessary to examine the possible temperature and concentration differencesbetween the bulk phase of reacting gas and the surface of the catalyst. If the reaction rate per catalyst particle, r_s, is known, the temperature difference between the bulk phase and the catalyst surface can be approximated by

$$T_s - T_b = \frac{r_s \Delta H}{h_p \pi d_p^2} \qquad \text{(VII-13)}$$

where h_p is the heat transfer coefficient between the particle surface and the bulk gas in the packed bed reactor. When particle-fluid radiation may be neglected, h_p can be calculated by [17]

$$J_H = \frac{h_p}{C_p G} N_{Pr}^{2/3} = 1.95 \left(\frac{d_p G}{\mu}\right)^{-0.51} \qquad \text{(VII-14)}$$

A maximum temperature difference $(T_s - T_b)_{max}$ can be calculated when the maximum reaction rate is used.

Figure VII-3 indicates the approximate maximum temperature difference as a function of gas mass velocity in the reactor for the three different feeds employed. As is evident when the gas velocity, G, is below 3×10^3 lb./hr.ft.^{2}, the maximum temperature difference, $(T_s - T_b)_{max}$, for the high CO case can become as high as 100°F. When the temperature difference is too great, many undesirable phenomena such as catalyst sintering, side reactions, carbon deposition, etc. may take place. Therefore, a minimum mass flow rate corresponding to an allowable temperature difference exists for a given reaction rate. This becomes one of the constraints in the reactor optimization. It is conceivable that when the feed

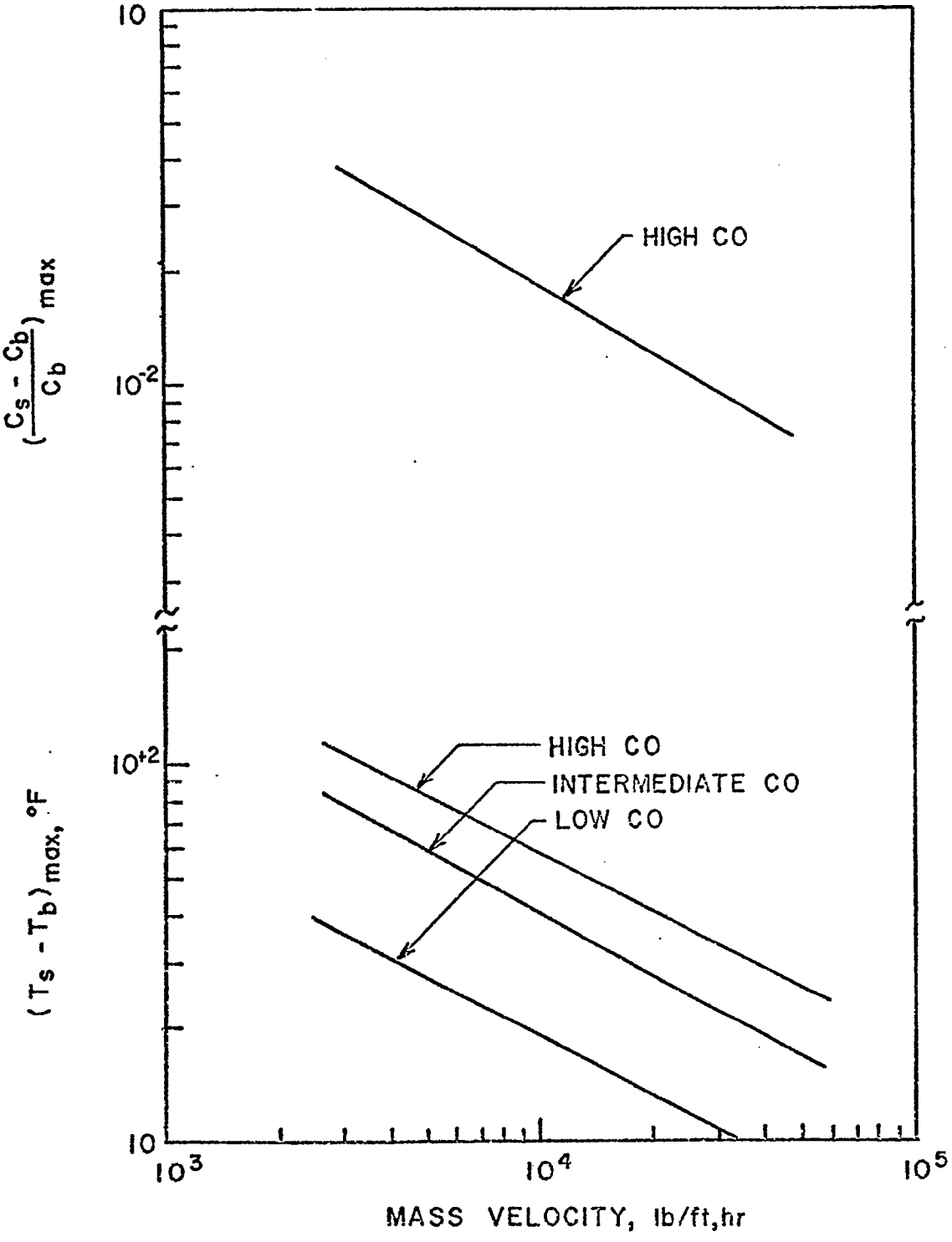

FIGURE VII-3 Mass Velocity Versus The Maximum Temperature Difference Between The Catalyst Surface and Bulk Fluid As Well As Mass Velocity Versus The Reduced Concentration Difference Of Methane When The Rate Is Maximum.

gas contains large amounts of CO and H_2, the minimum mass flow rate of gas may become so large that recycling of a portion of the product gas may become necessary. The experimental measurement of temperature difference on the Harshaw catalyst carried out by a high speed stirred reactor [15] indicates a maximum temperature difference of approximately 11°F for the intermediate CO case requiring no recycle of gas in this system.

As the reaction is quite exothermic, it would also be necessary to check the temperature gradient in the catalyst particles. If the reaction takes place uniformly in the catalyst particle, the heat balance equation in the catalyst can be written as

$$\frac{d^2T}{dr^2} + \frac{2}{r}\frac{dT}{dr} = \frac{r_s}{ke}\Delta H \ , \qquad \text{(VII-15)}$$

where ke, the effective thermal conductivity of the catalyst particles, is expressed as

$$\frac{1}{ke} = \frac{1}{(1-\theta)k_s + \theta kg} \qquad \text{(VII-16)}$$

where

θ is the internal porosity of the catalyst.
k_s is the thermal conductivity of the catalyst materials.
kg is the thermal conductivity of reacting gases.

Using the proper boundary conditions, Equation (VII-15) can be solved for the temperature within the catalyst pellet as,

$$T = T_s + \frac{1}{6}\left(-\frac{r_s}{ke}\Delta H\right)\left[\left(\frac{d_p}{2}\right)^2 - r^2\right] \qquad \text{(VII-17)}$$

It is clear when the reaction rate, r_s, is the largest, the temperature difference in the catalyst particle is also the largest.

Numerical calculation shows the largest temperature difference in the catalysts particle to be about 30°F. In actuality, the reaction at the surface is much faster than at the center of the catalyst particle due to diffusion effect. The maximum temperature difference in the catalyst particles therefore is expected to be much smaller than 30°F.

The concentration difference between the bulk phase and at the surface of catalyst pellets can be estimated by

$$C_s - C_b = \frac{r_s}{k_f \pi d_p^2} \qquad \text{(VII-18)}$$

where k_f is the fluid-particle mass transfer coefficient in a packed bed and is computed by [8]

$$\frac{J_M}{(1-\epsilon)^{0.2}} = 1.40 \left[\frac{d_p G}{\mu(1-\epsilon)}\right]^{-0.41} \qquad \text{(VII-19)}$$

Figure VII-3 also shows the effect of the mass velocity on the methane concentration difference when the reaction rates are maximum. From the figure, it may be concluded that the surface concentrations of each component are almost the same as that of the bulk gas. This conclusion is substantiated by the experimental results obtained by I.G.T. [15].

2. Reactor Performance Equations

Flow behavior in a fixed bed usually can be represented either by the dispersion model or by the cells-in-series model.

The following material balance equations are obtained around the n-th cell based on the cells-in-series model:

$$F_1^n = F_1^{n-1} + \rho_c V_c^n r_{CH_4} \qquad \text{(VII-20)}$$

$$F_2^n = F_2^{n-1} - \rho_c V_c^n r_{CH_4} \qquad \text{(VII-21)}$$

$$F_3^n = F_3^{n-1} - 3\rho_c V_c^n r_{CH_4} \qquad \text{(VII-22)}$$

$$F_4^n = F_4^{n-1} \qquad \text{(VII-23)}$$

$$F_5^n = F_5^{n-1} + \rho_c V_c^n r_{CH_4} \qquad \text{(VII-24)}$$

$$F_6^n = F_6^{n-1} \qquad \text{(VII-25)}$$

where F_1^n, F_2^n, F_3^n, F_4^n, F_5^n and F_6^n are the molar flowrates of methane, carbon monoxide, hydrogen, carbon dioxide, steam and nitrogen at the exit of the n-th cell, respectively. V_c^n is the volume occupied by the catalyst per unit cell. It has been shown that in a fixed bed, the traverse distance of a particle may be used to approximate the height of each individual cell. The length of a unit cell is assumed to be one inch in the present calculation. Although the reactor diameter is in the order of feet, a larger cell height is chosen for more conservative evaulation of the reactor size. It can be readily shown that a cell height of less than one inch makes the flow model of the reactor to approach closely to that of plug flow.

Chapter VII. METHANATION

The heat balance equations around the n-th cell can be obtained similarly as

$$T^n \sum_{i=1}^{6} C_{P_i}^n F_i^n - T^{n-1} \sum_{i=1}^{6} C_{P_i}^{n-1} F_i^{n-1} = (\Delta H)\, \rho_c\, V_c^n\, r_{CH_4} - Q^n \quad \text{(VII-26)}$$

where Q^r is the amount of heat removed (B.t.u./hr.) from the n-th cell in the reactor. The heat of reaction, ΔH, is in B.t.u. per pound mole of CH_4 formed and is given as

$$\Delta H = 87787.8 + 11.87\, T^n - 0.00668\, (T^n)^2 \quad \text{(VII-27)}$$

$C_{P_i}^n$ is the heat capacity of component i at T^n. The superscripts represent the number of cells from the top of the reactor.

The pressure drop across the n-th cell can be computed based on Ergun's equation [6]:

$$\Delta P = \frac{150(1-\epsilon)\left(\frac{\mu}{d_p G}\right) + 1.75}{[\epsilon^3/(1-\epsilon)](d_p/C_L)(g\rho/G^2)} \quad \text{(VII-28)}$$

where

ΔP is the pressure drop per unit cell (lb./sq.ft.).
ρ, μ and G are density (lb./ft.^{3}), viscosity (lb./ft.hr.), and mass flow rate of the gas (lb./ft.^{2}hr.), respectively.
d_p is the diameter of the catalyst (ft.).
C_L is height of a unit cell (ft.).
ϵ is the void fraction having approximate value of $0.35 \sim 0.4$ for fixed beds.

3. Process Optimization of Heat Exchangers

Since a large amount of heat is released in the methanation reaction, heat removal from reactors and product gases become the major problem in the optimization study. Three different types of heat exchangers are required in the methanation process, namely the preheater, the product gas cooler and the intermediate cooler. In this section, a process optimization of these heat exchangers is discussed.

3.1 Preheater

The feed gas must be preheated to a temperature above the reaction initiation temperature. The feed gas preheating is accomplished by exchanging heat between the product gas and the feed gas.

The total annual cost for the preheater can be represented by the following equation [13]

$$C_T = A_o K_F C_{Ao} + A_o E_i H_y C_i + A_o E_o H_y C_o \qquad \text{(VII-29)}$$

where

C_T is the total annual variable cost for heat exchanger and its operation ($/years).
C_{Ao} is the installed cost of heat exchanger per unit of outside-tube heat transfer area ($/ft.^{2}).
C_i is the cost for supplying 1 ft.-lb. force to pump fluid flowing through inside of tubes ($/ft.-lb. force).
C_o is the cost for supplying 1 ft.-lb. force to pump fluid flowing through shell side of unit ($/ft.-lb. force).
A_o is the area of heat transfer (ft.^{2}).
K_F is the annual fixed charges (-).
H_y is the hours of operation per year (hr./year).
E_o is the power loss outside tubes per unit of outside tube area (ft.-lb. force/hr.ft.).
E_i is the power loss inside tubes per unit of outside tube area (ft.-lb.force/hr.ft.^{2}).

The area for heat transfer, A_o, is a function of h_i, h_o and Δt_m as given by the following equation

$$\frac{F_T \Delta t_m}{q} = \frac{1}{U_P A_o} = \frac{1}{A_o}\left(\frac{D_o}{D_i h_i} + \frac{1}{h_o} + R_{dw}\right) \qquad \text{(VII-30)}$$

where

U_P is the overall heat transfer coefficient (B.t.u./ft.^{2}hr.°F).
Δt_m is logarithmic-mean temperature difference (°F).
F_T is correction factor on Δt_m (–)
D_i, D_o are inside and outside tube diameter (ft.).
q is total heat flux in the exchanger (B.t.u./hr.).
h_i, h_o are inside and outside film heat transfer coefficient in the tube. (B.t.u./ft.^{2}hr.°F)
R_{dw} is resistance to heat flow due to scaling. (ft.^{2}hr.°F/B.t.u.)
E_i is a function of the tube side fluid mass velocity which can be expressed in terms of h_i.
E_o is a function of the shell side fluid mass velocity which can be expressed in terms of h_o.

Thus Eq. (VII-29) may be written in terms of h_i, h_o and A_o as,

$$G = A_o K_F C_{Ao} + A_c \alpha_i h_i^{3.5} H_y C_i + A_o \alpha_o h_o^{4.75} H_y C_o \qquad \text{(VII-31)}$$

where α_i and α_o are the proportionality constants which depend on designing condition and fluid properties.

Applying the "Lagrange multiplier method," Eq. (VII-31) becomes

$$G = A_o K_F C_{Ao} + A_o \alpha_i h_i^{3.5} H_y C_i + A_o \alpha_o h_o^{4.75} H_y C_o + \lambda'\left[\frac{F_T \Delta t_m}{q} - \frac{1}{Ao}\left(\frac{D_e}{d_i h_i} + \frac{1}{h_o} + R_{dw}\right)\right] \qquad \text{(VII-32)}$$

where λ' is the Lagrange multiplier. A computer program of Eq. (VII-32) is already available [9]. Using this program, a typical example of the preheater design is calculated.

The optimum overall heat transfer coefficient is found to be about 70 B.t.u./ft.^{2}hr.°F. This value is used in the subsequent design calculation of the preheaters associated with the various methanation processes.

3.2 Product Gas Cooler

After flowing through the preheater, the product gas is cooled to 100°F by the three stage heat exchangers as shown in Figure VII-4. The exit product gas from the preheater has the temperature ranging between 400°F and 750°F. Steam having 400 psia pressure is recovered from the first heat exchanger while low pressure steam of about 35 psia is recovered from the second heat exchanger. The product gas is finally cooled down to 100°F by the counter-current product gas cooler. The cooling water enters at a temperature of 85°F and leaves at 150°F. If the inlet gas temperature to the first heat exchanger is below 500°F, only two heat exchangers are required.

In the first heat exchanger, treated water enters the tube side. Approximately 50 per cent of the water entered is vaporized producing high pressure steam. The product gas flows in the shell side and provides the main heat transfer resistance of this exchanger. The shell side film coefficient can be calculated by

$$\left(\frac{h_o D_e}{k}\right) = 0.36 \left(\frac{D_e G_s}{\mu}\right)^{0.55} \left(\frac{C_p \mu}{k}\right)^{1/3} \qquad \text{(VII-33)}$$

Pressure drop for shell side fluid is calculated by the following equation [10]

$$\Delta P_S = \frac{f G_S^2 D_S L_H}{5.22 \times 10^{10} D_e s B'} \qquad \text{(VII-34)}$$

and

$$f = 1.2 \times 10^{-2} \left(\frac{DeG_S}{\mu}\right)^{-0.189} \qquad \text{(VII-35)}$$

where

De is equivalent diameter for heat transfer tube (ft.).
k is thermal conductivity (B.t.u./ft.hr.°F).
μ is viscosity (lb./ft.hr.).
G_S is mass velocity (lb./ft.^{2}hr.).

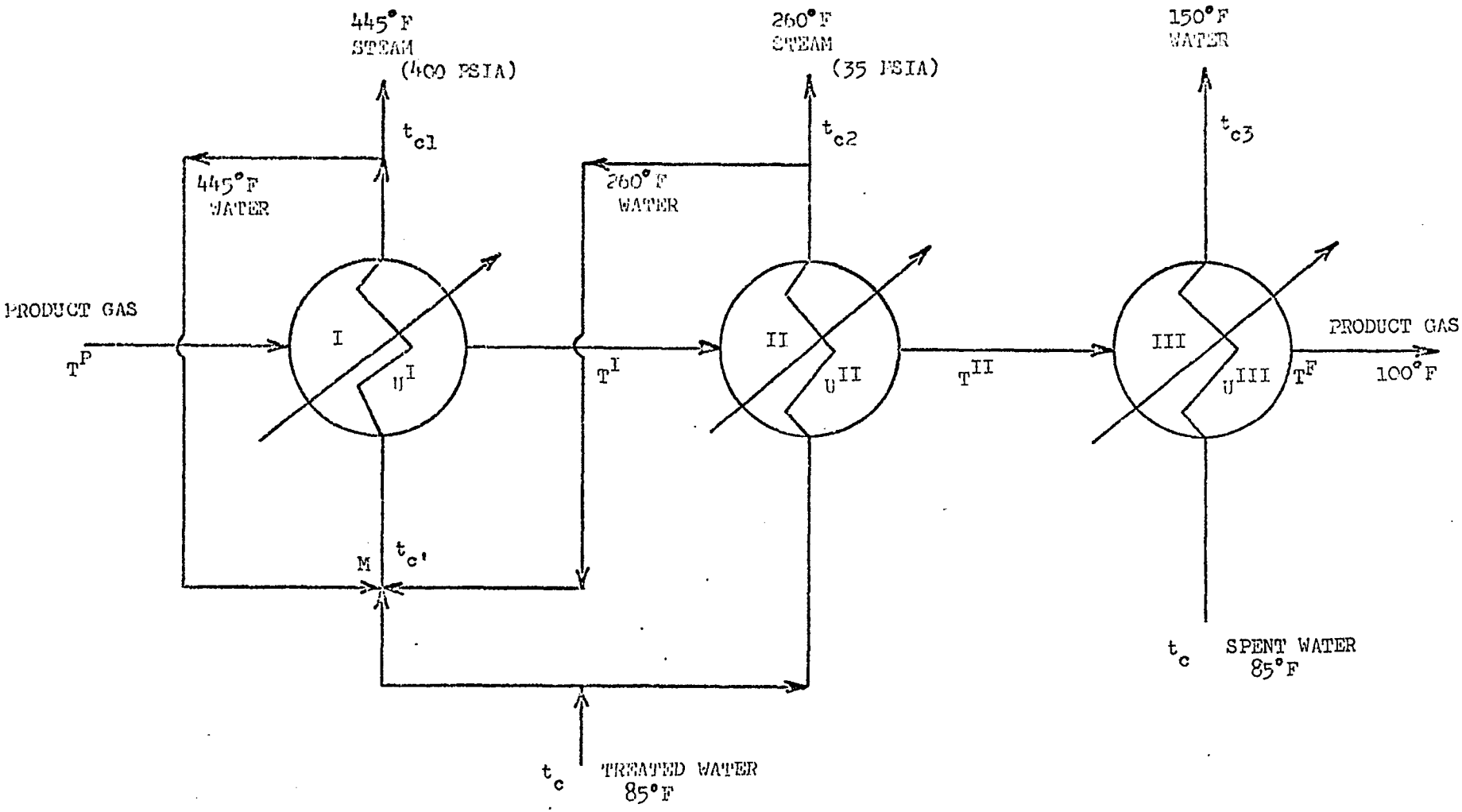

FIGURE VII-4 FLOW DIAGRAM OF PRODUCT GAS COOLER

C_p is the heat capacity (B.t.u./lb.°F).
D_S is the inside diameter of the shell (ft.).
L_H is the length of the heat exchanger (ft.).
B' is baffle spacing (ft.).
s is the specific gravity (-).
ΔP is pressure drop of the heat exchanger (psi).

It is evident from Eqs. (VII-33) and (VII-34) that both h_o and ΔP_S are increased as the mass velocity is increased. Thus the maximum allowable shell side heat transfer coefficient or the optimum heat transfer coefficient is calculated based on the mass velocity corresponding to the maximum allowable pressure drop through the heat exchanger. If the combined pressure drop of the three product gas coolers is limited to 10 psia, the corresponding maximum mass velocity is about 100,000 lb./ft.^{2}hr.

The shell side film heat transfer coefficient corresponding to this mass velocity is about 110 B.t.u./ft.^{2}hr.°F . As water is being vaporized in the tube, the tube side film coefficient, which depends greatly on the temperature gradients across the tube, is expected to be larger than 1000 B.t.u./hr.ft.^{2}°F . The tube side film coefficient without accompanying phase change can be calculated by the following equation,

$$\frac{h_i D_i}{k} = 0.027 \left(\frac{D_i G_i}{\mu}\right)^{0.8} \left(\frac{C_p \mu}{k}\right)^{1/3} \left(\frac{\mu}{\mu_o}\right)^{0.14} \qquad \text{(VII-36)}$$

where

D_i is the inside diameter of the tube (ft.).
G_i is the mass velocity of water (lb./ft.hr.°F).

A numerical calculation based on Eq. (VII-36) gives an inside tube film heat transfer coefficient of about 200 B.t.u./ft.^{2}°Fhr. The overall heat transfer coefficient of the first heat exchanger then becomes approximately 85 B.t.u./ft.^{2}hr.°F .

Similar to the previous case treated, water is introduced into the second heat exchanger with 50 per cent of the water being vaporized in the tube side. The product gas is passed through the shell side, which again provides the main heat transfer resistance of this exchanger. However, when the temperature of the product gas is reduced below 370°F, partial condensation of the water takes place in the shell side. The quantity of condensation depends upon the partial pressure of water in the product gas.

Heat flux accompanied by steam condensation is expressed as

$$q_c = K_G M_v \lambda_c (P_v - P_c) \qquad \text{(VII-37)}$$

where

q_c is the heat removed by condensation (B.t.u./ft.^{2}hr.).
M_v is the molecular weight of steam (lb./lb.mole).
λ_c is the heat of condensation of steam (B.t.u./lb.).
P_v and P_c are partial pressures of steam at the bulk fluid and at the surface of the tube, respectively (atm.).
K_G is the mass transfer coefficient (lb.mole/hr.ft.^{2}atm.).

Since steam condensing on the tube may be regarded as simultaneous heat and mass transfer phenomena, K_G may be expressed as

$$K_G = \frac{h_o (C_p \mu / k)^{2/3}}{C_p p_{gf} M_m (\mu / p k_d)^{2/3}} \qquad \text{(VII-38)}$$

where

M_m is the mean molecular weight of the fluid (lb./lb.mole).
k_d is the diffusion coefficient (ft.^{2}/hr.).
p_{gf} is logarithmic-mean pressure difference of non-condensing gas (atm.).
h_o is the film heat transfer coefficient for shell side fluid and can be calculated by Eq. (VII-33).

The total heat flux is the sum of the heat flux due to non-condensing vapor and the heat flux accompanied by the condensation. Hence,

$$q_T = h_o(T_g - T_c) + K_G M_v \lambda_c (P_v - P_c) = h_c(T_g - T_c) \quad \text{(VII-39)}$$

Calculations using Eqs. (VII-33) and (VII-39) give the range of the shell side film heat transfer coefficient to be between 110 and 210 B.t.u./hr.ft.^{2}°F under an allowable combined pressure drop of 10 psi.

The tube side film heat transfer coefficient is practically the same as that for the first heat exchanger. The overall heat transfer coefficient of the second heat exchanger then becomes approximately 90 B.t.u./ft.^{2}hr.°F .

In the third heat exchanger, spent water is used in the tube side and product gas is passed through the shell side. Using Eqs. (VII-33) and (VII-39) the film coefficient of shell side fluid, which is also affected by the partial condensation of water, is calculated to be between 110 to 150 B.t.u./hr.ft.^{2}°F under the allowable pressure drop. The tube side heat transfer coefficient is about 250 ~ 300 B.t.u./hr.ft.^{2}°F for this operating condition. Thus, the overall heat transfer coefficient of the third heat exchanger is calculated to be approximately 80 B.t.u./ft.^{2}hr.°F. Table VII-2 summarizes the heat transfer coefficients used in the optimization of the three heat exchangers.

TABLE VII-3 HEAT TRANSFER COEFFICIENTS OF THE THREE HEAT EXCHANGERS ($B.t.u./ft.^2 hr.°F$)

	First Exchanger	Second Exchanger	Third Exchanger
shell side heat transfer coefficient	110	110 ~ 210	160 ~ 110
tube side (vaporization) heat transfer coefficient	1500	1500	1500
tube side (no vaporization) heat transfer coefficient	200	200	250 ~ 300
overall heat transfer coefficient	85	90	80

In the process optimization of product gas coolers, the optimum temperatures of gas entering the second and the third heat exchanger are to be found so as to minimize the total equipment and operation costs of the three heat exchangers under the specified temperature constraints. The total cost, C_T, consisting of the equipment cost of the three heat exchangers, the water cost and the steam benefit, is expressed as

$$C_T = \phi' E_H + (C_1 W_1 + C_2 W_2) - (C_3 W_{S1} + C_4 W_{S2}) \qquad \text{(VII-40)}$$

where

E_H is the total equipment cost of the three heat exchangers ($).
W_1 and W_2 are the total flow rates of treated and spent water in the product gas coolers (lb./hr.).
W_{S1} and W_{S2} are the flow rates of high and low pressure steam, respectively (lb.hr.).
ϕ' is the cost factor (1/hr.).
C_1 and C_2 are the treated water and spent water cost per unit weight.
C_3 and C_4 are high pressure and low pressure steam cost per unit weight.

The heat duties of the first, the second and the third heat exchanger are expressed as:

$$q^I = \bar{M} W^N (\bar{C}_P^P T^P - \bar{C}_P^I T^I) \qquad \text{(VII-41)}$$

$$q^{II} = \bar{M} W^N (\bar{C}_P^I T^I - \bar{C}_P^{II} T^{II}) + 18 \left(\frac{P_w}{P_t} - \frac{P_v}{P_t}\right) \lambda_c W^N \qquad \text{(VII-42)}$$

$$q^{III} = \bar{M} W^N (\bar{C}_P^{II} T^{II} - \bar{C}_P^F T^F) + 18 \frac{P_v}{P_t} \lambda_c W^N \qquad \text{(VII-43)}$$

where

W^N is the molar flow rate of the product gas (lb.mole/hr.).
$\bar{M}$ is the average molecular weight of the product gas (lb./lb.mole).
T^I and T^{II} are the outlet temperatures of the product gas from the first and second heat exchanger (°F).
P_w is the partial pressure of steam in the product gas (atm.).
P_v is the vapor pressure of water at T^{II} (atm.).
$\bar{C}_P^P$, $\bar{C}_P^I$ and $\bar{C}_P^{II}$ are the heat capacities of the product gas at temperature T^P, T^I and T^{II}, respectively (B.t.u./lb.°F).

The heat transfer area of the first exchanger is calculated as follows:

First, the water flow rate through the first exchanger, WC^I is calculated from q^I as

$$WC^I = \frac{q^I}{C_{pw}(t_{c1}-t_c')+0.5\lambda_c} \qquad \text{(VII-44)}$$

where

C_{pw} is the heat capacity of water.
t_c' is the temperature of coolant water and is calculated by a heat balance around point M in Figure VII-4.

After entering the first heat exchanger, the water is preheated to the vaporization temperature. This assures a near constant water temperature in the tube as long as the constant steam pressure is maintained. The product gas temperature corresponding to the point at which steam starts to vaporize can be found from,

$$T_m^I = T^I + \frac{WC^I \cdot C_{pw}}{\bar{M}\, W^N \bar{C}_P^I}(t_{c1} - t_c') \qquad \text{(VII-45)}$$

The heat transfer area of the first heat exchanger is

$$A^I = \frac{WC^I}{U^I}\left\{\frac{C_{pw}(t_{c1} - t_c')}{\Delta t_1} + \frac{0.5\lambda_c}{\Delta t_1'}\right\} \qquad \text{(VII-46)}$$

where Δt_1 and $\Delta t_1'$ are,

$$\Delta t_1 = \frac{(T_m^I - t_{c1}) - (T^I - t_c')}{\ln \dfrac{(T_m^I - t_{c1})}{(T^I - t_c')}}, \qquad \Delta t_1' = \frac{(T^P - t_{c1}) - (T_m^I - t_{c1})}{\ln \dfrac{(T^P - t_{c1})}{(T_m^I - t_{c1})}}$$

Next, the heat transfer area of the second heat exchanger is calculated by the same procedure as the first exchanger. The flow rate of water, WC^{II}, in the second heat exchanger is

$$WC^{II} = \frac{q^{II}}{C_{pw}(t_{c2}-t_c)+0.5\lambda_c} \qquad \text{(VII-47)}$$

The heat transfer area of the second heat exchanger is

$$A^{II} = \frac{WC^{II}}{U^{II}} \left\{ \frac{C_{pw}(t_{c2} - t_c)}{\Delta t_2} + \frac{0.5\lambda_c}{\Delta t_2'} \right\} \qquad \text{(VII-48)}$$

where Δt_2 and $\Delta t_2'$ are defined as

$$\Delta t_2 = \frac{(T_m^{II} - t_{c2}) - (T^{II} - t_c)}{\ln \frac{(T_m^{II} - t_{c2})}{(T^{II} - t_c)}}, \quad \Delta t_2' = \frac{(T^{I} - t_{c2}) - (T_m^{II} - t_{c2})}{\ln \frac{(T^{I} - t_{c2})}{(T_m^{II} - t_{c2})}}$$

T_m^{II}, the corresponding product gas temperature at the point where the steam vaporization starts, is calculated from

$$T_m^{II} = T^{II} + \left\{ WC^{II} \cdot C_{pw}(t_{c2} - t_c) - 18 \left(\frac{P_{vm} - P_v}{P_t}\right) \cdot \lambda_c \cdot W^N \right\} \frac{1}{\overline{M}w^N \cdot C_p^{II}} \qquad \text{(VII-49)}$$

where P_{vm} is the vapor pressure of water at temperature, T_m^{II}.

The heat transfer area of the third heat exchanger is calculated as follows:

$$A^{III} = \frac{q^{III}}{U^{III}\Delta t_3} \qquad \text{(VII-50)}$$

where

$$\Delta t_3 = \frac{(T^{II} - t_{c3}) - (T^{F} - t_c)}{\ln \frac{(T^{II} - t_{c3})}{(T^{F} - t_c)}}$$

The water flow rate in the third heat exchanger is calculated from

$$W_2 = \frac{q^{III}}{C_{pw}(t_{c3}-t_c)} \qquad \text{(VII-51)}$$

Then the total heat exchanger cost, E_H, in Equation (VII-40) is calculated by Equations (VII-46), (VII-48) and (VII-50). The consumption of treated water W_1 is

$$W_1 = WC^{II} + 0.5\ (WC^{I} - WC^{II}) \qquad \text{(VII-52)}$$

Here, WC^{II} and WC^{I} are calculated from Eqs. (VII-47) and (VII-44), respectively. W_2, W_{s1} and W_{s2} are also calculated from Eqs. (VII-51), (VII-47) and (VII-44) and are expressed as the function of the temperature T^{I} and T^{II}. The terms appearing in Equation (VII-40) are in turn expressed as functions of the gas inlet temperatures to the second and the third heat exchanger. Figure VII-5 shows the relation between the inlet temperatures of the second and the third heat exchanger and the total cost.

From Figure VII-5 it is readily seen that the optimum temperatures of the gas entering the second and the third exchangers are 460°F and 270°F, respectively. The negative total cost, C_T, means that the steam benefit is the predominant factor affecting the process.

It is realized that a large quantity of steam particularly high pressure steam, will be required in other phases of operations, such as the primary gasification, the gas purification, the water gas shifting, etc. It is not possible, however, at this stage to estimate how much is required for each of the various routes to be considered. Therefore, low costs of \$0.35/1,000 lb. for 400 psi steam and \$0.15/1000 lb. for 35 psi steam are used.

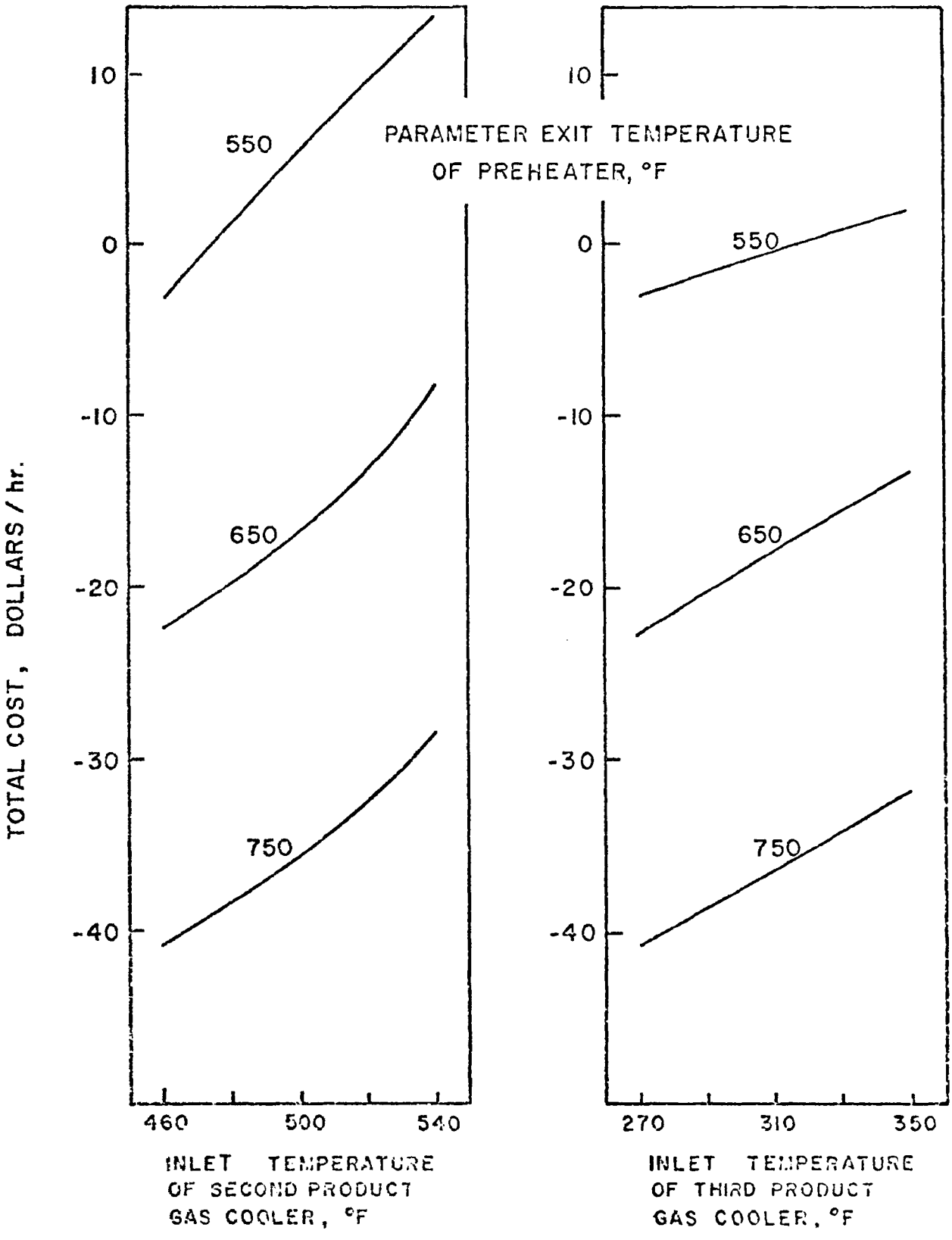

FIGURE VII-5 Total Cost Versus Inlet Temperatures Of Second And Third Product Gas

3.3 Intermediate Cooler

In the cold quench system with a high CO content feed gas, the heat generated in the reactor is so large that it is necessary to cool the reactant intermediately below a suitable temperature as shown in Figure VII-6. In this intermediate cooler, high pressure steam (400 psia) is recovered. The gas enters the heat exchanger at 850°F and must leave at a temperature higher than the reaction initiation temperature of 550°F. Since steam benefit is the over riding factor, it is clear that the optimum outlet temperature of the intermediate cooler must be the lowest possible temperature of 550°F. Since the fluid properties in the intermediate cooler are almost the same as that in the first heat exchanger of the product gas cooler, the overall heat transfer coefficient of this heat exchanger may be taken to be 85 B.t.u./ft.^{2}hr.°F. Water flow rate, W_{im}, and steam rate obtained in the intermediate cooler are,

$$W_{im} = \frac{w^o(\bar{C}_p^N T^N - \bar{C}_p^A T^A)}{\{C_{pw}(t_{cl}-t_c'')+0.5\lambda\}} \qquad \text{(VII-53)}$$

where

w^o is the mass flow rate of reactant gas (lb./hr.).
t_c'' is the inlet water temperature (°F).
T^A is the outlet reactant gas temperature from the intermediate cooler (°F).

The heat transfer area of the intermediate cooler is obtained from

$$A_{in} = \frac{W_{im}}{U^I}\left\{\frac{C_{pw}(t_{cl} - t_c'')}{\Delta t_A} + \frac{0.5\lambda_c}{\Delta t_B}\right\} \qquad \text{(VII-54)}$$

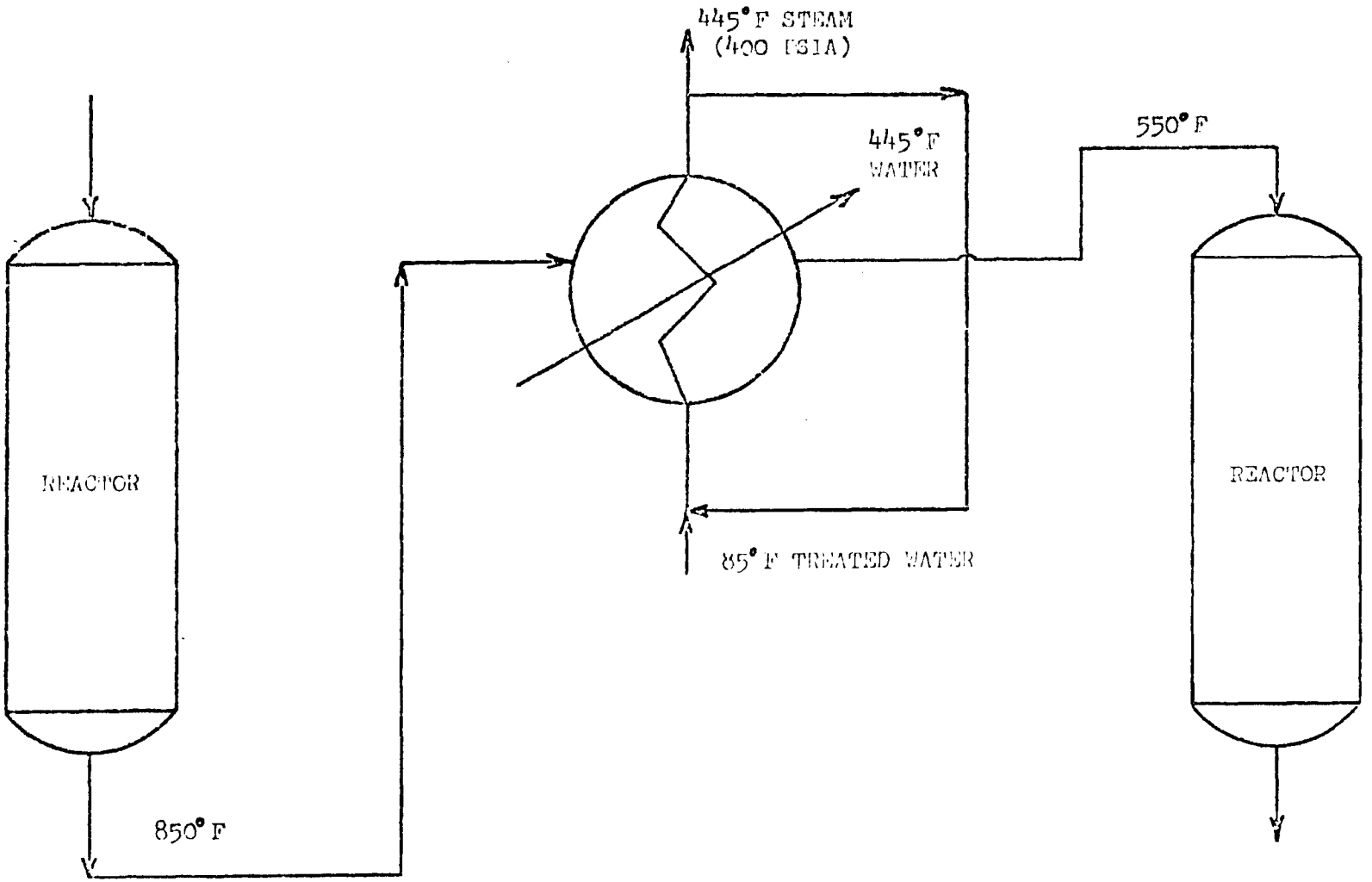

FIGURE VII-6 FLOW DIAGRAM OF INTERMEDIATE COOLER

4. The Heat Extraction System

4.1 Process Analysis

A flow diagram for the heat extraction system is shown in Figures VII-7 and VII-8. The gaseous effluent from the primary gasification system, after being purified and the H_2 to CO ratio being adjusted to approximately 3 by water-gas shift reaction, is fed into the methanation system at 100°F and 1065 psia. The gas has been preheated to $T^{(1)}$, a temperature high enough to initiate the reaction, before it is introduced to the top of the reactor. The temperature of 550°F is selected for $T^{(1)}$ although a lower temperature of about 500°F is believed sufficient for starting the reaction.

In the upper portion of the reactor, reaction is carried out adiabatically until the maximum allowable temperature of 850°F is reached. The reaction thereafter is carried out isothermally by the removal of the excess heat of reaction from the reactor through the embedded fin tubes.

The temperature of 850°F is selected as the operating temperature for two reasons. First, at above 900°F, carbon deposition on catalysts may take place, which drastically reduces the effectiveness of the catalysts. Second, in order to minimize the required heat transfer area of fin tubes, the temperature difference between the reacting gas and the coolant should be kept as large as possible.

But in the high CO case, the temperature near the exit of the reactor is reduced to 810°F in order to avoid equilibrium hindrance. Pressurized hot water at temperature of 445°F is used as a coolant

where

$$\Delta t_A = \frac{(T^m - t_{cl}) - (T^A - t_c'')}{\ln \frac{(T^m - t_{cl})}{(T^A - t_c'')}} \qquad \Delta t_B = \frac{(T^N - t_{cl}) - (T^m - t_{cl})}{\ln \frac{(T^N - t_{cl})}{(T^m - t_{cl})}}$$

$$T^m = T^A + \frac{W_{im} C_{pw}}{w \bar{C}_p^A} (t_{cl} - t_c'')$$

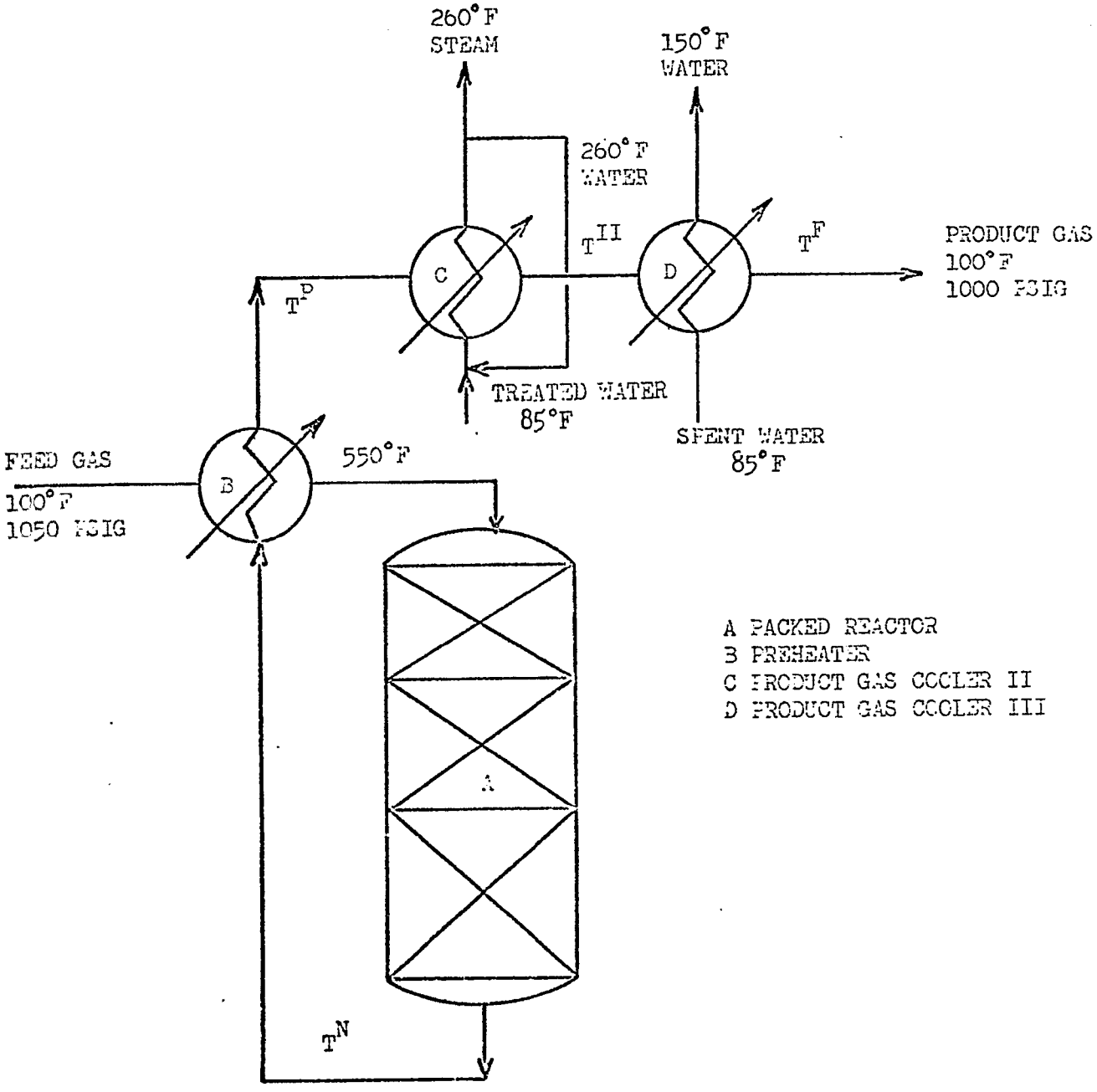

FIGURE VII-7 FLOW DIAGRAM IN LOW CO CASE

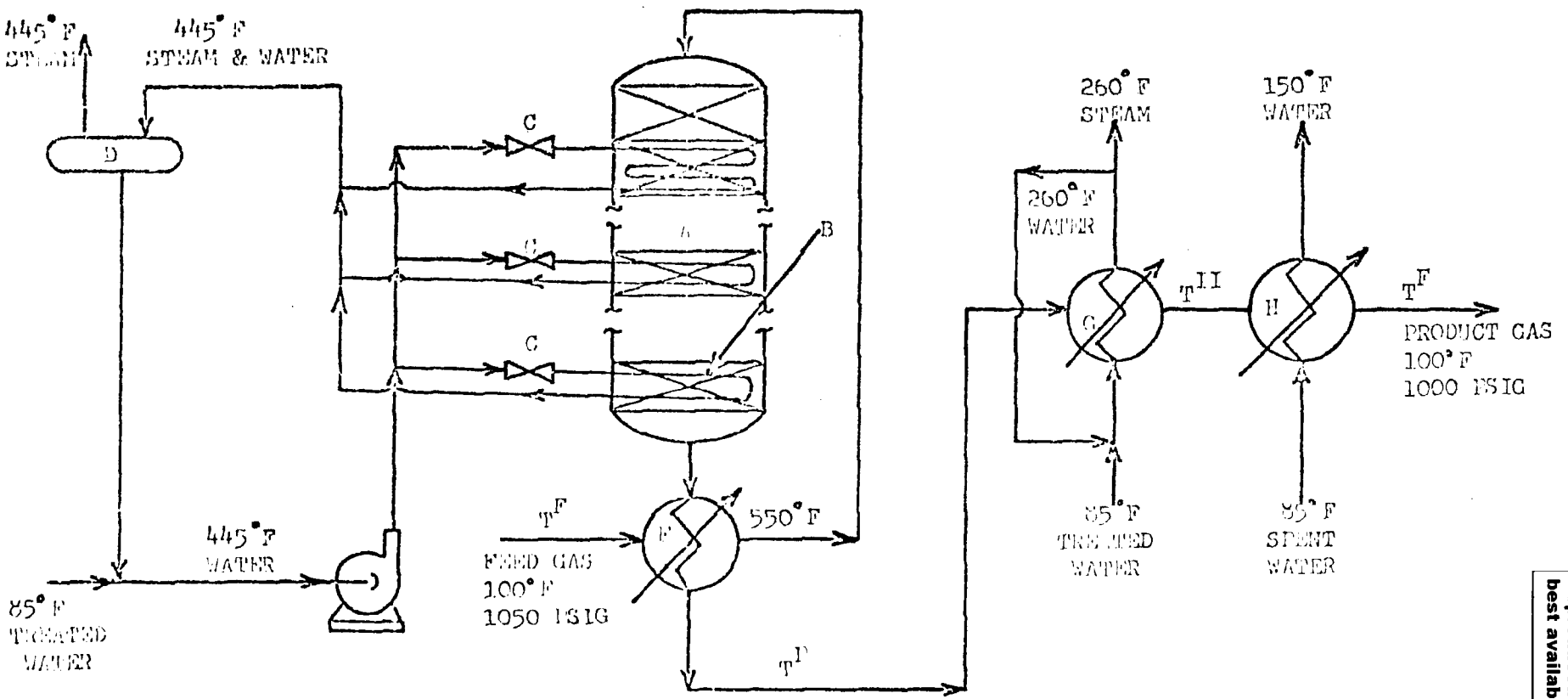

A PACKED REACTOR
B FIN TUBES
C CONTROL VALVE
D SEPARATOR DRUM
E PUMP
F PREHEATER
G PRODUCT GAS COOLER II
H PRODUCT GAS COOLER III

FIGURE VII-8 FLOW DIAGRAM IN BOTH INTERMEDIATE AND HIGH CO CASES FOR HEAT EXTRACTION SYSTEM.

in the fin tubes. A large portion of water is evaporated as it passes through the fin tubes in the reactor. The main resistance to heat transfer would be across the gas film outside the embedded fin tubes. In the reactor H_2 and CO are converted to methane until the composition in the product gas reaches 92.1% methane on a dry base. The product gas is subsequently cooled to 100°F by the preheater and the product gas cooler.

The exit gas pressure of the methanation process is fixed at 1015 psia. Therefore the total pressure drop, both in the reactor and in the heat exchangers must be kept less than 50 psia. These are the constraints in the design of the optimum reactor diameter.

4.2 Calculation Procedure

As previously stated, in the heat extraction system the reactor is operated adiabatically until the temperature of 850°F is reached, after which the reactor is operated isothermally. Thus, the heat balance around the n-th cell can be written as,

For $T_1 \leq T \leq 850°F$

$$\sum_{i=1}^{6} C_{P_i}^{n} F_i^{n} T^{n} - \sum_{i=1}^{6} C_{P_i}^{n} F_i^{n-1} T^{n-1} = (\Delta H)\, \rho_c V_c^{n}\, r_{CH_4} \qquad \text{(VII-55)}$$

and $T = 850°F$,

$$Q^{n} = (\Delta H)\rho_c V_c^{n}\, r_{CH_4} = U_o A_t^{n} (T^{n} - T_w) \qquad \text{(VII-56)}$$

where

Q^n is the amount of heat removed from the n-th cell.(B.t.u./hr.)
U_o is the overall heat transfer coefficient.(B.t.u./hr.°F)
T^n and T_w are the reactor temperature and the coolant temperature, respectively.(°F)
A_t^n is the total heat transfer area of the fin tubes in the n-th cell.($ft.^2$)

Since the main resistance to heat flow is across the gas film outside of the fin tubes, the resistance across the tube wall and that due to inside film of the coolant can be neglected. The overall heat transfer coefficient based on the outside surface of the fin tube is approximated to be 11.12 B.t.u./hr.ft.^{2}°F.

From the equations developed, the concentration of each component, the temperature and the pressure at each cell can be calculated under the adiabatic condition from the previous cell. The calculation is continued until the reactor temperature reaches 850°F. The calculation thereafter is repeated but under the isothermal condition until the concentration of methane reaches 92.1 per cent on a dry base. Since heat transfer area in a single cell does not have a practical meaning, an average heat transfer area of 40 cells-in-series which make up one tray length is calculated.

Since the heat generated in the low CO case is not very great, no heat removal from the reactor is necessary for this case. For the high CO case, the heat generation rate near the entrance of the reactor is so large that the catalyst are packed only partially in order to keep the gas temperature at 850°F. Also the temperature near the exit of the reactor is reduced to 810°F to avoid equilibrium hindrance of the methanation reaction.

The heat transfer areas of the preheater and the product gas cooler are calculated by the method mentioned in Section 3.

The total cost of the system can be computed from the summation of the individual cost of preheater, product gas cooler, catalyst, insulation, reactor, supporting tray, control valves and fin tubes.

Here, the number of the control valves is estimated from the number of trays. Thus, the control valve cost, E_{CV}, is calculated by,

$$E_{CV} = C_{CV} \cdot N \qquad \text{(VII-57)}$$

C_{CV} is the cost of a control valve (4000 dollars per valve is used in this study.)

From the optimization point of view, the decision variables are the reactor diameter, D, the inlet pressure, P^o, and the inlet gas temperature to the reactor, $T^{(1)}$. A search technique as described in the next section is developed to determine these three variables by minimizing the total equipment cost. Since the gas temperature at the reactor inlet should be kept as low as possible to minimize the heat removal cost, the problem is reduced to that involving two decision variables; the reactor diameter and the inlet pressure.

4.3 Optimum Search Techniques

One of the simple procedures commonly employed for the optimization involving several variables is to vary each of the variables in turns until no further improvement can be made on the objective function. This method is very effective when the contours are nearly circular. Although in most of the practical problems the contours are not necessarily circular, the search can still be made effective by finding a procedure that will follow a valley to its minimum point.

In the present study, the method of the steepest descent can be efficiently applied. This method starts with locating the direction of the steepest descent from an initial point. The search is then made

along this line until no further improvement can be made. A new direction of the steepest descent is located at this point and searching is continued along the new line until no further improvement is possible. At this point, another new direction is found and the search continues.

For the search involving two independent variables, once the starting point is selected the search direction can be located by varying one variable at a time. When there are more than two variables involved, Powell's method which does not require the computation of derivatives is more conveniently employed. However, this procedure has no way of recognizing constraints on the variables and consequently this method is not effective for the problems with inequality constraints [7].

The computer flow diagram for searching reactor diameter and pressure for the heat extraction system is shown in Appendix B-5

4.4 Results and Discussion

The results obtained from the computer study of the heat extraction system indicate that (1) the optimum inlet pressure is equal to the feed gas pressure at 1065 psia, (2) the optimum reactor diameter is a function of the feed composition.

i. Low CO Case

Since the heat generated in the low CO case is not very large, no heat removal from the reactor is necessary. The reactor is essentially operated adiabatically without internal heat removal

or cold shot cooling. The effect of reactor diameter on the equipment cost is shown in Figure VII-9. Table VII-4 lists the optimum operating conditions as well as the optimum equipment costs. The reaction rate, the composition of each gaseous component and the temperature profiles along the reactor are shown in Figures VII-10 and VII-11, respectively.

ii. Intermediate CO and High CO Case

The effects of reactor diameter on the equipment cost are shown in Figs. VII-12 and VII-13 for the catalytic methanation employing the heat extraction system for the intermediate CO and the high CO cases. Tables VII-5 and VII-6 list the operating conditions and the corresponding equipment costs. Figures VII-14 and VII-15 indicate the reaction rate, the concentration of each gaseous component and temperature profiles along the reactor, respectively, for the intermediate CO case. Similarly, the reaction rate, the composition and temperature profiles along the reactor for the high CO case are shown in Figures VII-16 and VII-17, respectively.

Although the decision variables selected for optimization are the reactor diameter, the inlet pressure and the feed gas temperature, the feed gas temperature has been fixed at 550°F in actual calculation. This is because the reaction is not affected by temperature significantly after 600°F is reached as shown in Figure VII-1, probably on account of the slow catalyst pore diffusion. Hence, there is no reason to increase the inlet temperature above 600°F.

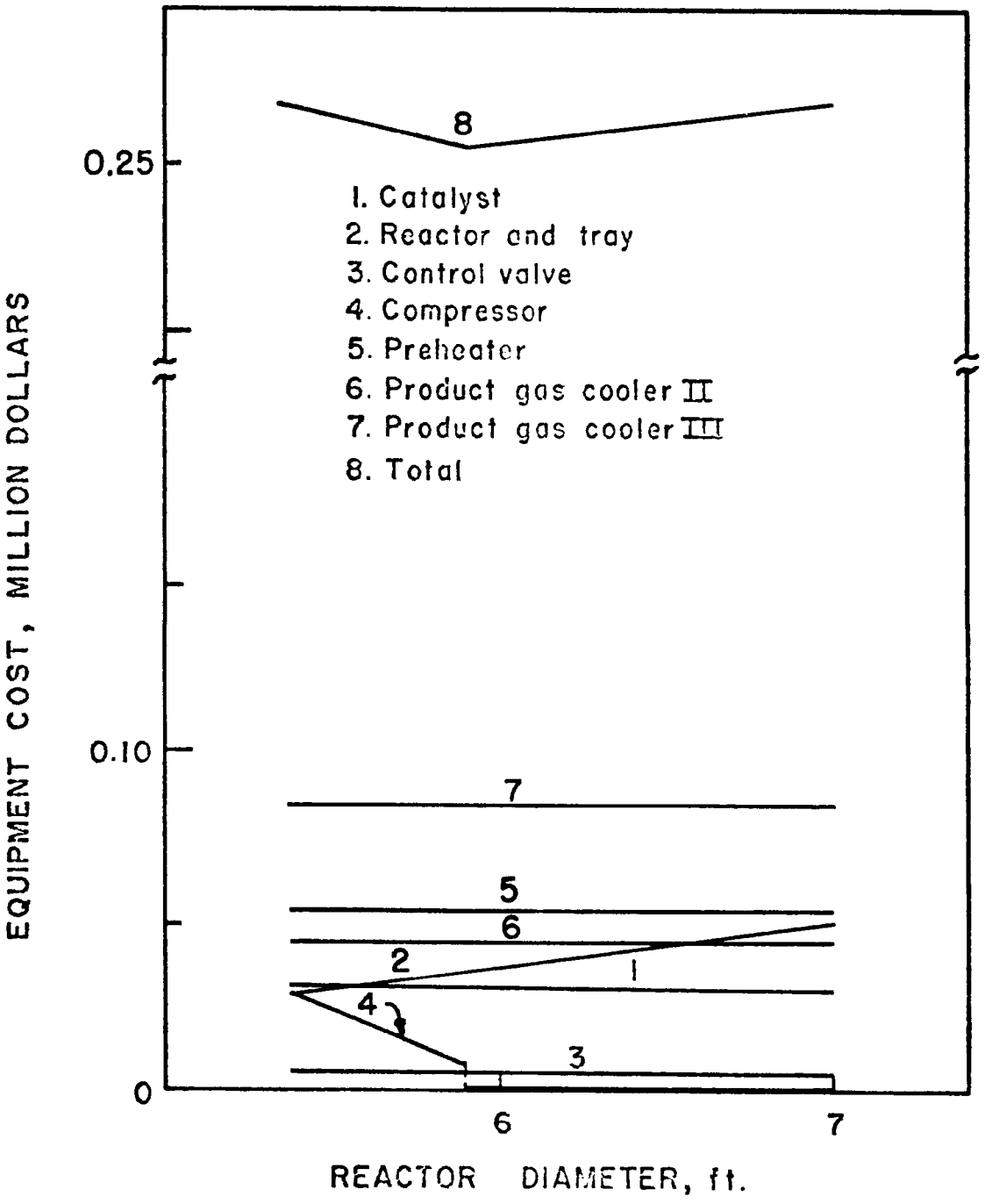

FIGURE VII-9 Equipment Cost Versus Reactor Diameter In Low CO Case.

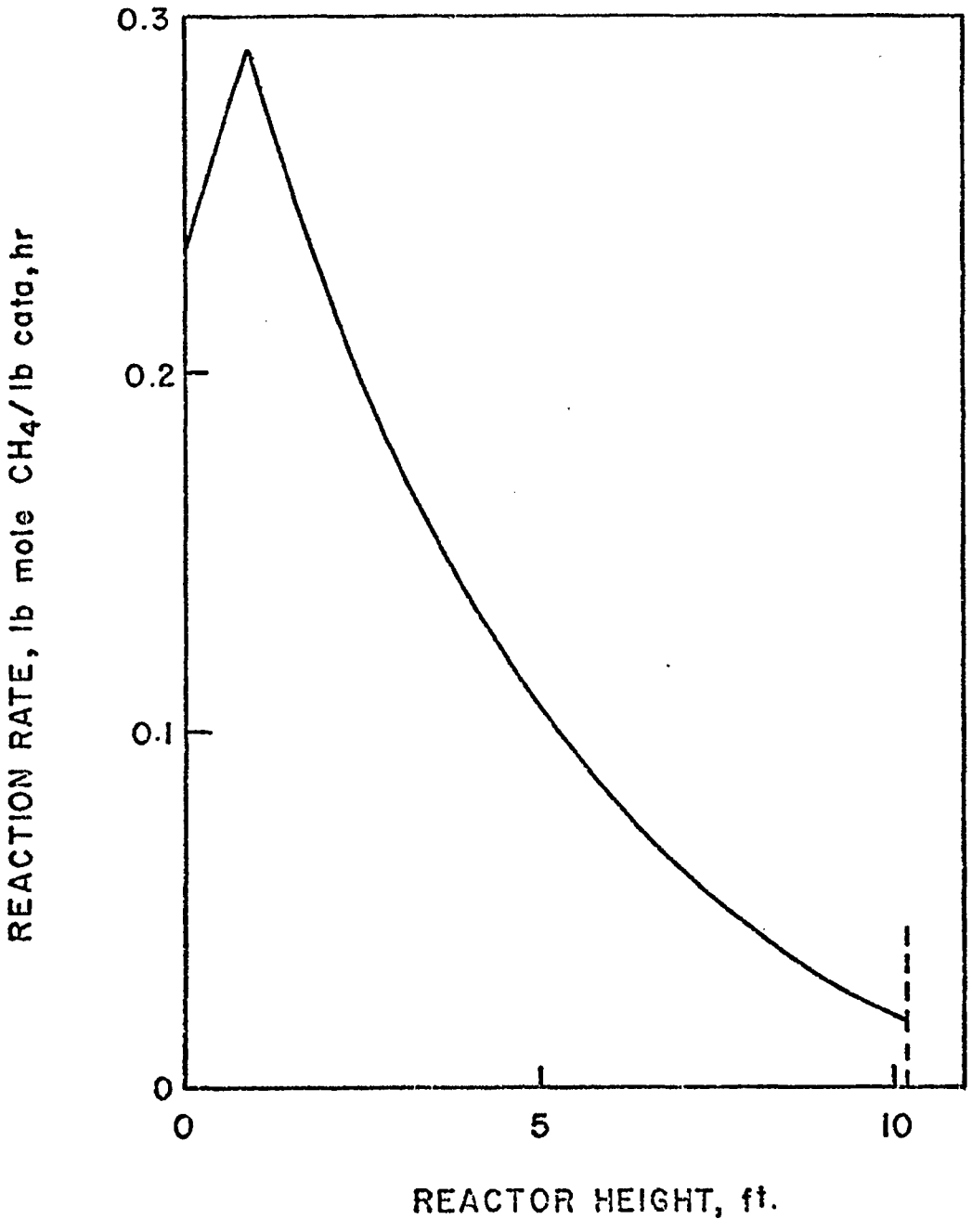

FIGURE VII-10 Reaction Rate Along The Reactor Height In Low CO Case.

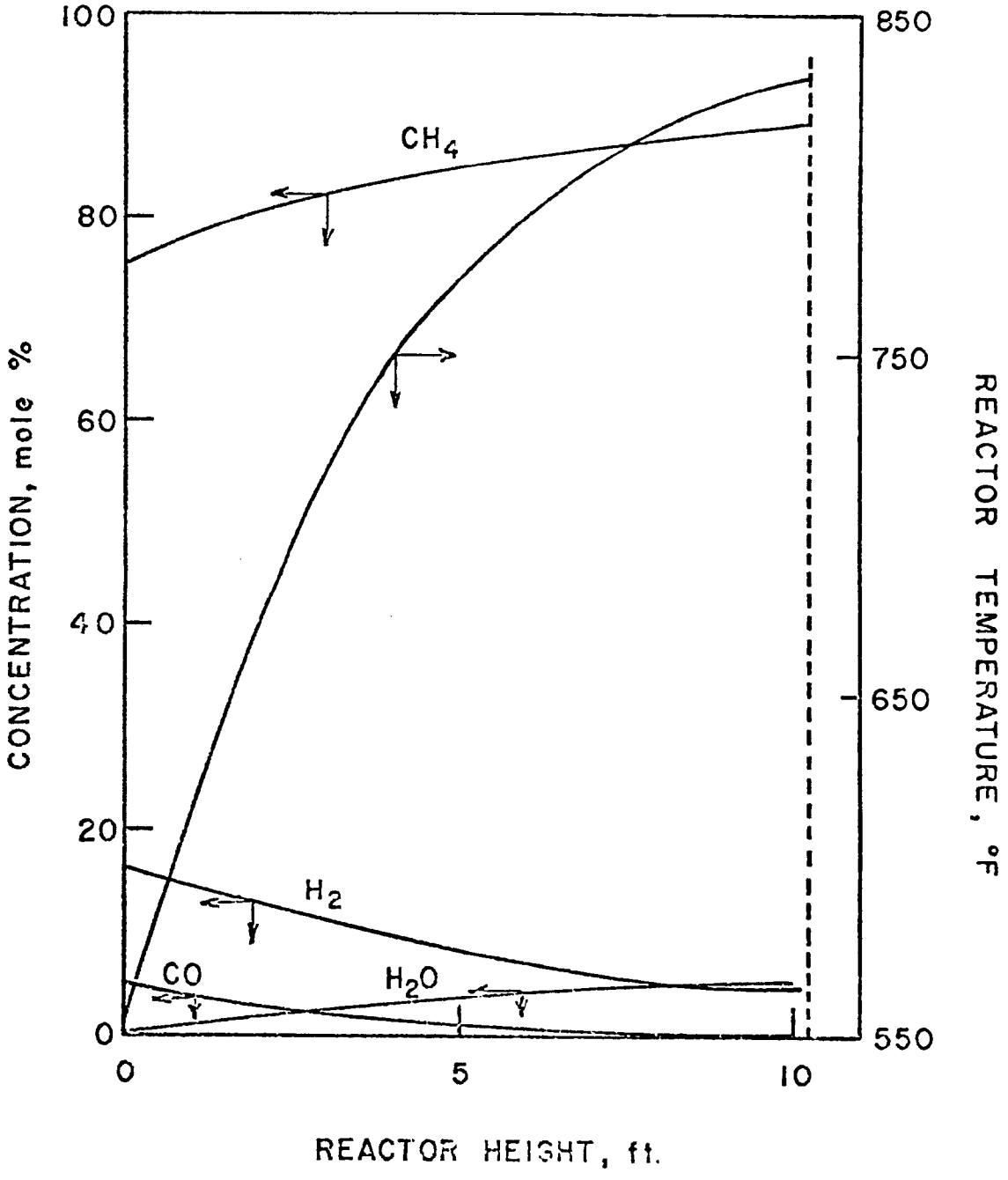

FIGURE VII-11 Concentration And Temperature Profiles Along The Reactor Height In Low CO Case.

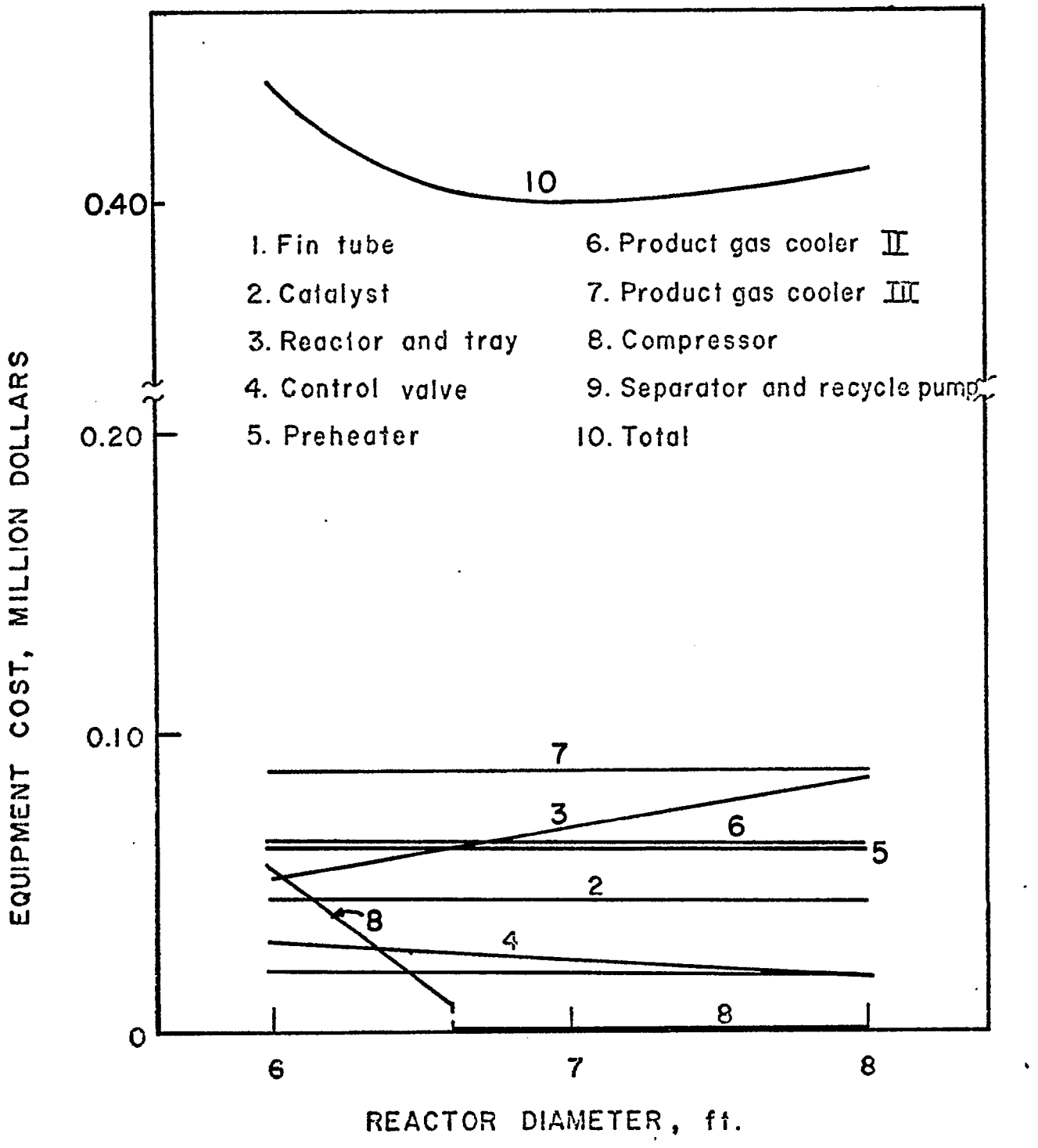

FIGURE VII-12 Equipment Cost Versus Reactor Diameter In Intermediate CO Case For Heat Extraction System.

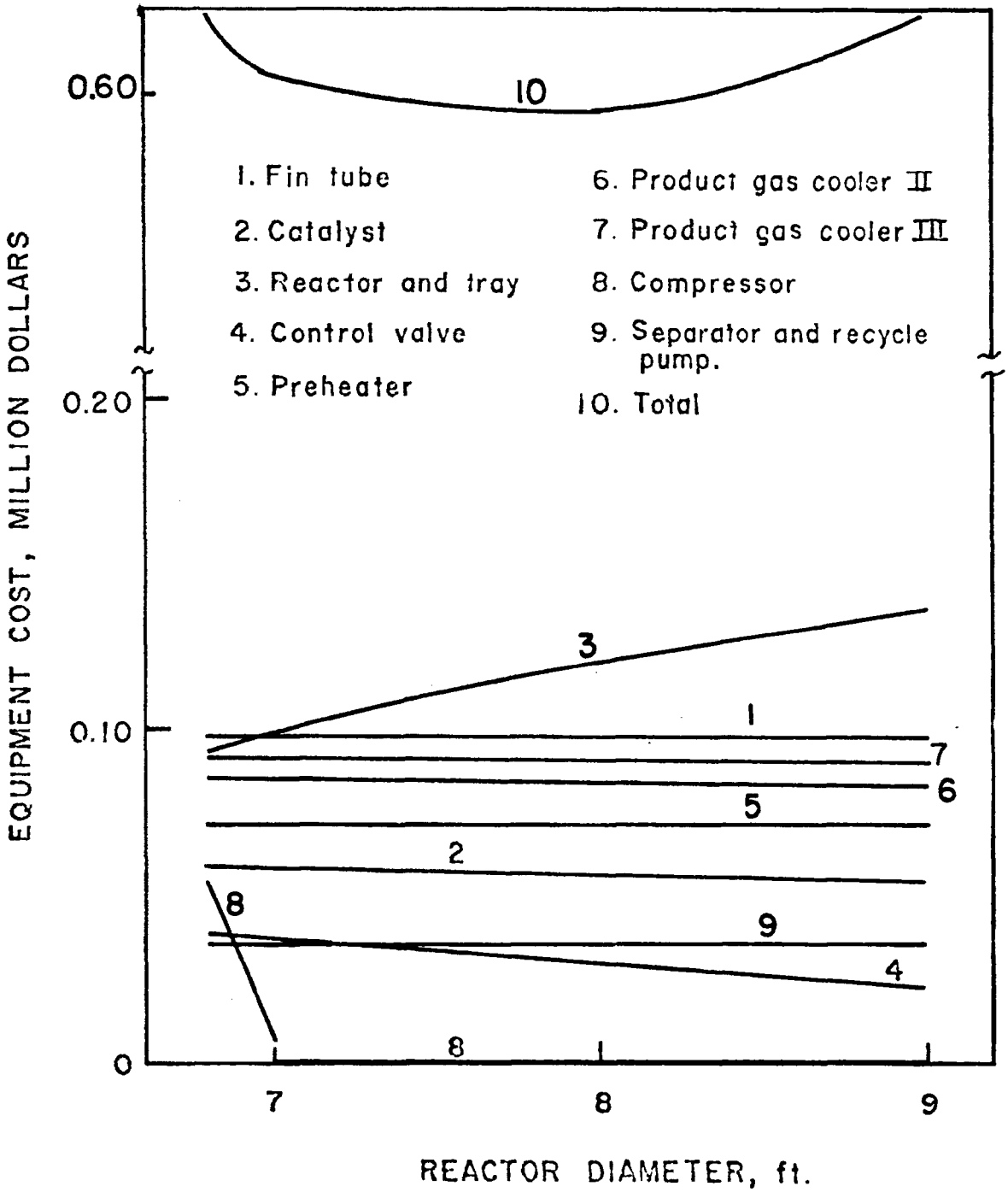

FIGURE VII-13 Equipment Cost Versus Reactor Diameter In High CO Case For Heat Extraction System.

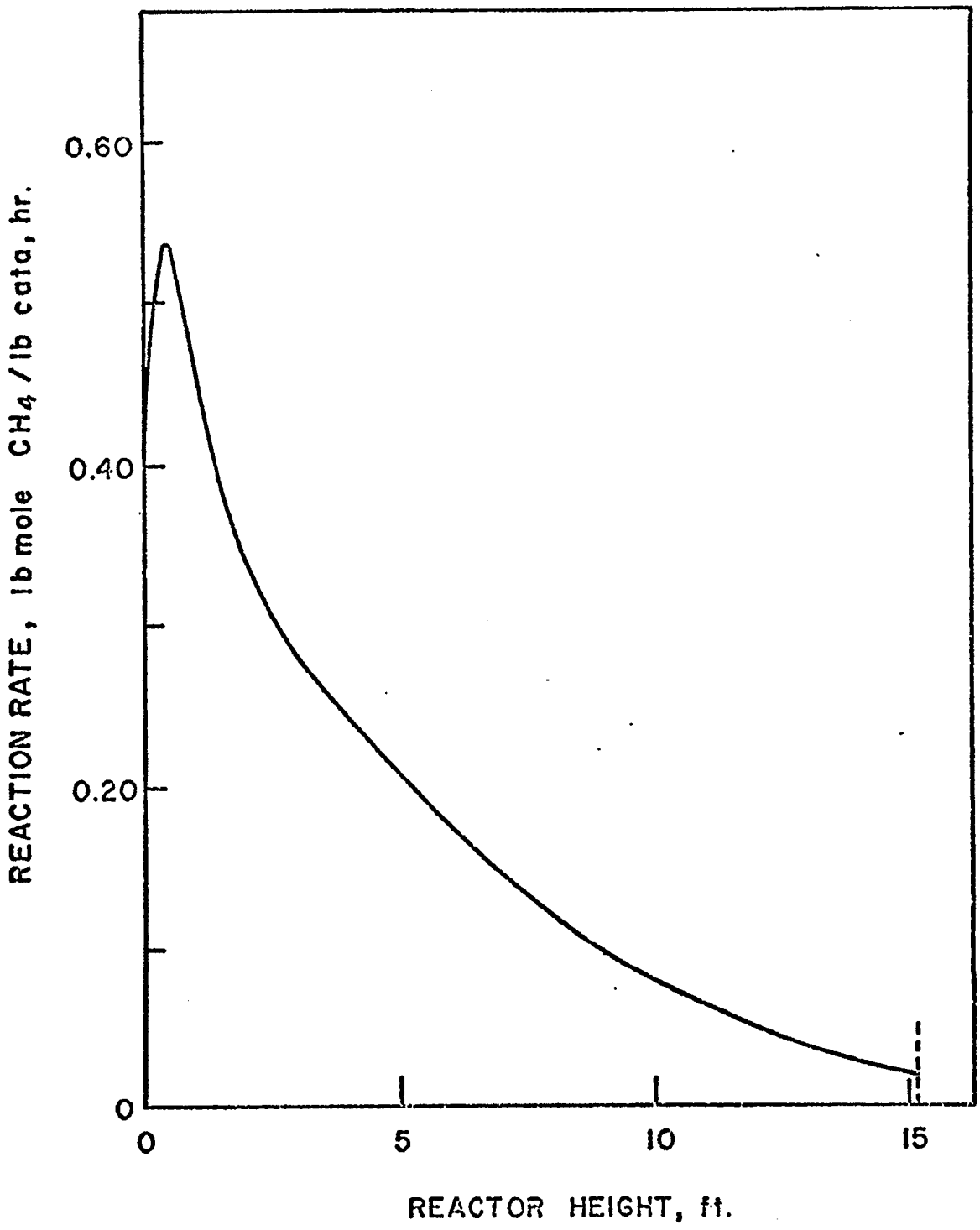

FIGURE VII-14 Reaction Rate Along The Reactor Height In Intermediate CO Case For Heat Extraction System.

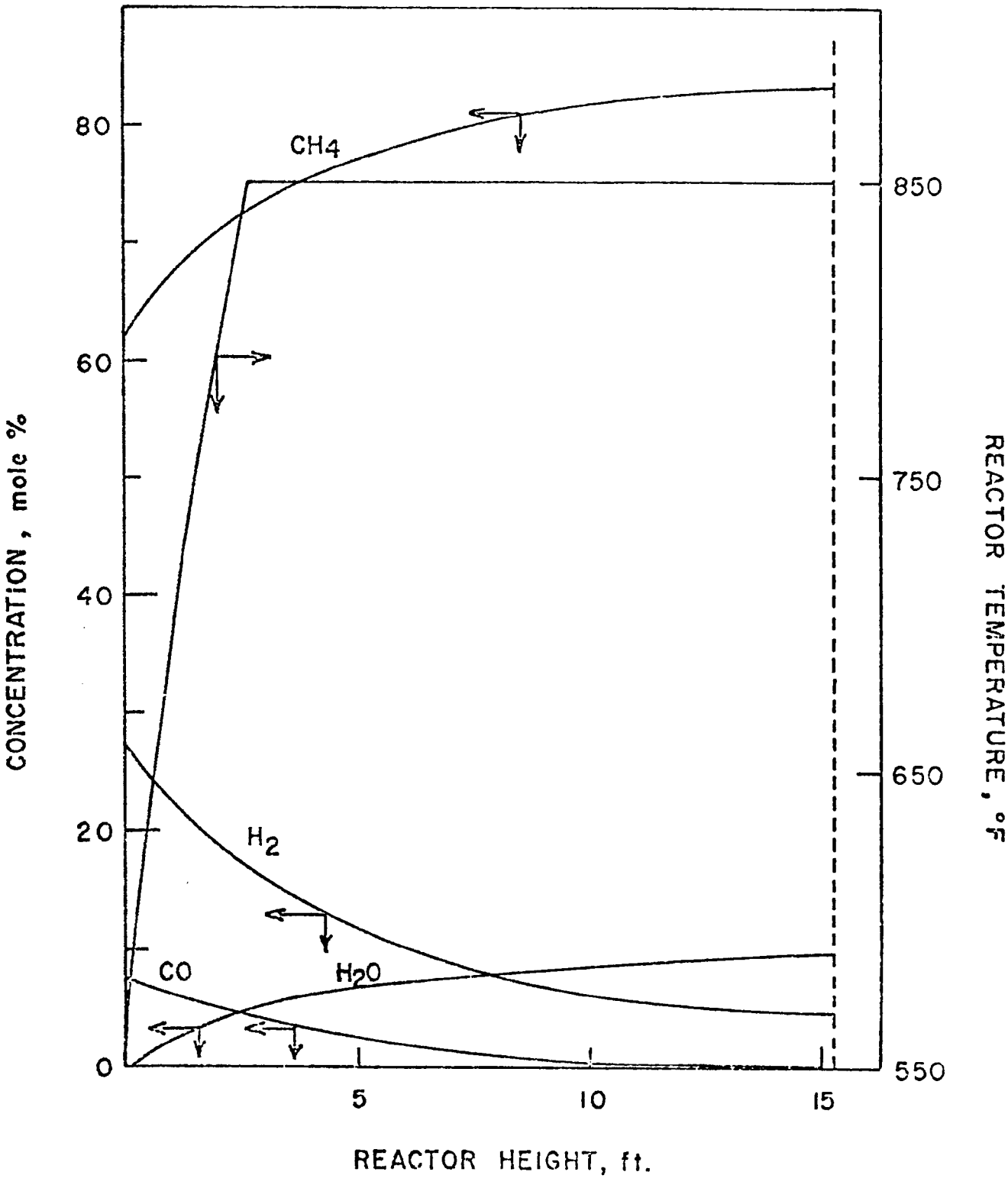

FIGURE VII-15 Concentration And Temperature Profiles Along The Reactor Height In Intermediate CO Case For Heat Extraction System

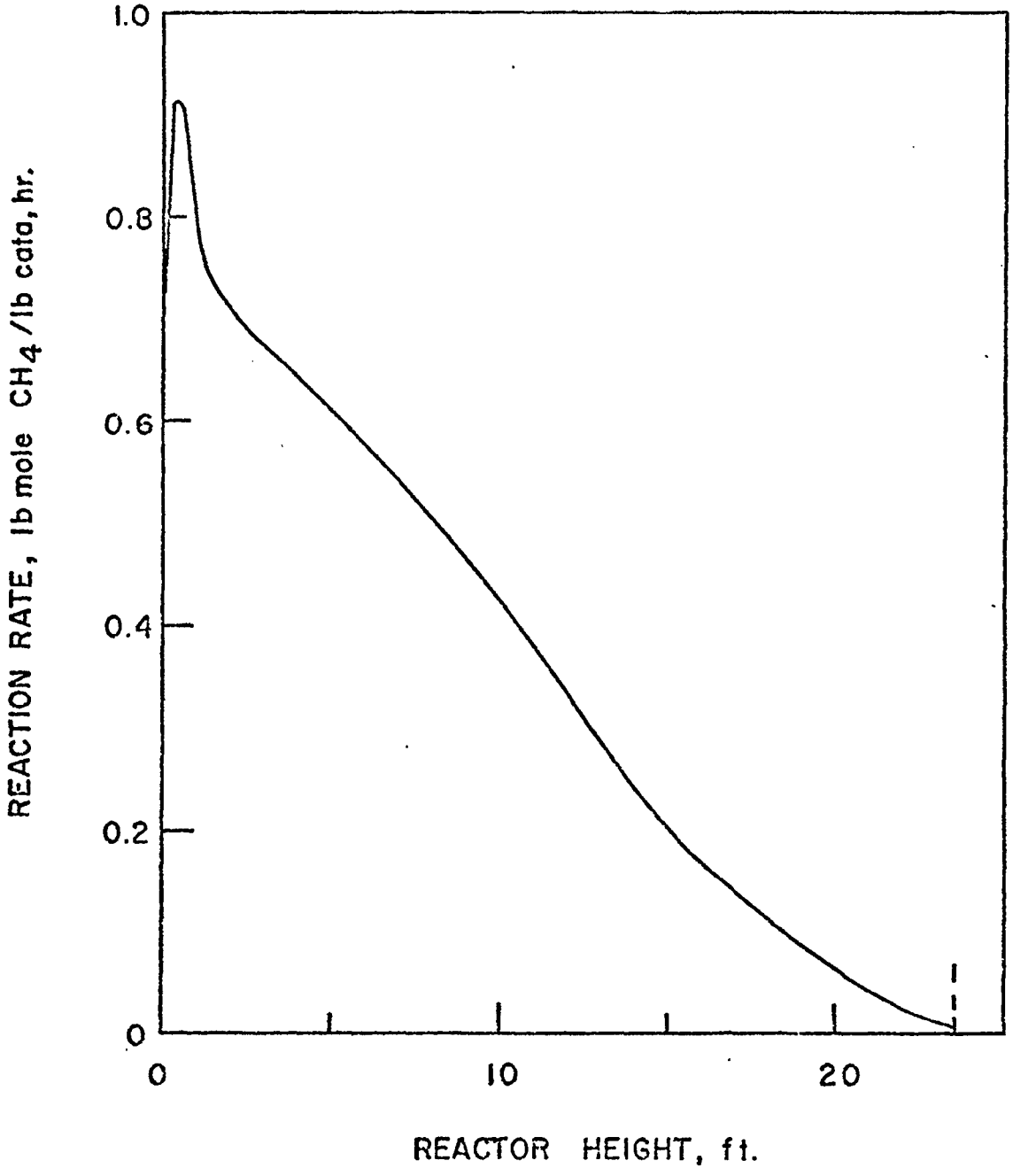

FIGURE VII-16 Reaction Rate Along The Reactor Height In High CO Case For Heat Extraction System.

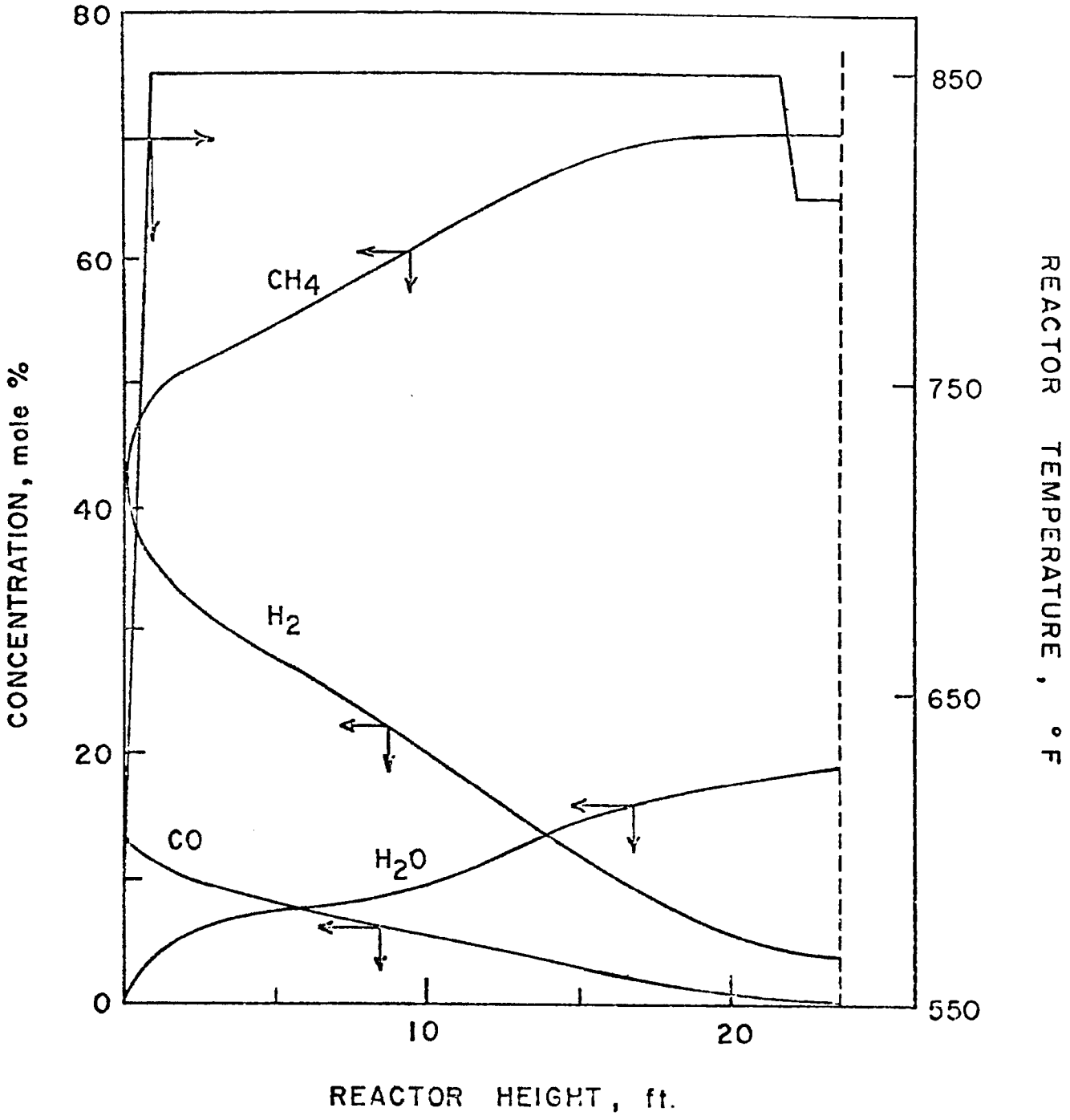

FIGURE VII-17 Concentration And Temperature Profiles Along The Reactor Height In High CO Case For Heat Extraction System.

TABLE VII-4 OPTIMUM OPERATING CONDITIONS AND OPTIMUM EQUIPMENT COSTS IN LOW CO CASE

Operating Conditions		Equipment Costs, $	
Inlet temperature, °F	100	Catalyst	30,000
Outlet temperature, °F	100	Reactor and tray	35,600
Inlet pressure, psig	1,050	Control valve	6,000
Outlet pressure, psig	1,000	Preheater	56,700
Reactor diameter, ft.	5.9	Product gas cooler II	44,700
Reactor height, ft.	10.1	Product gas cooler III	85,100
Space velocity*, $hr.^{-1}$	11,230	Total	258,100
Catalyst weight, lbs.	12,030		
Heat transfer surface area of preheater, $ft.^2$	9,015		
Heat transfer surface area of product gas cooler II, $ft.^2$	5,920		
Heat transfer surface area of product gas cooler III, $ft.^2$	18,600		
Flow rate of 35 psia steam in heat exchangers, lb./hr.	38,450		
Flow rate of treated water in heat exchangers, lb./hr.	76,900		
Flow rate of spent water in heat exchangers, lb./hr.	138,000		

*Based on inlet condition

TABLE VII-5 OPTIMUM OPERATING CONDITIONS
IN TWO DIFFERENT FEEDS
FOR HEAT EXTRACTION SYSTEM

	Intermediate CO	High CO
Inlet temperature, °F	100	100
Outlet temperature, °F	100	100
Inlet pressure, psig	1,050	1,050
Outlet pressure, psig	1,000	1,000
Reactor diameter, ft.	7.0	8.0
Reactor height, ft.	15.2	23.5
Space velocity*, $hr.^{-1}$	9,130	8,530
Catalyst weight, lbs.	17,390	22,340
Total heat transfer surface area of fin tube, $ft.^2$	31,400	94,500
Heat transfer surface area of preheater $ft.^2$	10,320	13,520
Heat transfer surface area of product gas cooler II, $ft.^2$	10,900	18,360
Heat transfer surface area of product gas cooler III, $ft.^2$	20,000	21,140
Flow rate of 35 psia steam in heat exchangers, lb./hr.	55,530	76,670
Flow rate of treated water in heat exchangers, lb./hr.	111,000	153,400
Flow rate of spent water in heat exchangers, lb./hr.	149,200	157,600
Flow rate of 400 psia steam in fin tubes, lb./hr.	105,790	356,600
Flow rate of treated water in fin tubes, lb./hr.	105,790	356,500

*Based on inlet condition.

TABLE VII-6 OPTIMUM EQUIPMENT COSTS
IN TWO DIFFERENT FEEDS
FOR HEAT EXTRACTION SYSTEM

	Intermediate CO	High CO
Catalyst, $	43,500	55,900
Reactor and tray, $	67,100	120,450
Control valve, $	24,200	34,200
Fin tube, $	37,200	98,400
Preheater, $	61,200	71,200
Product gas cooler I, $	0	0
Product gas cooler II, $	63,100	84,600
Product gas cooler III, $	88,700	91,550
Separator drum and recycling pump (in fin tube system), $	20,250	36,850
Total equipment, $	405,250	593,150

It has been also discussed that the temperature of 500°F is probably sufficient to start the methanation reaction but lacking actual experimental data at this temperature, 550°F has been selected. Since this temperature is less than 600°F, the catalyst cost is slightly increased but the preheater cost and the fin tube cost are reduced substantially, resulting in a net reduction of the total equipment cost. As is evident from Tables VII-5 and VII-6, heat exchanger costs, particularly the preheater cost and the product gas cooler cost, are the major items of the total equipment cost. Any effective scheme to reduce the size of heat exchanger will reduce the total cost most significantly. Had the reactor been permitted to operate at a feed gas temperature of 500°F, the total cost would have been reduced further. Temperature much below 400°F is not desirable not only because of the low reaction rate but also due to a concern about carbonyl formation.

Each section of the reactor between the two adjacent trays is made up of 40 cells equivalent to 40 inches of fixed bed packed with catalyst and fin tubes. The fin tubes have equal heat transfer area in each section. Therefore, the temperature in the isothermal portion of the reactor is not necessarily maintained at the specified 850°F. The temperature deviation is not serious, however, with the largest deviation of only 16°F occurring at the final tray in the high CO case.

The study of the effect of pressure on the equipment cost indicates that the optimum pressure is the highest pressure obtainable without additional compression to meet the given gas line pressure.

5. THE COLD QUENCH SYSTEM

5.1 Process Analysis and Calculation Procedure

In the cold quench system, only a small portion of the fresh feed is preheated and enters the top of the reactor. The remainder of the fresh feed enters at relatively low temperature at prescribed intervals into the reactor in such a way that the effluent from the preceding bed is cooled substantially to maintain the reactor temperature below the maximum allowable temperature. In effect, the excess heat generated by the reaction is absorbed into the sensible heat of the feed gas. If the excess heat generated by the reaction is more than that can be absorbed by the sensible heat of the feed gas, it is necessary to use more than one reactor with provisions for intermediate cooling. The maximum allowable temperature is again taken to be 850°F for all cases except for the high CO case in which the exit temperature from the last reactor is reduced to 810°F for reasons previously discussed. The pressure drop in both the reactor and the product gas coolers is limited to less than 50 psia.

Since the amount of heat generated by the reaction, Q_c, is strongly affected by the feed gas composition as can be seen from the equation:

$$Q_c = (\Delta H)\, F^O \cdot y^N \qquad \text{(VII-58)}$$

where

F^O is the total molar flow rate of feed gas (lb.mole/hr.).
y^N is the conversion of CO to CH_4 at the exit (—).
ΔH is the heat of reaction in B.t.u./mole of CH_4 formed.

As mentioned previously, the heat generated for the low CO case is less than the sensible heat of the reactant gas so it is not necessary

to perform cold quenching. From the heat generation as well as from the economics points of view, only one reactor without the intermediate cooling will be necessary for the intermediate CO case. However, for the high CO case, three reactors with two intermediate coolers will be needed.

i. Intermediate CO Case

The schematic flow diagram of this case is presented in Figure VII-18. A portion of the feed gas is preheated to $T^{(1)}$ by the preheater prior to entering the top of the reactor. The first cold shot of feed is introduced to cool the reacting gas at a point where the gas temperature has reached the maximum allowable value of 850°F. Since the reaction rate is not significantly affected by the temperature above 600°F, an exact amount of cold quench that will bring down the gas temperature to 600°F should be introduced.

The heat balance across the reactor can be written as

$$T^N \sum_{i=1}^{6} C_{P_i}^N F_i^N = (1 - \lambda_1')T^F \sum_{i=1}^{6} C_{P_i}^F F_i^O + \lambda_1' T^{(1)} \sum_{i=1}^{6} C_{P_i}^{(1)} F_i^O + Q_c \qquad \text{(VII-59)}$$

where

λ_1' is the fraction of the feed gas passing through the preheater (-).
T^N is the temperature of gas at the exit of the reactor (850°F).
$T^{(1)}$ is the temperature of gas leaving the preheater (°F).
F_i^O is the molar flow rate of i-th component in the feed gas (lb.mole/hr.).
F_i^N is the molar flow rate of i-th component in the product gas (lb.mole/hr.).
$C_{P_i}^N$, $C_{P_i}^{(1)}$ and $C_{P_i}^F$ are the heat capacity of i-th component at T^N, $T^{(1)}$ and T^F, respectively (B.t.u./lb.mole°F).
Q_c is the amount of heat generated per unit time and can be calculated from Equation (VII-58)
T^F is feed gas temperature (100°F).

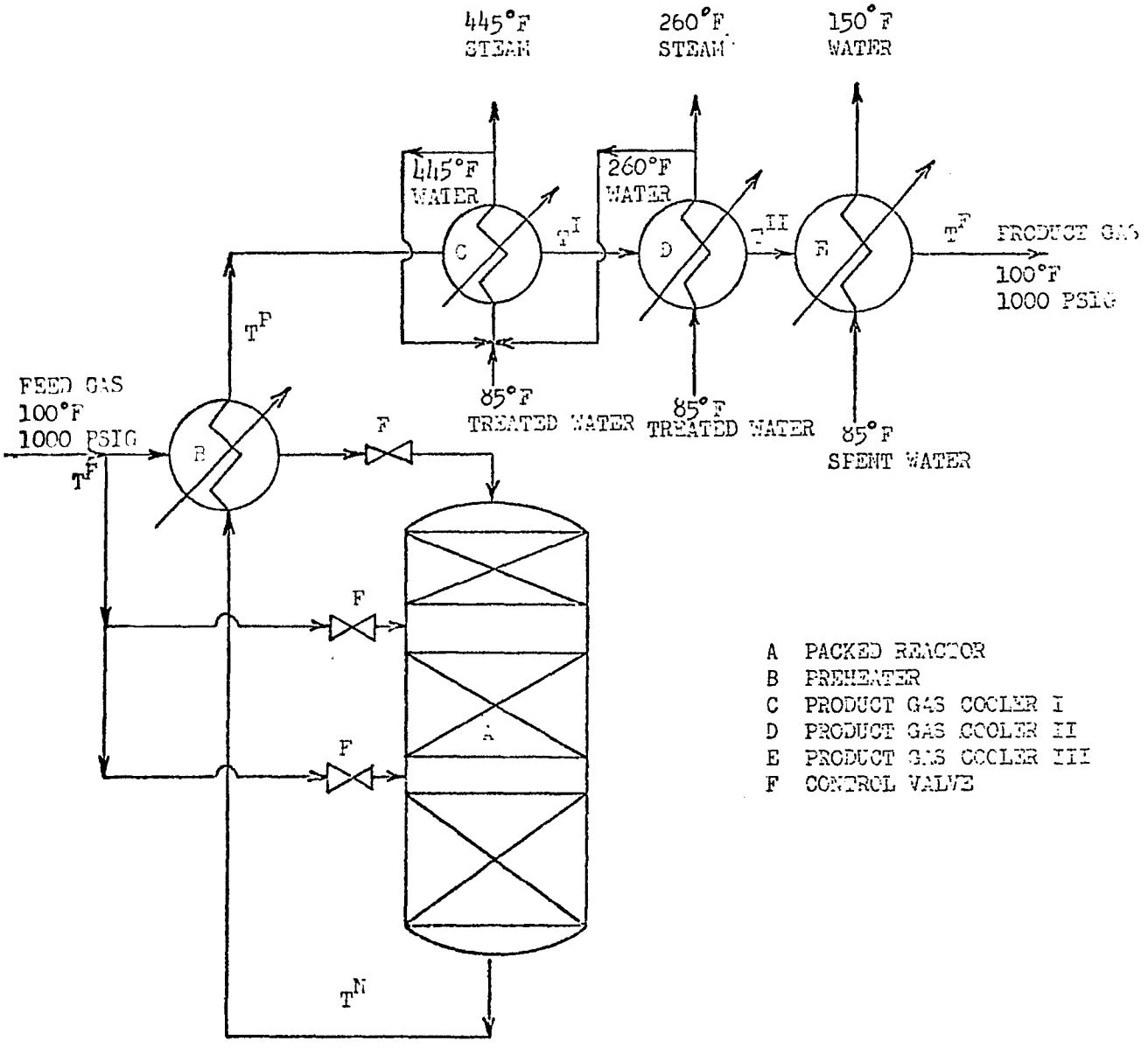

FIGURE VII-18 FLOW DIAGRAM IN INTERMEDIATE CO CASE FOR COLD QUENCH SYSTEM.

If $T^{(1)}$ is known, λ_i' is calculated from Equation (VII-52). The concentration of each gaseous component and temperature profiles can then be calculated by the same method described in the heat extraction system. The calculation is continued until the temperature in the reactor reaches 850°F.

In the cold quench system, the reactor is subdivided into a number of sections which are separated by the cold quench point. At each quenching point, both the flow rate of the cold quenching gas required and the gas composition after the quenching can be calculated from the flow rate and the temperature of the gas before quenching. Therefore knowing the inlet temperature, $T^{(1)}$, the concentrations of each component and the temperature distribution in the reactor can be calculated.

The total equipment cost for the intermediate CO case is obtained by the summation of the individual equipment cost of preheater, product gas cooler, catalyst, reactor and tray, control valves and thermal insulation. These costs are calculated from the design conditions of the reactor and the heat exchangers together with the cost equations described in Chapter II.

In obtaining the reactor and tray cost, the distance between the two adjacent sections of catalyst bed allowed for the quenching gas to mix with the hot gas, is taken to be 0.5 feet.

The decision variables studied in the optimization of this system for the intermediate CO case are the gas temperature at the reactor inlet, $T^{(1)}$, and the reactor diameter, D. The optimization technique used is the same as that for the high CO case in the cold quench system and the flow diagram is shown in Appendix B.5.

ii High CO Case

Since a large amount of heat is released in this case, a single reactor cannot accommodate the necessary conversion. Two different arrangements as shown in Figure VII-19 are considered. In System I, a portion of the fresh feed gas is preheated and enters the top of the first reactor. The remainders of the feed are introduced at intervals along the reactor in order to cool the reactant gas.

When the gas temperature in the first reactor reaches 850°F after the final quenching, the reactant gas leaves the first reactor and is cooled by the preheater and the intermediate cooler I.

A portion of the reactant gas then enters the top of the second reactor. The remainder of the reactant gas is cooled by the intermediate cooler II and is fed at intervals along the second reactor to cool the reactant gas. After leaving the second reactor, the product gas is cooled in the product gas coolers I, II and III to 100°F. 400 psia steam is recovered from the intermediate cooler I and the product gas cooler I, and 35 psia steam is recovered by the intermediate cooler II and the product gas cooler II.

In System II, the arrangement for the first reactor is the same as in System I. When the gas temperature in the first reactor reaches 850°F after the last quenching, the reactant gas is introduced to the intermediate cooler I and is cooled to $T^{(2)}$ and fed to the second reactor. When the temperature in the second reactor reaches 850°F, the reactnat gas leaves the second reactor and is cooled by the intermediate cooler II to $T^{(3)}$ and thereafter enters the third reactor.

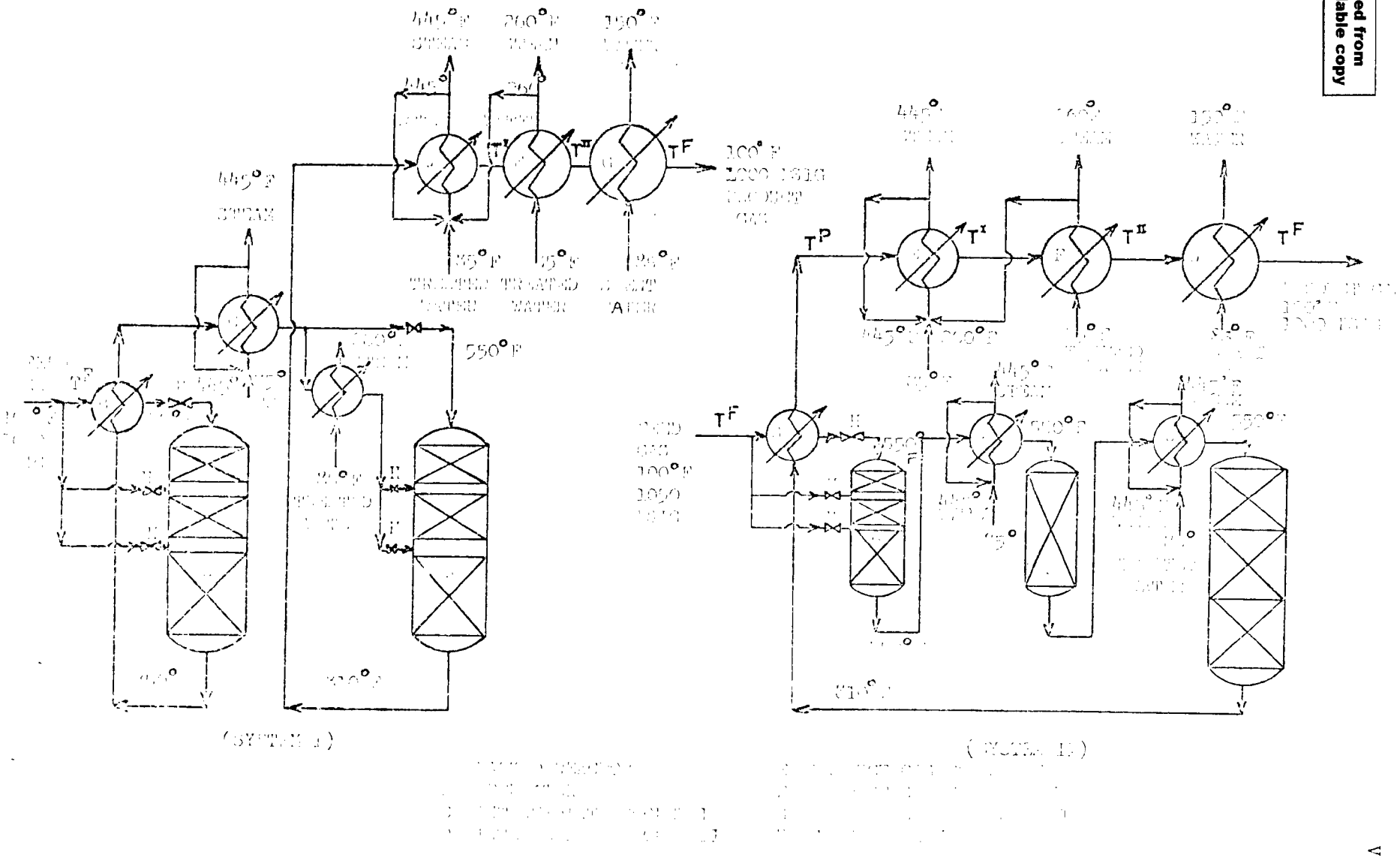

FIGURE VII-19 FLOW DIAGRAM IN HIGH CO CASE FOR COLD QUENCH SYSTEM.

As the product gas leaves the third reactor, it is cooled by the feed gas preheater and subsequently by the product gas coolers I, II and III to 100°F. Again 400 psia steam is recovered from the intermediate coolers I and II and the product gas cooler I, while 35 psia steam is recovered from the product gas cooler II.

A rough calculation shows that the total heat exchanger cost for System II is smaller than that for System I and the steam benefit for System II is larger than that for System I. It also shows that the catalyst weight for System II is smaller than that for System I because no quenching for the second and the third reactor is required. Therefore, System II is selected for the optimization study. The calculation procedure for the optimization of System II is as follows:

The heat balance across the third reactor can be written as

$$T^E \sum_{i=1}^{6} C_{P_i}^E F_i^E - T^{(3)} \sum_{i=1}^{6} C_{P_i}^{(3)} F_i^{(3)} = \Delta H\, F^0 (y^N - y^{(3)}) \qquad \text{(VII-60)}$$

where

T^E is the exit temperature of the third reactor (°F).
$T^{(3)}$ is the inlet temperature of the third reactor(°F).
$y^{(3)}$ is the conversion of CO to CH_4 at the inlet of the third reactor (-).
F_i^E and $F_i^{(3)}$ are the molar flow rate of i-th component at the inlet of the third reactor and the exit of the reactor respectively (lb.mole/hr.).
$C_{P_i}^E$ and $C_{P_i}^{(3)}$ are the molar heat capacity of the i-th component at the temperatures T^E and $T^{(3)}$, respectively.(B.t.u./lb.mole°F)

If the temperature, $T^{(3)}$, is known, the conversion, $y^{(3)}$, is calculated from Equation (VII-60)

The heat balance across the second reactor is

$$T^N \sum_{i=1}^{6} C_{P_i}^N F_i^{(3)} - T^{(2)} \sum_{i} C_{P_i}^{(2)} F_i^{(2)} = \Delta H\, F^0 (y^{(3)} - y^{(2)}) \qquad \text{(VII-61)}$$

where

$T^{(2)}$ is the inlet temperature of the second reactor (°F).
$y^{(2)}$ is the conversion of CO to CH_4 at the inlet of the reactor (—).
$F_i^{(2)}$ is the molar flow rate of i-th component at the inlet of the second reactor (lb.-mole/hr.).
$C_{P_i}^{(2)}$ are the molar heat capacity of the i-th component at the temperature T^3.(B.t.u./lb.mole hr.)

If the inlet temperature $T^{(2)}$ is known, the conversion $y^{(2)}$ is calculated from Equation (VII-61).

The heat balance across the first reactor can be written as,

$$T^N \sum_{i=1}^{6} C_{P_i}^N F_i^{(2)} = (1 - \lambda_1')T^F \sum_{i=1}^{6} C_{P_i}^F F_i^0 + \lambda_1' T^{(1)} \sum_{i=1}^{6} C_{P_i}^{(1)} F_1^0 + \Delta H \cdot F^0 \cdot y^{(2)}$$

If the inlet temperature of the first reactor $T^{(1)}$ is given, the fraction of feed gas required for the first quenching, λ_1', is calculated by Equation (VII-62). The catalyst weight and reactor sizes of three reactors are calculated from λ_1', $y^{(2)}$ and $y^{(3)}$.

The total equipment cost for the high CO case is obtained by the summation of the individual equipment cost of preheater, product gas, coolers I, II and III, intermediate coolers I and II, catalyst, reactors and trays, control valves, and heat insulation.

In the optimization of System II, the decision variables are the diameters and inlet temperatures for the three reactors. The inlet temperature for the first reactor should be as low as possible, because under this condition the preheater cost is the lowest and steam benefit for the product gas cooler I is the highest. The inlet temperatures of the second and the third reactors also should be be as low as possible because the steam benefits for the intermediate coolers I and II are the highest under this condition. Thus, the optimum inlet temperature for the three reactors must be selected at 550°F. Hence the optimization problem

for this case is reduced to that of searching the optimum reactor diameters. The flow diagram of computer calculation is shown in Appendix B.5.

5.2 Results and Discussion

i. Intermediate CO Case

Figure VII-20 shows the effect of the reactor diameter on the equipment costs for the intermediate CO case, indicating the optimum reactor diameter to be 6.2 feet. The gas temperature and concentration profiles and the reaction rate along the reactor under the optimum conditions are shown in Figure VII-21, to VII-23, respectively.

ii. High CO Case

Figures VII-24, VII-25, and VII-26 show the effect of the reactor diameters of the three reactors on the equipment costs for the high CO case, respectively. The optimum diameters of the first, second and third reactor are seen to be 6.2 feet, 6.6 feet, and 7.2 feet, respectively. The temperature profile, the reaction rate, and the concentration distribution in the reactor under the optimum conditions are shown in Figure VII-27, VII-28, and VII-29, respectively. Tables VII-7 and VII-8 show the operating conditions and the optimum equipment costs for the cold quench system under the two different feeds.

The quantity of the quenching gas and the locations of the quenching points are determined by assuming the reactant temperature before and after quenching to be at 850°F and 600°F, respectively. The reactor and catalyst costs calculated based on such temperature constraints are not necessarily the true optimum values, however.

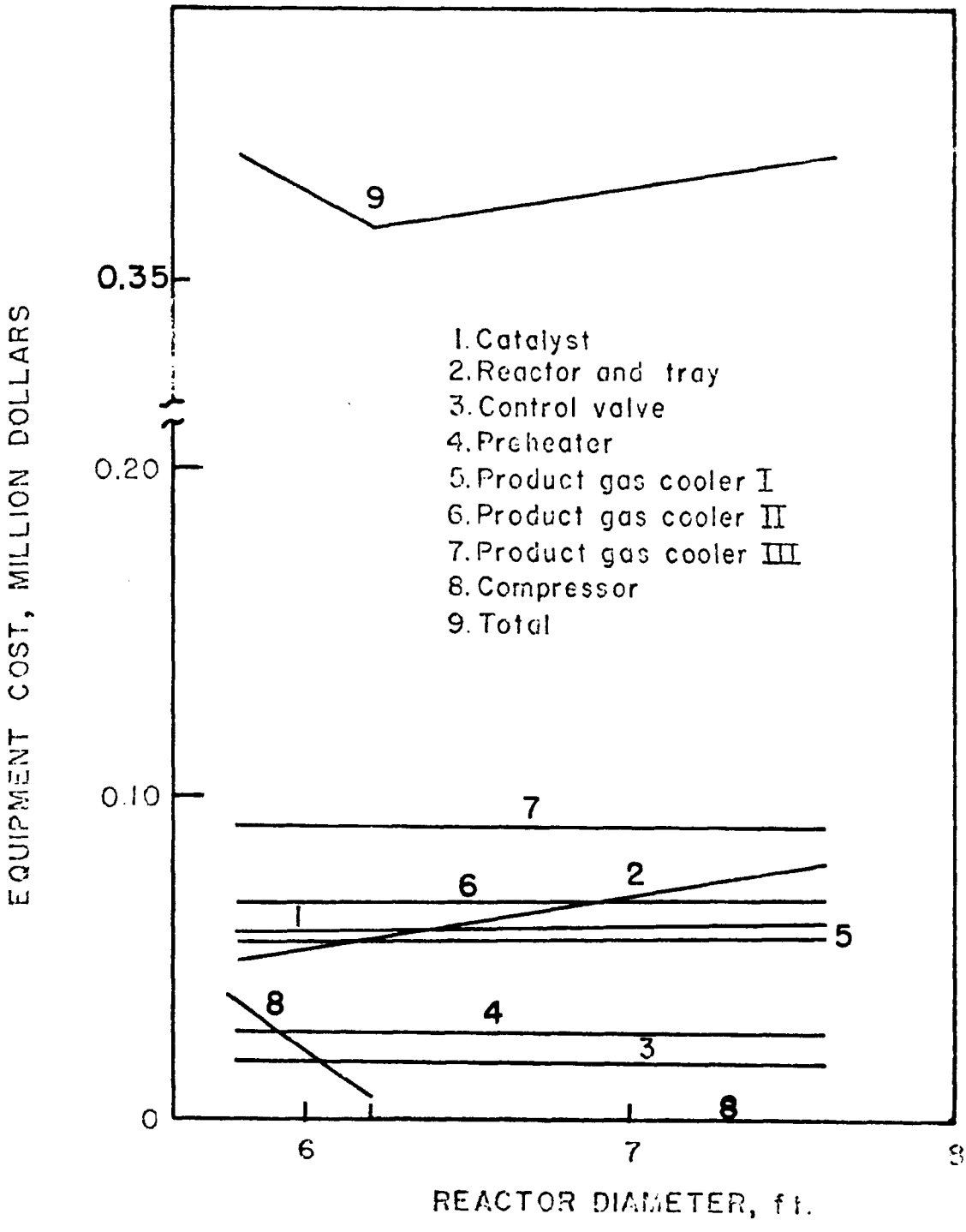

FIGURE VII-20 Equipment Cost Versus Reactor Diameter In Intermediate CO Case For Cold Quench System.

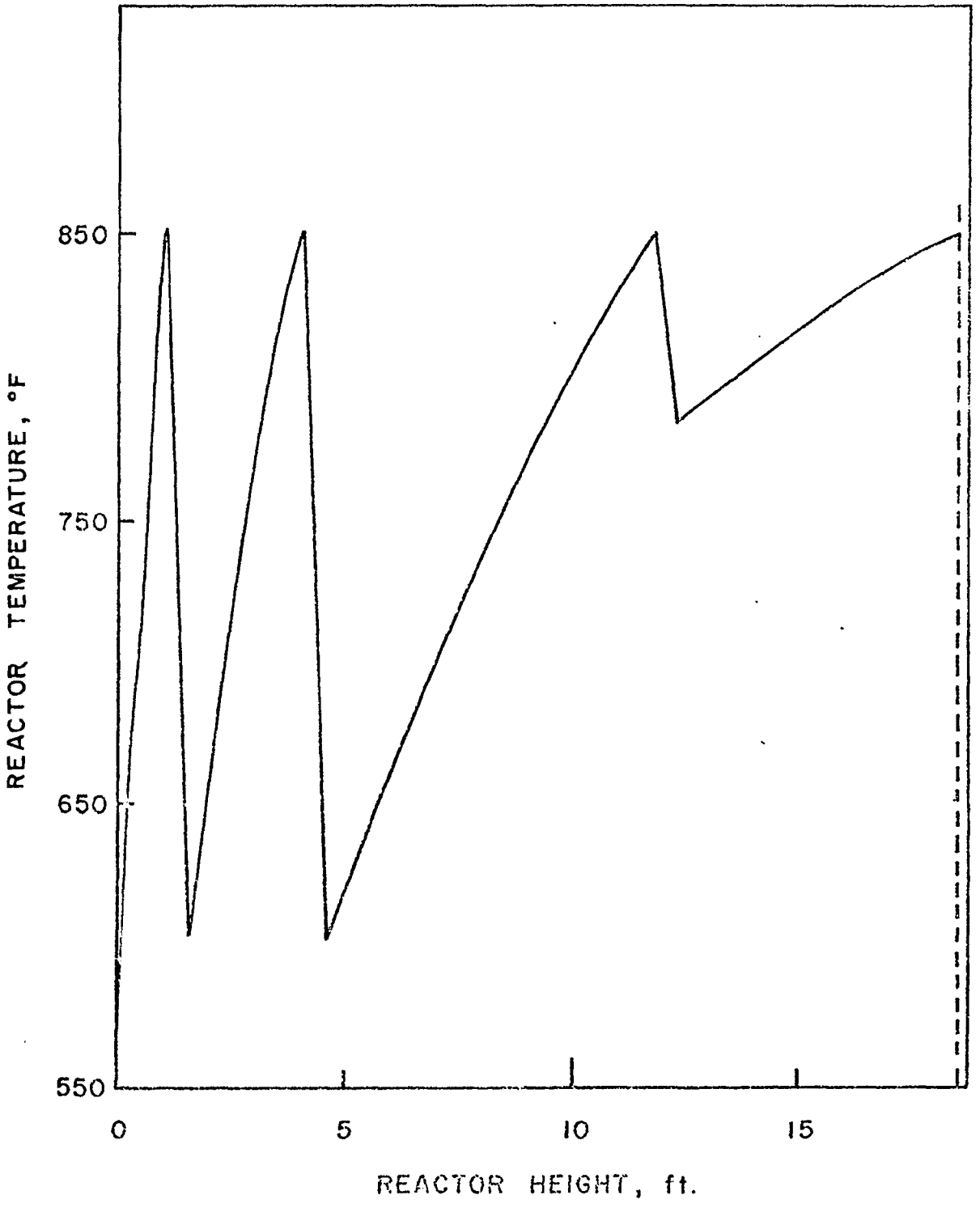

FIGURE VII-21 Temperature Profile Along The Reactor Height In Intermediate CO Case For Cold Quench System.

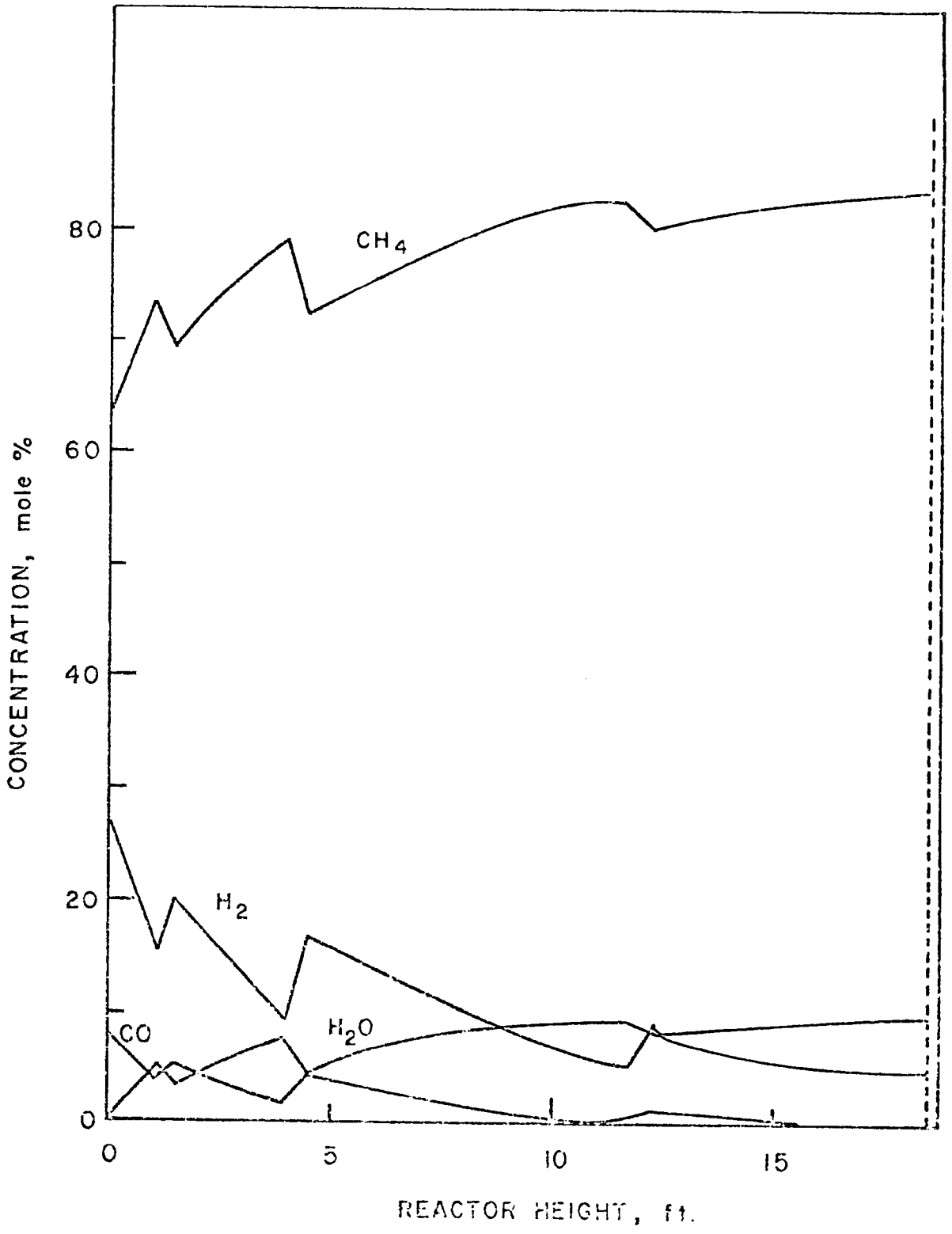

FIGURE VII-22 Concentration Profile Along The Reactor Height In Intermediate CO Case For Cold Quench System

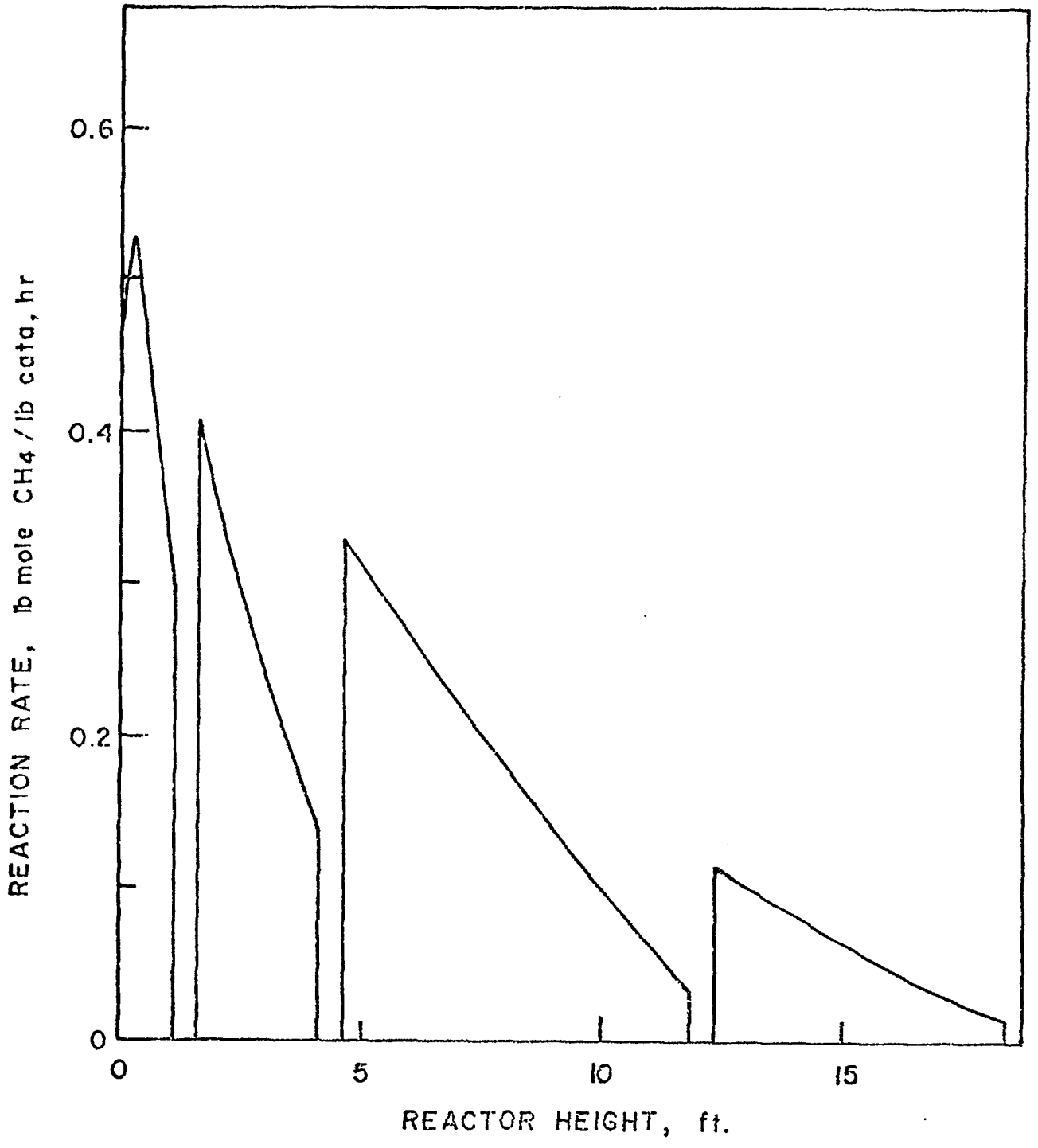

FIGURE VII-23 Reaction Rate Along The Reactor Height In Intermediate CO Case For Cold Quench System.

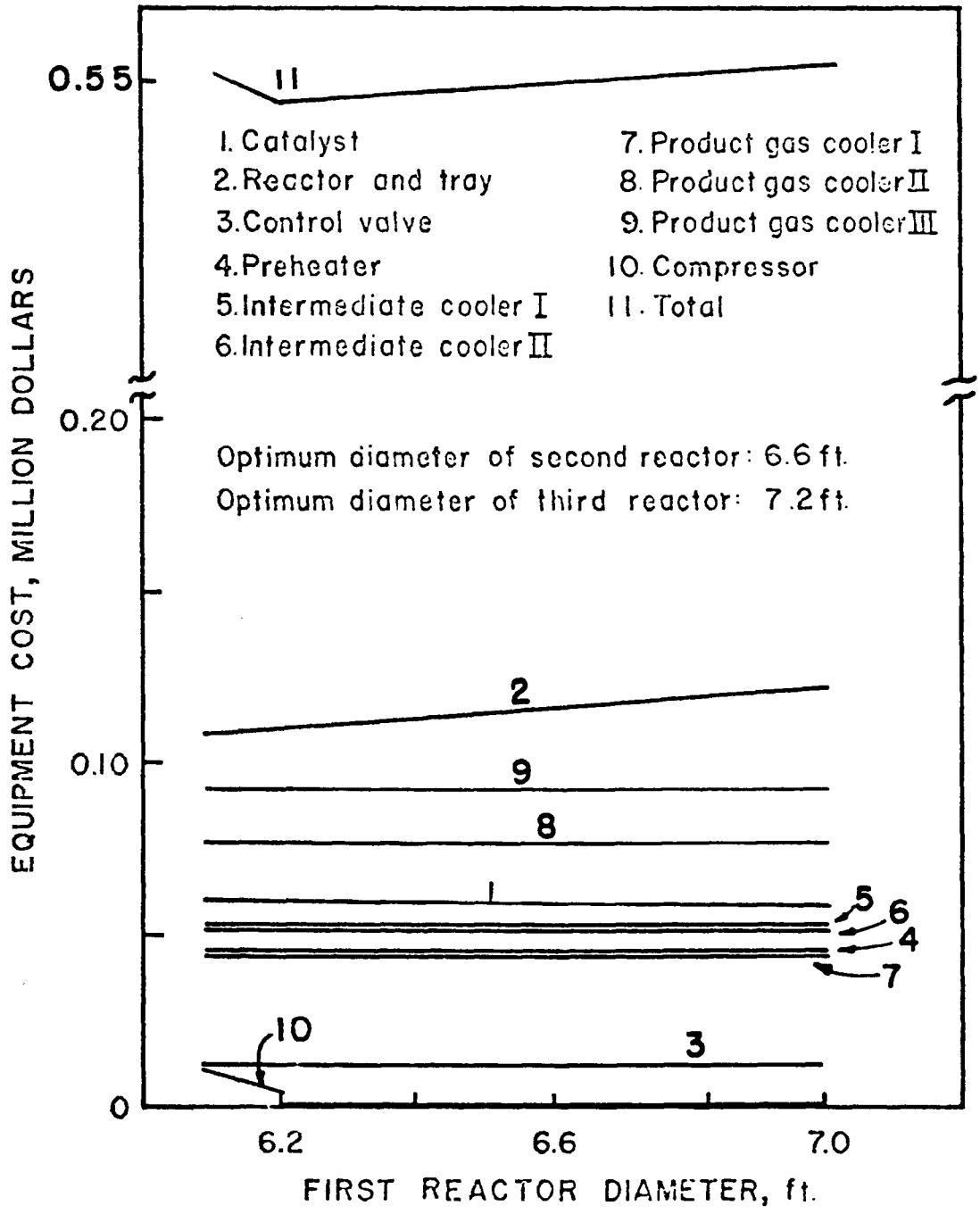

FIGURE VII-24 Equipment Cost Versus First Reactor Diameter In High CO Case For Cold Quench System.

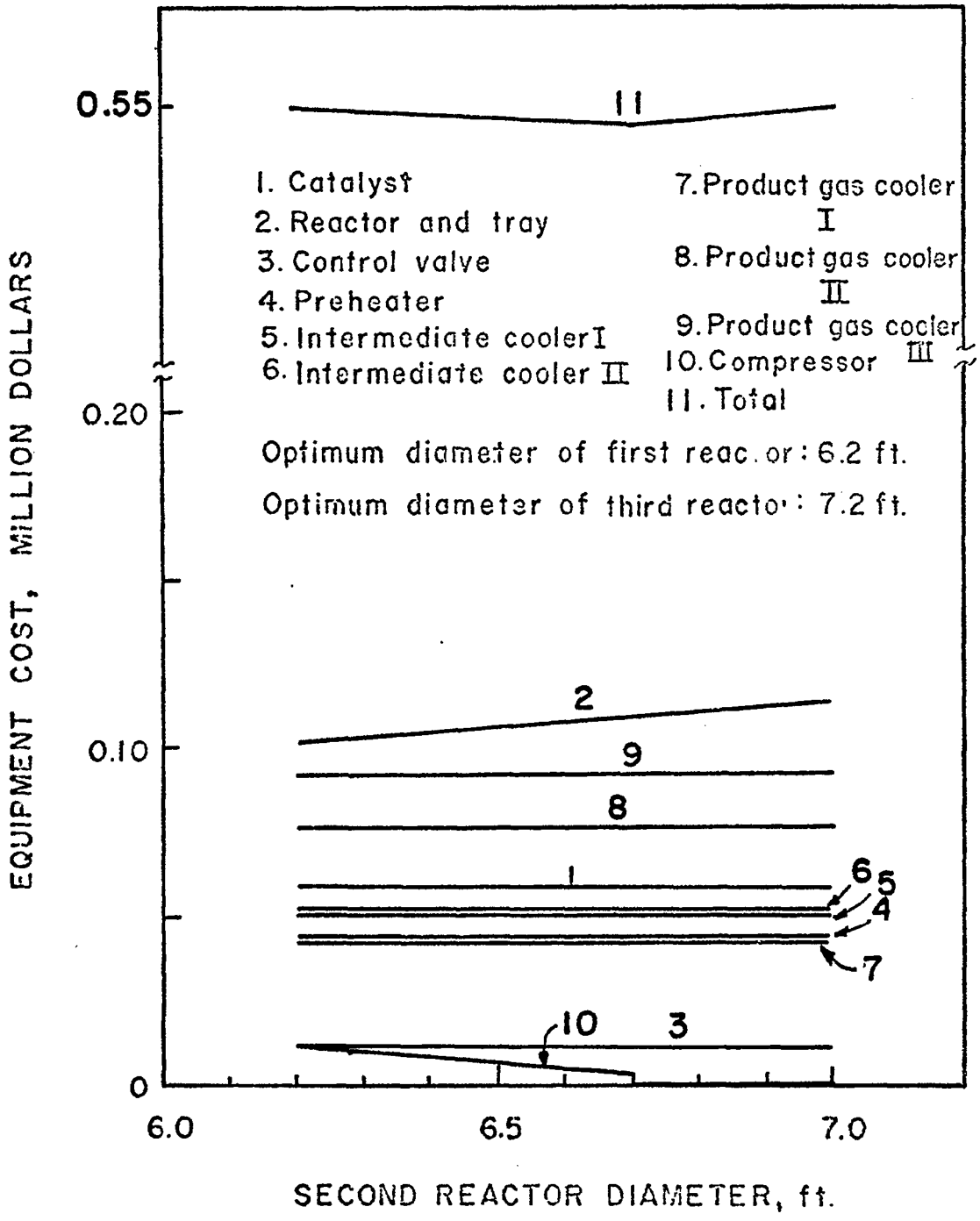

FIGURE VII-25 Equipment Cost Versus Second Reactor Diameter In High CO Case For Cold Quench System.

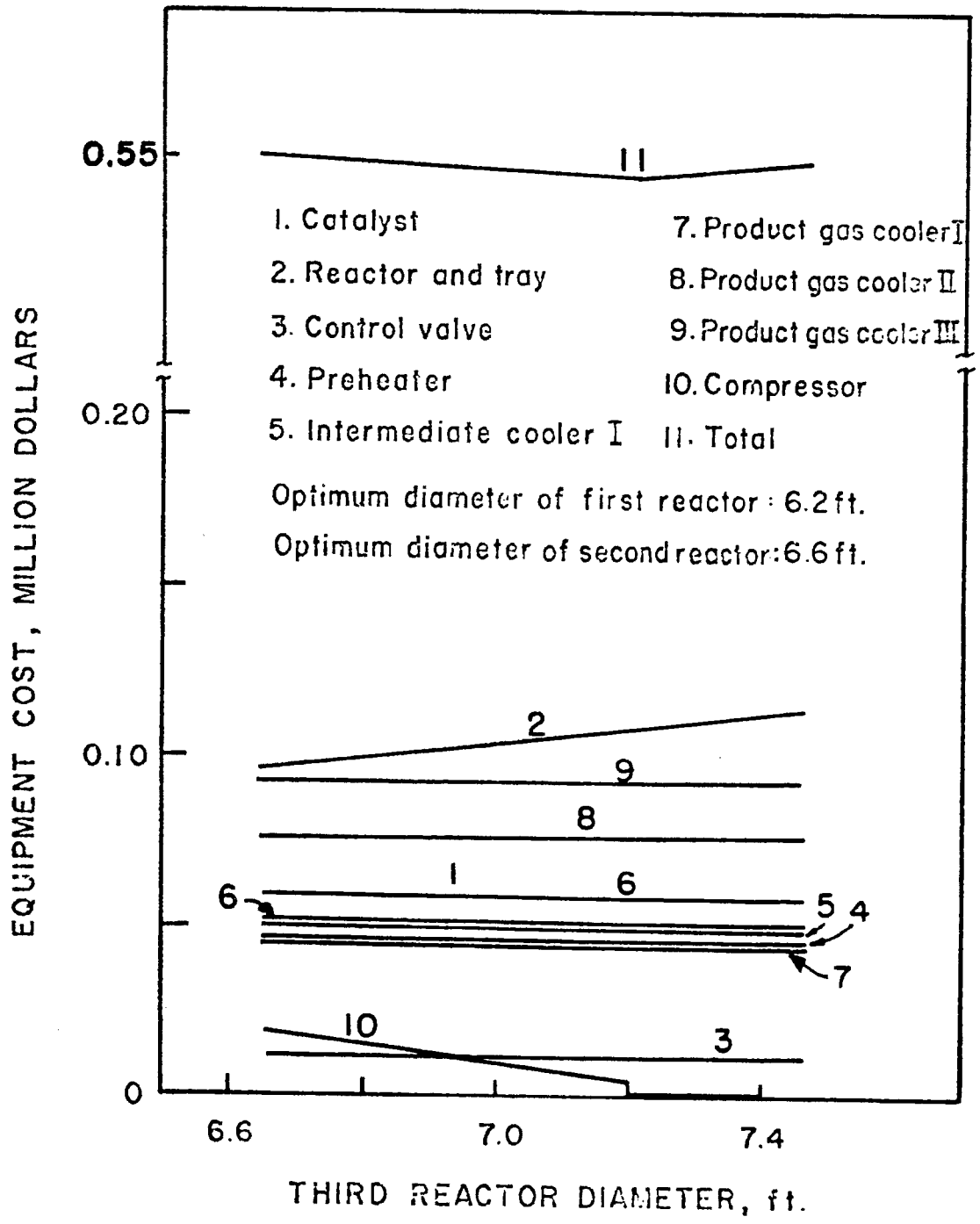

FIGURE VII-26 Equipment Cost Versus Third Reactor Diameter In High CO Case For Cold Quench System.

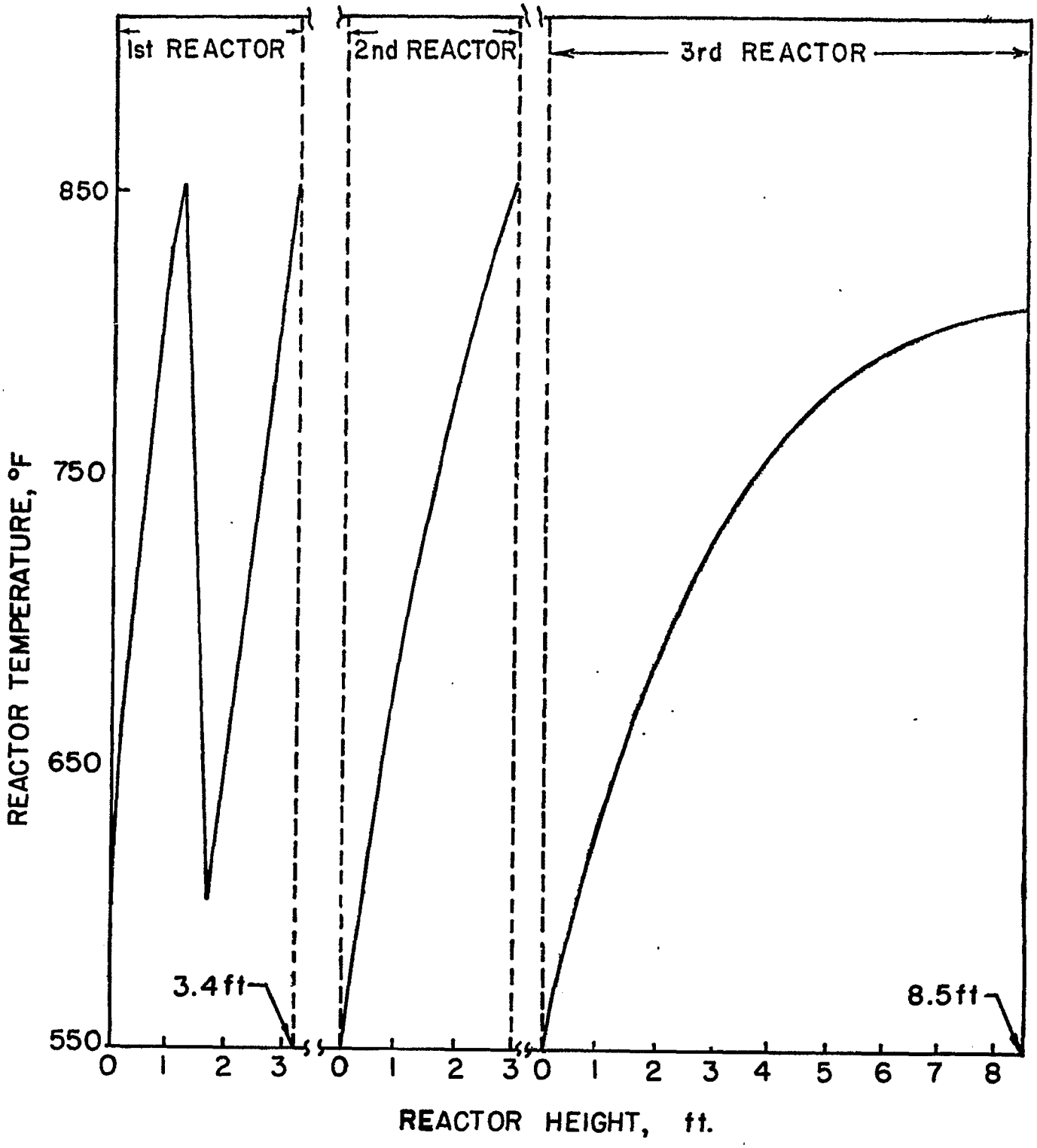

FIGURE VII-27 Temperature Profile Along The Reactor Height In High CO Case For Cold Quench System

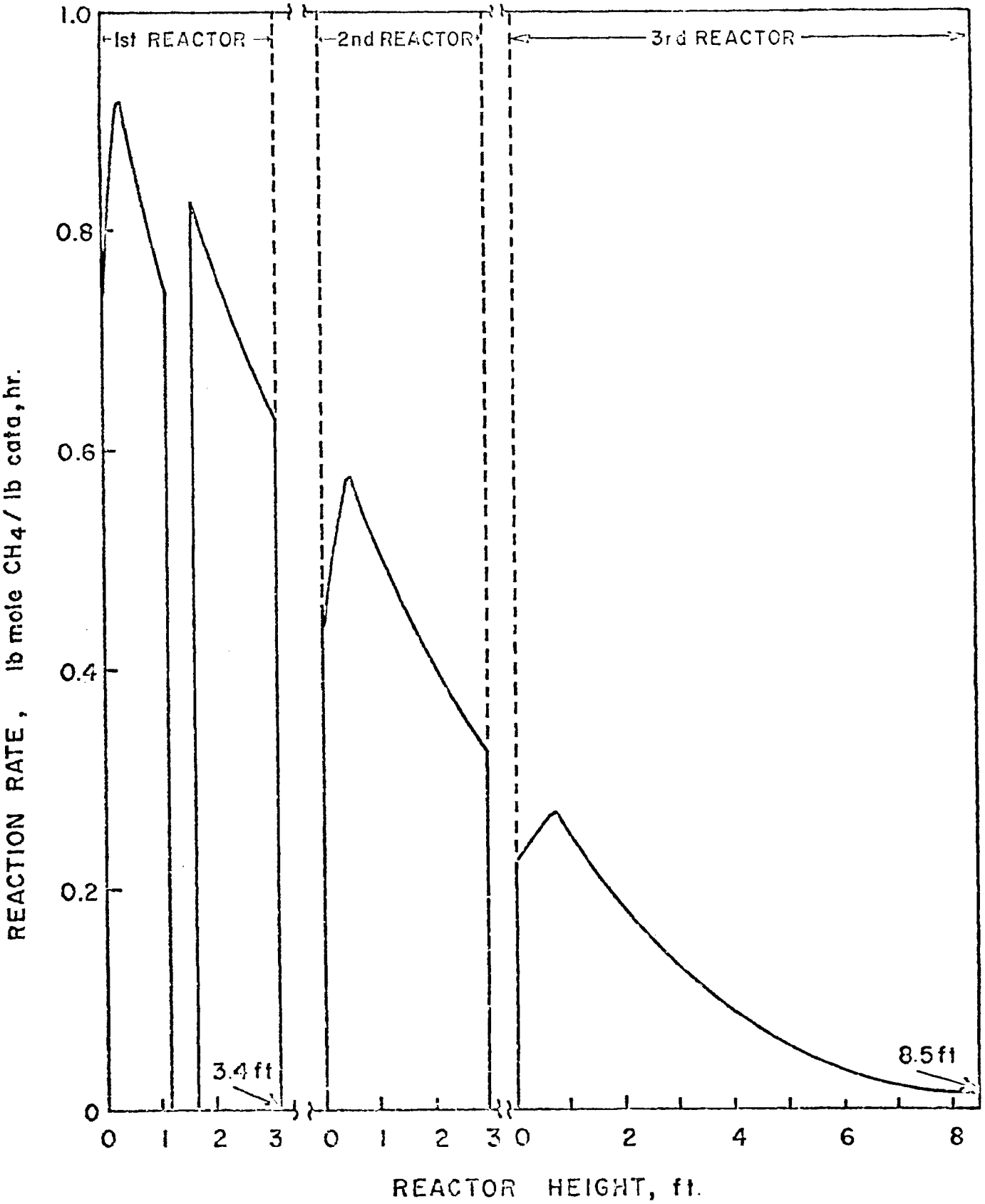

FIGURE VII-28 Reaction Rate Along The Reactor Height in High CO Case For Cold Quench System.

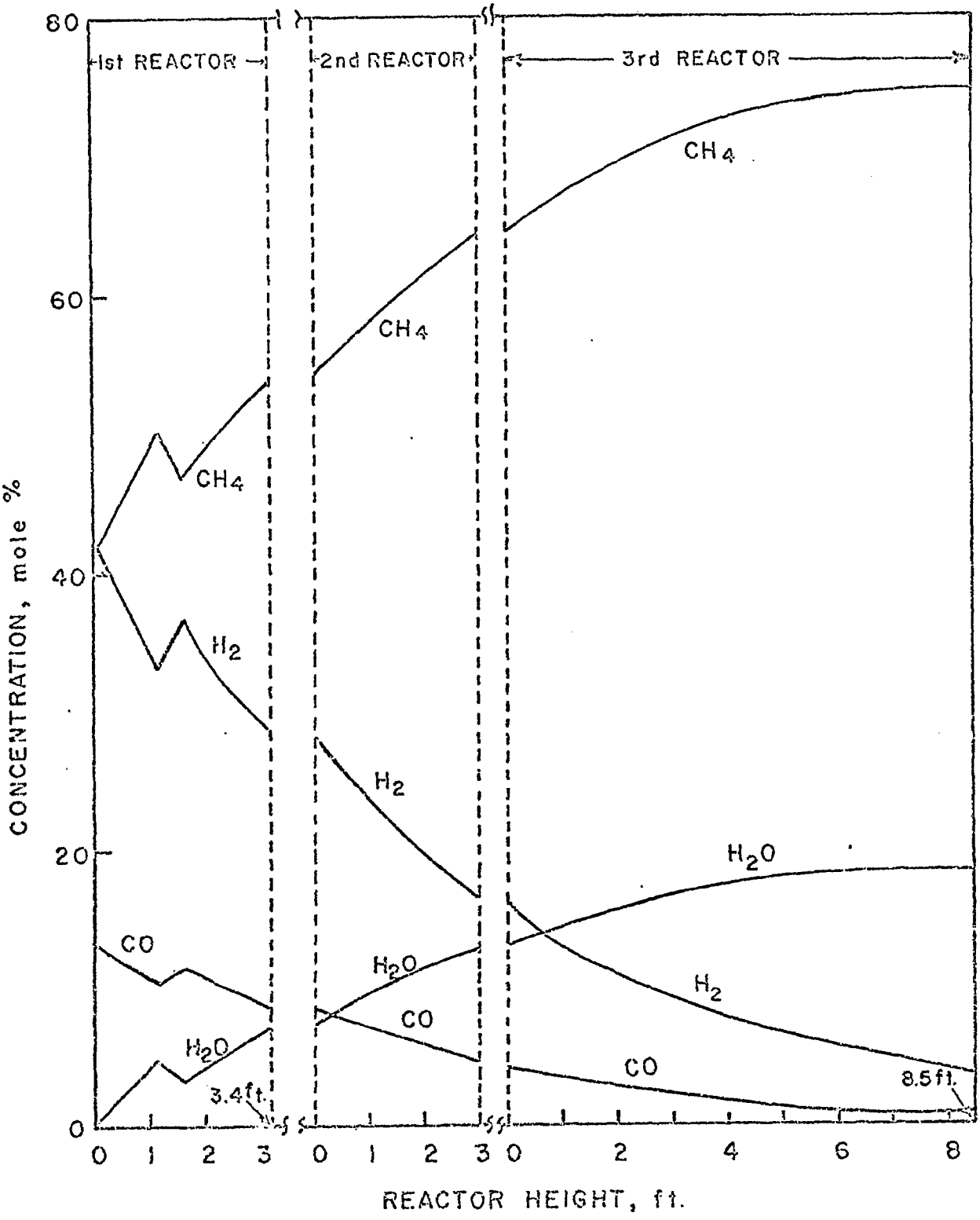

FIGURE VII-29 Concentration Profile Along The Reactor Height In High CO Case For Cold Quench System.

TABLE VII-7 OPTIMUM OPERATING CONDITIONS
IN TWO DIFFERENT FEEDS
FOR COLD QUENCH SYSTEM

	Intermediate CO	High CO
Inlet temperature, °F	100	100
Outlet temperature, °F	100	100
Inlet pressure, psig	1,050	1,050
Outlet pressure, psig	1,000	1,000
First reactor diameter, ft.	6.2	6.2
First reactor height, ft.	18.75	3.4
Second reactor diameter, ft.	--	6.6
Second reactor height, ft.	--	3
Third reactor diameter, ft.	--	7.2
Third reactor height, ft.	--	8.5
Space velocity*, $hr.^{-1}$	6,910	8,030
Catalyst weight, lbs.	22,930	23,740
Heat transfer surface area of preheater, $ft.^2$	2,175	6,090
Heat transfer surface area of intermediate cooler I, $ft.^2$	--	7,680
Heat transfer surface area of intermediate cooler II, $ft.^2$	--	7,530
Heat transfer surface area of product gas cooler I, $ft.^2$	8,480	6,075
Heat transfer surface area of product gas cooler II, $ft.^2$	11,930	15,670
Heat transfer surface area of product gas cooler III, $ft.^2$	26,630	21,240
Flow rate of 400 psia steam in intermediate cooler I and II, lb./hr.	--	336,670

TABLE VII-7 (CONT.)

	Intermediate CO	High CO
Flow rate of treated water in intermediate cooler I and II, lb./hr.	--	336,670
Flow rate of 400 psia steam in heat exchangers, lb./hr.	108,100	22,000
Flow rate of 35 psia steam in heat exchangers, lb./hr.	101,000	138,130
Flow rate of treated water in heat exchangers, lb./hr.	202,000	276,280
Flow rate of spent water in heat exchangers, lb./hr.	1,249,500	1,319,470

*Based on inlet condition.

According to Tables VII-7 and VII-8, the catalyst cost for the cold quench system is no more than 1.3 times that for the heat extraction system. Therefore the cost of reactor and catalyst estimated can be considered to be very close to the true optimum value.

TABLE VII-8 OPTIMUM EQUIPMENT COSTS
IN TWO DIFFERENT FEEDS
FOR COLD QUENCH SYSTEM

	Intermediate CO	High CO
Catalyst, $	57,300	59,350
Reactor and tray, $	56,850	107,800
Control valve, $	18,000	14,000
Preheater, $	25,500	45,480
Intermediate cooler I, $	--	51,800
Intermediate cooler II, $	--	51,250
Product gas cooler I, $	54,800	45,400
Product gas cooler II, $	66,350	77,400
Product gas cooler III, $	88,950	91,800
Total equipment, $	367,750	544,280

6. THE RECYCLE SYSTEM

6.1 Process Analysis and Calculation Procedure

In the recycle system, total heat generated in the reactor is absorbed by the portion of the product gas being recycled to become the sensible heat. Figure VII-30 shows the flow diagram of the recycle system.

From the heat balance across the reactor, the following equations are obtained.

$$T^N \sum_i^6 C_{P_i}^N F_i^N - T^{(1)} \sum_i^6 C_{P_i}^{(1)} F_i^{(1)} = Q_c \qquad \text{(VII-63)}$$

and

$$F_i^{(1)} = F_i^0 + F_i^r \qquad \text{(VII-64)}$$

where

F_i^0 is the molar flow rate of i-th component in the feed gas (lb.mole/hr.).
F_i^r is the molar flow rate of i-th component in the recycle gas (lb.mole/hr.).

If the total amount of heat generated in the reactor, Q_c, is known, the recycle flow rate $\sum_i^6 F_i^r$ is calculated from Equations (VII-63) and (VII-64). The inlet flow rate and the compositions are then calculated. The reactor size and the catalyst weight for this system are determined from the performance equations.

When the enthalpy of the inlet gas $T^{(1)} \sum_i^6 C_{P_i}^{(1)} F^{(1)}$ is larger than both the enthalpy of the feed gas, $T^F \sum_i^6 C_{P_i}^F F_i^0$ and that of the recycle gas, $T^N \sum_i C_{P_i}^N F_i^r$, it is necessary to preheat the feed gas to $T^{(PF)}$. In this case, System I as shown in Figure VII-30 is used. The temperature $T^{(PF)}$ to which the gas must be preheated is calculated

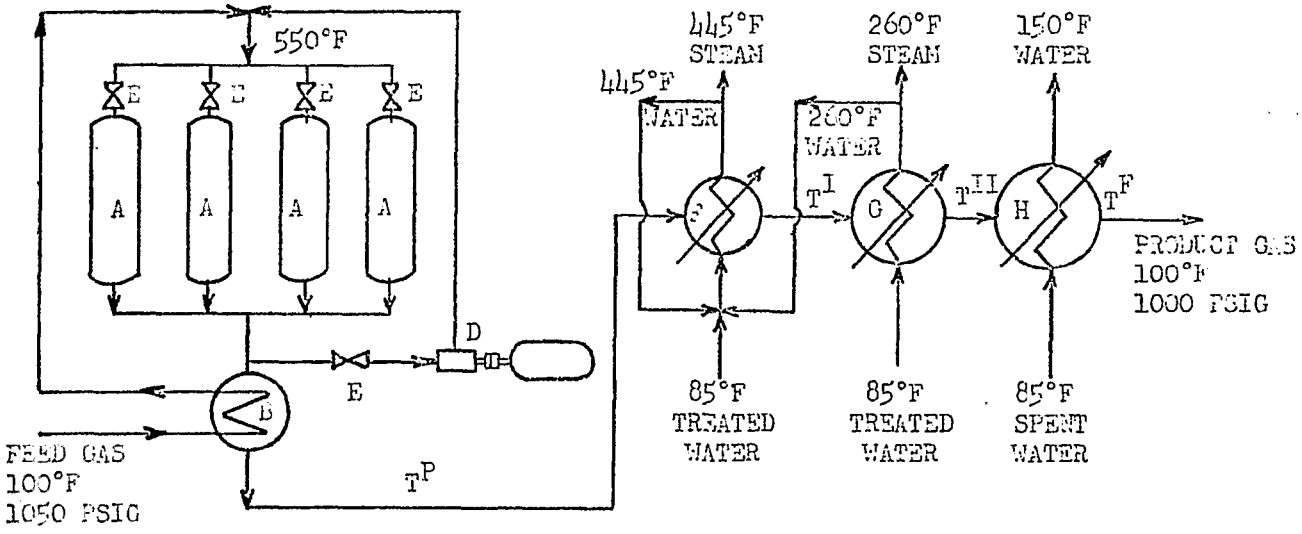

(SYSTEM I)

A REACTORS
B PREHEATER
C RECYCLE GAS COOLER
D COMPRESSOR
E CONTROL VALVE
F PRODUCT GAS COOLER I
G PRODUCT GAS COOLER II
H PRODUCT GAS COOLER III

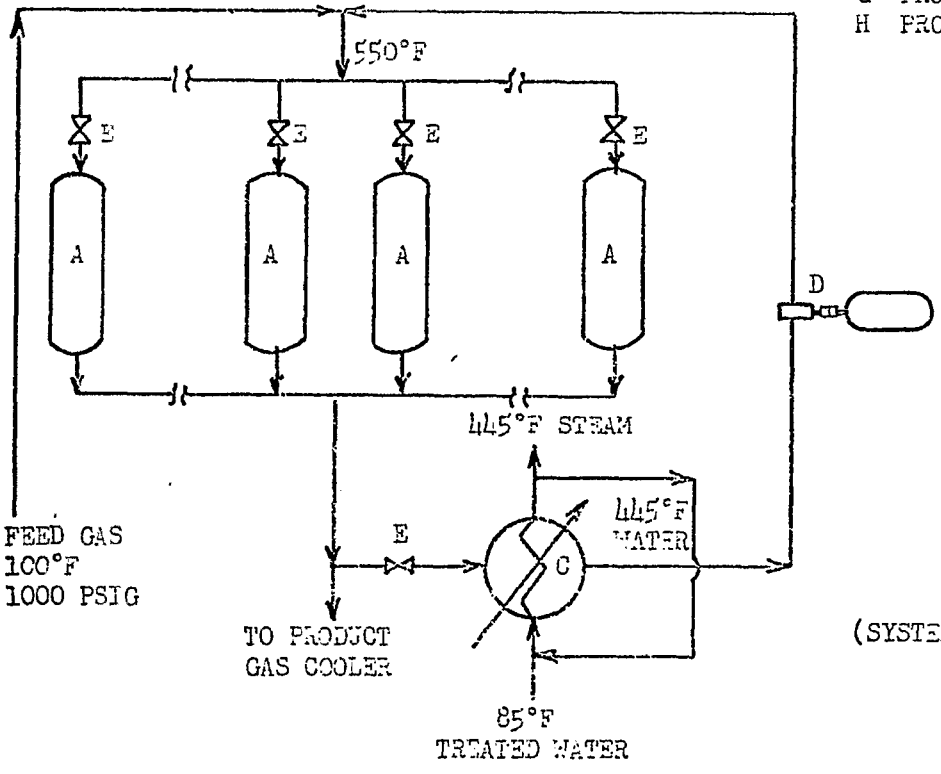

(SYSTEM II)

FIGURE VII-30 Flow Diagram In Both Intermediate And High CO Cases For Recycle System.

from the heat balance around the point where the feed mixes with the recycle gas, according to the following equation:

$$T^{(PF)} \sum_{i}^{6} C_{P_i}^{(PF)} F_i^0 + T^N \sum_{i}^{6} C_{P_i}^N F_1^r = T^{(1)} \sum_{i}^{6} C_{P_i}^{(1)} F_i^{(1)} \qquad \text{(VII-65)}$$

where

$C_{P_i}^{(PF)}$ is the molar heat capacity of i-th component at the temperature $T^{(PF)}$ (B.t.u./lb.mole°F).

The size of the preheater required is calculated from $T^{(PF)}$ by the same procedure described in Section 3.

When the enthalpy of the inlet gas is smaller than that of the feed gas and the recycle gas, it is necessary to cool the recycle gas to $T^{(Nr)}$. The temperature $T^{(Nr)}$ of the gas leaving the recycle gas cooler is calculated from the heat balance around the mixing point M as

$$T^F \sum_{i}^{6} C_{P_i}^F F_i^0 + T^{(Nr)} \Sigma C_{P_i}^{(Nr)} F_i^r = T^{(1)} \sum_{i}^{6} C_{P_i}^{(1)} F_i^{(1)} \qquad \text{(VII-66)}$$

where

$C_{P_i}^{(Nr)}$ is the molar heat capacity of the i-th component at the temperature $T^{(Nr)}$.

The size of the recycle gas cooler producing 400 psia steam is calculated from $T^{(Nr)}$ by the same procedure used in the intermediate cooler. The size of the recycle pump is calculated based on the pressure drop in the reactor and the flow rate of the recycle gas.

In the optimization of this process, the decision variables considered are the reactor diameter, the inlet and outlet temperatures of the gas $T^{(1)}$ and T^N, and the number of reactors in parallel. In the recycle system the volumetric flow rate in the reactor and

consequently the reactor diameter is so large, especially for the high CO case, it is necessary to find the optimum number of reactors for this case. In the cost estimation of this process, as the number of reactors is increased, $8,000 per reactor is added as the costs of control valves and other instrumentation.

However, as the temperature difference between $T^{(1)}$ and T^{N} increases, the recycle gas rate is decreased, reducing the reactor cost, catalyst cost and recycle pump cost. Therefore, the optimum gas temperature at the reactor inlet is 550°F for each CO case, and the optimum gas temperatures at the outlet of the reactor are 850°F for the intermediate CO case and 810°F for the high CO case

Consequently, the remaining decision variables are the number of reactors in parallel and the reactor diameters, which are searched in the optimization study of this system.

6.2 Results

Figure VII-31 and VII-32 show the effect of the reactor diameter on the total equipment cost with the number of reactors as parameter for the intermediate CO case and the high CO case, respectively. From Figure VII-31, the optimum number of reactors in parallel is seen to be 4, and the optimum reactor diameter to be 5.8 ft. for the intermediate CO case. From Figure VII-32, the optimum number of reactors and the reactor diameter for the high CO case are 8 and 6.0 ft., respectively. Comparing Figure VII-31 with VII-20, a considerable effect of the number of reactors in parallel on the total equipment cost is noted for the cases where large diameter

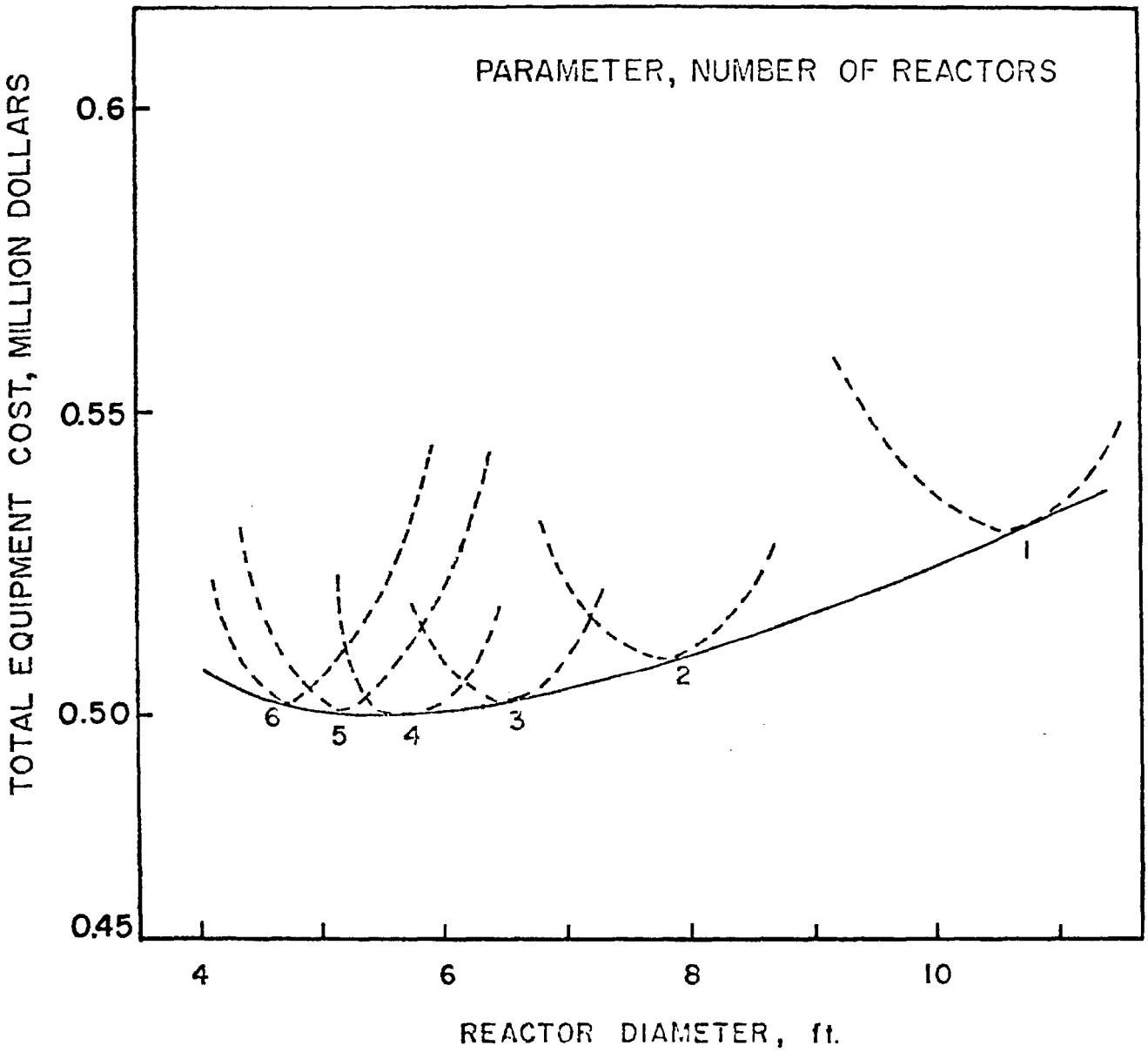

FIGURE VII-31 Total Equipment Cost Versus Reactor Diameter In Intermediate CO Case For Recycle System.

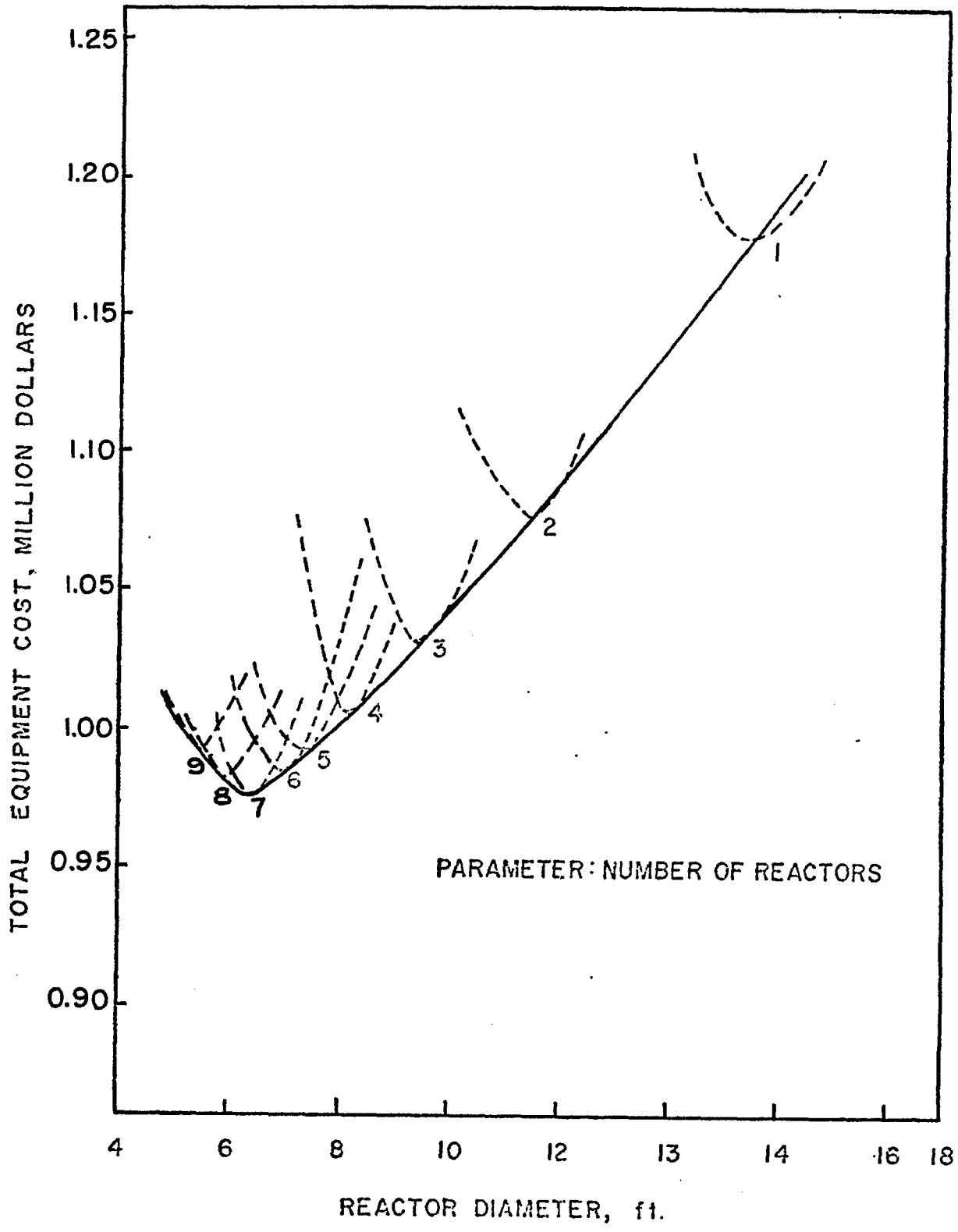

FIGURE VII-32 Total Equipment Cost Versus Reactor Diameter In High CO Case For Recycle System.

reactors are used. The differences between the optimum equipment cost for one reactor and that with optimum number of reactors in parallel are $190,000 for the high CO case, but only $13,000 for the intermediate CO case. Table VII-9 and VII-10 list the optimum operating conditions and the optimum equipment costs for the recycle system.

From Table VII-10, the reactor and catalyst costs for this system are seen to be the most expensive among the three systems. In addition, the recycle pumps are also considerably expensive resulting in the highest total equipment cost among the three systems investigated.

TABLE VII-9 OPTIMUM OPERATING CONDITION
IN TWO DIFFERENT FEEDS
FOR RECYCLE SYSTEM

	Intermediate CO	High CO
Inlet temperature, °F	100	100
Outlet temperature, °F	100	100
Inlet pressure, psig	1,050	1,050
Outlet pressure, psig	1,000	1,000
Number of reactors	4	8
Reactor diameter	5.8	6.0
Reactor height, ft.	6.02	5.95
Catalyst weight, lbs.	28,030	58,730
Space velocity*, $hr.^{-1}$	5,640	3,240
Heat transfer surface area of preheater, $ft.^2$	1,593	--
Heat transfer surface area of recycle gas cooler I, $ft.^2$	--	6,140
Heat transfer surface area of product gas cooler I, $ft.^2$	8,500	10,150
Heat transfer surface area of product gas cooler II, $ft.^2$	11,775	15,630
Heat transfer surface area of product gas cooler III, $ft.^2$	19,900	21,195
Flow rate of treated water in heat exchangers, lb./hr.	320,000	317,930
Flow rate of spent water in heat exchangers, lb./hr.	1,236,170	1,316,140
Flow rate of 400 psia steam in heat exchangers, lb./hr.	108,330	178,330

TABLE VII-9 (CONT.)

	Intermediate CO	High CO
Flow rate of 35 psia steam in heat exchangers, lb./hr.	95,330	139,670
Recycle ratio	0.7796	2.911
Flow rate of treated water in recycle gas cooler, lb./hr.	--	147,860
Flow rate of 400 psia steam from recycle gas cooler, lb./hr.	--	147,860

*Based on inlet condition.

TABLE VII-10 OPTIMUM EQUIPMENT COSTS
IN TWO DIFFERENT FEEDS
FOR RECYCLE SYSTEM

	Intermediate CO	High CO
Catalyst, $	70,080	143,130
Reactor and tray, $	93,850	314,290
Valve and flow meter, $	48,000	72,000
Preheater, $	21,400	0
Recycle gas cooler, $	0	45,540
Product gas cooler I, $	54,900	60,620
Product gas cooler II, $	65,900	77,270
Product gas cooler III, $	88,500	91,670
Recycling compressor, $	56,150	169,190
Total equipment, $	498,780	973,610

7. DISCUSSION

7.1 Comparison of the Equipment Costs for the Three Different Feeds

i. Heat Exchanger Costs

It has been demonstrated that the major problem associated with the methanation processes is the heat removal from the reactor. Since the amount of heat generated in the reactor is directly related to the feed composition, an examination of how the feed gas composition affects the inlet gas temperature of an adiabatic reactor may be made based on the heat balance in a given reactor. Figure VII-33 shows the relation between the maximum CO concentration in the feed gas and the inlet feed gas temperature for an adiabatic reactor. If the concentration of CO in the feed gas is above the line, say the 850°F line, some devices for heat removal are necessary in order to keep the temperature of the reactor below 850°F. The intermediate CO case and the high CO case correspond to this situation. On the other hand, if the CO concentration is below the line, no provision for the heat removal is needed. The low CO case corresponds to this situation.

For heating and cooling of the process fluids, the preheaters, product gas coolers, intermediate coolers, recycle coolers and embedded fin tubes are used. The preheater cost for the heat extraction system is the most expensive among the three systems considered. This is because the entire feed gas must be heated to the required reactor inlet temperature. In the cold quench system, only a fraction of the feed gas is preheated, while in the recycle system, the preheater is not needed except for the intermediate CO case.

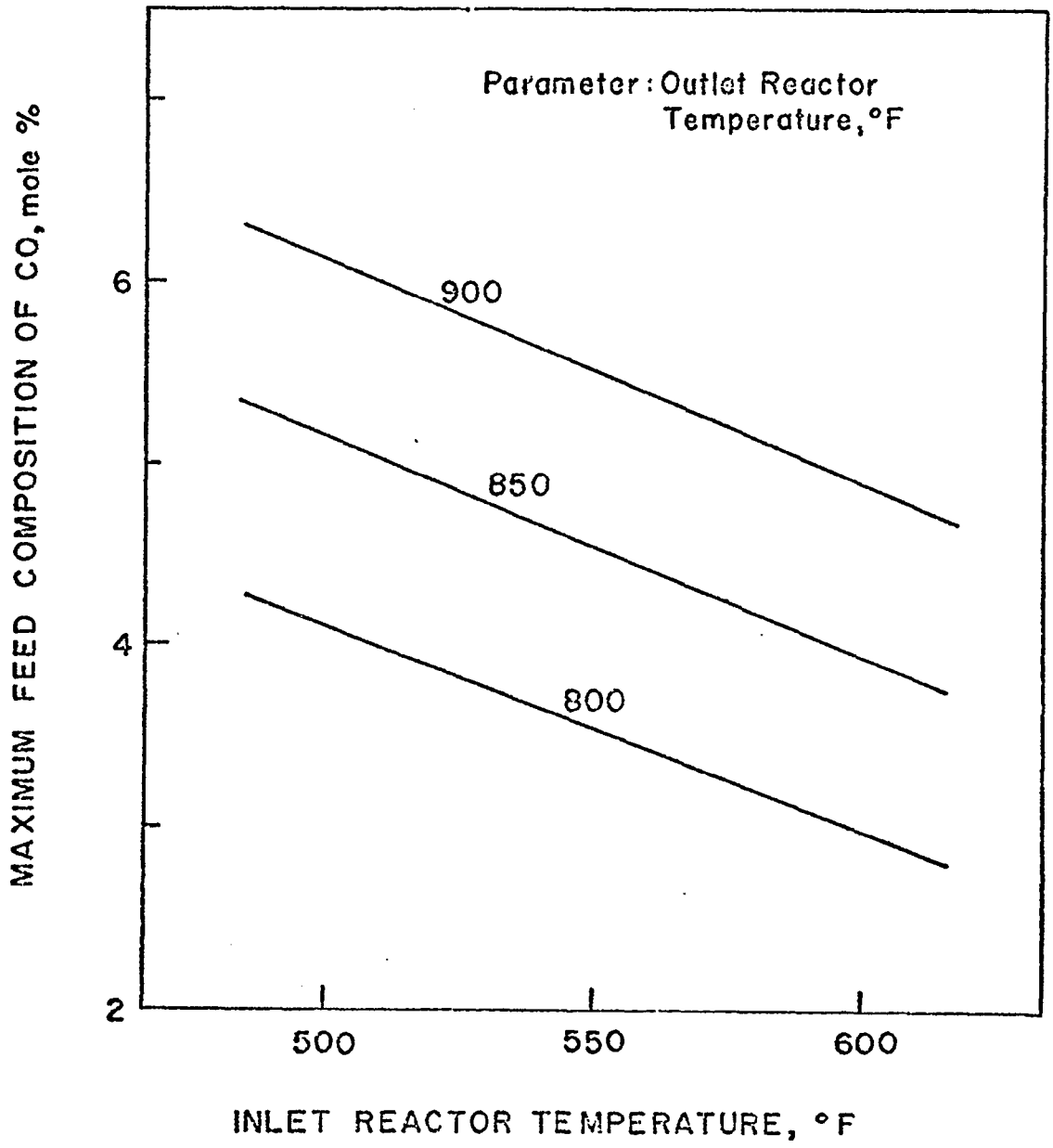

FIGURE VII-33 Maximum Feed Composition Of CO Versus Inlet Reactor Temperature For Different Outlet Reactor Temperatures.

It appears evident that the cost of the product gas cooler is the highest for the recycle system and is the lowest for the heat extraction system. For the cold quench system, the cost of the product gas cooler depends largely on the fraction of the feed gas introduced to the top of the reactor, λ_1', and is in general between that of the recycle system and the heat extraction system. As to the costs of fin tubes, intermediate coolers and recycle gas coolers, they are related to the amount of heat removed during the reaction and therefore are higher as the CO content of the feed gas is increased.

ii. Catalyst and Reactor Costs

It is readily seen that the catalyst cost for the heat extraction system is the cheapest and that for the recycle system is the most expensive among the three systems. The catalyst cost for the cold quench system ranks in the middle of the two, leaning closely to that of the heat extraction system. In contrast to the lowest catalyst cost for the heat extraction system, the reactor cost is higher than the cold quench system because a large portion of reactor volume is occupied by the embedded fin tubes. However, for the high CO case when three reactors are needed to accomplish the cold quenching, the reactor costs of the two systems become approximately the same.

The reactor cost for the recycle system is the highest because the catalyst volume required is the largest among the three systems.

In view of the high reactor and the catalyst costs as well as the high recycle gas compressor cost in the recycle system, this system is the least economical system.

Figure VII-34 shows the relation between the total equipment cost and the concentration of CO in the feed gas. From this figure, it may be concluded that the cold quench system is the most economical system among the three systems for the intermediate CO case and the high CO case.

7.2 Steam Benefit in Methanation Processes

In order to remove the excess heat generated in the reactor, a large amount of water is used which is converted into high pressure and low pressure steam. Fig. VII-35 shows the relation between the amount of steam produced per hour and the concentration of CO in the feed gas for the three different systems. Since the quantity of steam produced is roughly proportional to the amount of heat generated in the reactor, the two curves in Fig. VII-35 have the same trend with respect to the feed concentration of CO.

7.3 Effects of Temperature and Pressure of the Feed Gas on Total Equipment Cost

Although in this study the feed gas is assumed to be available at a temperature of 100°F and a pressure of 1065 psia, the optimum temperature and pressure are largely affected by the undecided choice of the primary gasification phases and to a lesser extent by the gas purification phase and the water-gas shift reaction phase which precedes the methanation phase. It is therefore necessary to study how the feed gas temperature and pressure will affect the equipment cost and what the optimum temperature and pressure should be as far as the methanation process is concerned.

Figure VII-36 shows the relation between the total equipment costs and the feed gas temperature for the low CO case in the adiabatic

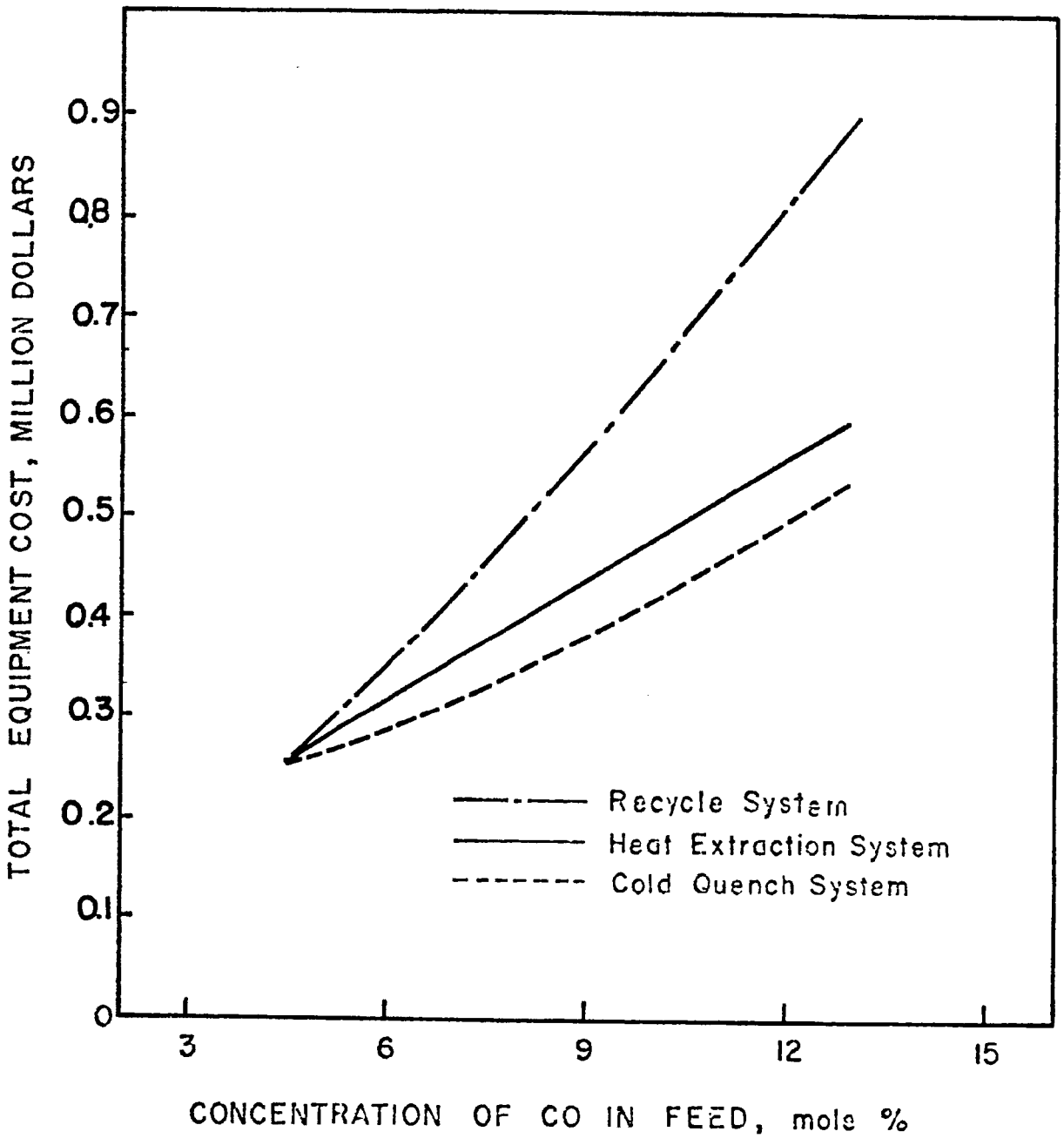

FIGURE VII-34 Relation Between Total Equipment Cost And Concentration Of CO In The Feed Gas For Three Different Systems.

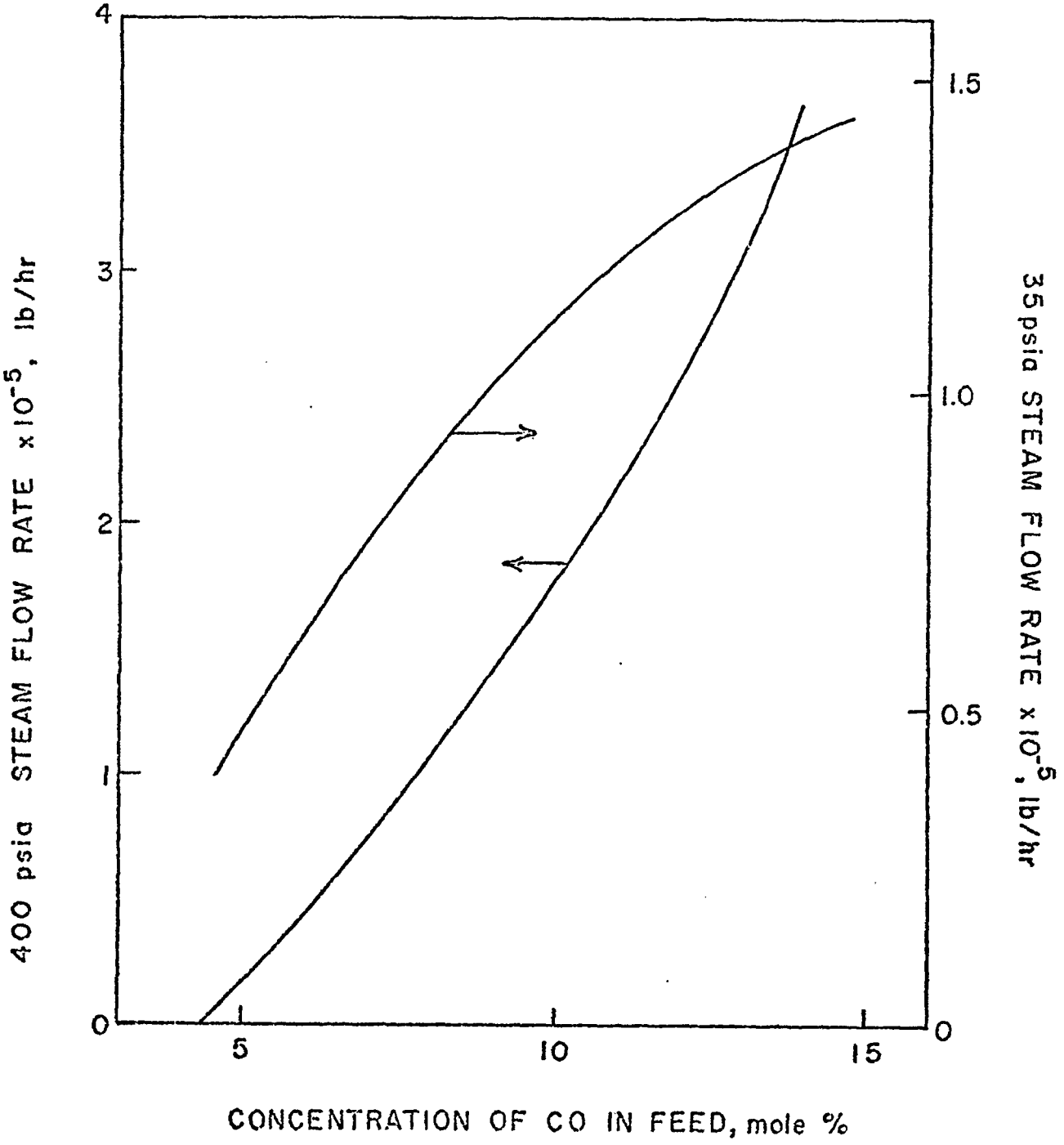

FIGURE VII-35- Relation Between Steam Recovery And The Concentration Of CO In The Feed Gas.

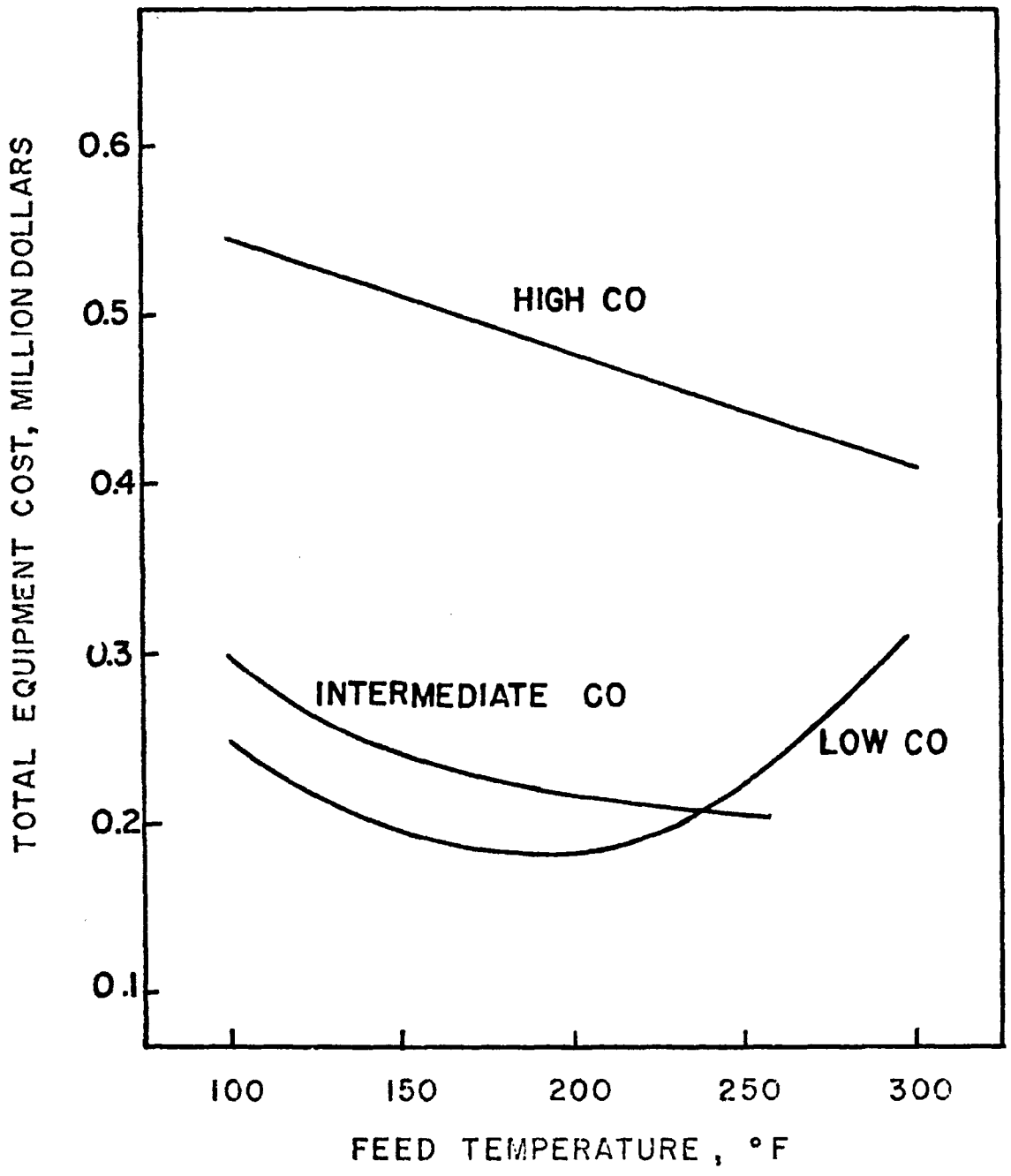

FIGURE VII-36 Total Equipment Cost Versus Feed Temperature In Low CO Case and In Two Cases For Cold Quench System.

reactor and for the intermediate CO case and the high CO case in the cold quench systems. In the low CO case, since the reactor is under the adiabatic condition, as the feed gas temperature is increased, the size of the preheater becomes smaller but the product gas cooler I becomes larger. As shown in Figure VII-36 when T_F is 200°F, the total equipment cost becomes the minimum.

In the cold quench system, as the feed gas temperature is increased, the fraction of the feed gas that must be introduced from the top of the reactor becomes smaller reducing the size of the preheater considerably. Consequently the total equipment cost becomes smaller as shown in the figure. However, an increase in the feed gas temperature decreases the capacity of the gas in the reactor to absorb the heat of reaction. Therefore, above a certain feed gas temperature, the operation becomes impossible without an additional reactor. The feed gas temperatures at which this will take place are 250°F for the intermediate CO case and 300°F for the high CO case. Hence, these temperatures become the optimum feed gas temperatures for the two cases.

Figure VII-37 shows how the feed gas pressure affects the total equipment cost for the low CO case, and the high CO case in the cold quench system. Since it is necessary to maintain the outlet product gas pressure above 1000 psig in order to meet the pipeline gas specification, the product gas must be compressed to this pressure when the gas effluent from the methanation reactor does not have enough pressure to meet this requirement. As shown in Figure VII-37 the compressor cost is by far the largest portion of the total

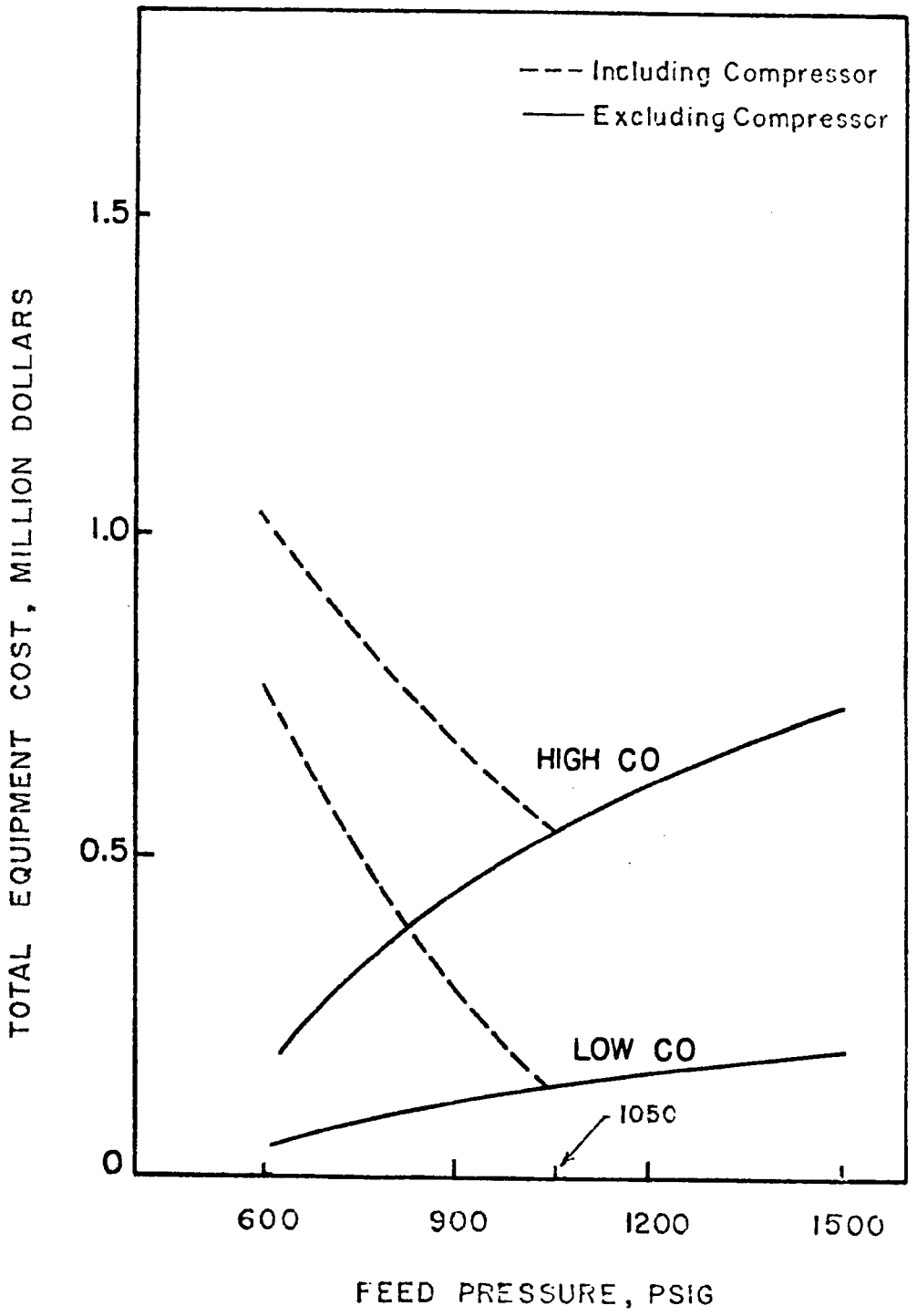

FIGURE VII-37 Total Equipment Cost With And Without Compressor Cost Versus Feed Pressure In Low CO Case And High CO Case For Cold Quench System

equipment cost, clearly indicating the undesirability of the product gas compression. It is therefore logical to conclude that the use of gas compressors to attain the pipeline gas pressure in any part of coal gasification processes should be avoided if possible.

7.4 Some Maintenance and Operational Problems Associated with the Three Systems

As a rule, a reactor should be designed so that the same product gas quality is maintained even though the feed gas concentration and the catalyst activity may slightly change during the course of the operation.

For example, if the CO content in the feed gas falls slightly below the specified level, it is still relatively simple to maintain the product gas heating value in the cold quench system and in the recycle system but not in the heat extraction system. In the cold quench system, the amount of the feed gas entering at the top of the reactor is simply increased, while in the recycle system, the flow rate of recycle gas is decreased. However, in the heat extraction system, not only the gas flow rate must be decreased but also the heat transfer coefficient of the fin tubes must be lowered. This cannot be accomodated easily.

The heat extraction system is also not as flexible as the other two systems from the viewpoint of catalyst loading and unloading. When the catalyst pellets are to be removed for regeneration and the fresh pellets are to be repacked, a greater effort is required to accomplish this in the heat extraction system. Not only the quantity

of catalyst pellets packed in each tray is different, but the pellets must also be packed between the fin tubes, requiring considerable time and effort for loading and unloading.

In the heat extraction system, since the main heat transfer resistance of the fin tubes is in the outside surface of the fin tubes, if the operating temperature in the reactor falls accidentally below 750°F, the temperature of the catalyst surface which is in contact with the fin tube may possibly fall below 500°F. Under such conditions, the formation of carbonyl at the cold spots could occur causing severe catalyst deactivation. Thus, the operation and the maintenance of the heat extraction system are considerably more difficult in comparison with that of the cold quench system and the recycle system.

In many senses, the recycle system is the easiest system to operate although it is the most expensive system among the three systems. Particularly when the CO concentration is very high, the temperature of the catalysts near the entrance of the reactor and the temperature difference between the surface of the catalyst and the bulk gas phase could become excessive at some localities due to non-uniform distribution of the gas flowing in the reactor. In such situations, the recycle system could become the only system operable without causing disastrous results of "temperature run-away."

7.5 Sensitivity Analysis

In this study, the optimum conditions (decisions) are obtained based on the specific values of system parameters which characterize the performance (kinetic constants, heat transfer coefficient, etc.) to minimize the total equipment cost (the objective function). The values of these parameters are usually obtained from the experimental studies or from careful evaluations based on established correlations. Often these values are somewhat inaccurate due to lack of time and funds required for an accurate evaluation. If the performance of the system under the optimal conditions is significantly dependent on these parameters, and if these values are uncertain, the actual system performance may deviate considerably from the specification. Therefore, to insure a better system performance under parameter uncertainty, it is necessary to analyze how sensitive the objective function (total equipment cost) is over a range of values of parameters. The sensitivity of a given parameter, σ, is defined [16] as

$$\sigma = [(\alpha - \bar{\alpha})/\bar{\alpha}] \,/\, [(\beta - \bar{\beta})/\bar{\beta}] \qquad \text{(VII-67)}$$

where

α and $\bar{\alpha}$ are the objective function (total equipment cost) for a given value of parameter and the objective function at the optimum condition, respectively
β and $\bar{\beta}$ are the parameter subject to variation and that at a specific value considered, respectively

Table VII-11 shows the result of parameter sensitivity study on the equipment cost for the methanation process. Among the parameters studied, the accuracy of kinetic expressions seems to be moderately sensitive to the total equipment cost for both the low CO case and

TABLE VII-11 PARAMETER SENSITIVITY ON TOTAL EQUIPMENT COST OF OPTIMUM METHANATION PROCESSES

Parameters	Sensitivity	
	Low CO	High CO
U^I	--	-0.05152
U^{II}	-0.10320	-0.08749
U^{III}	-0.19620	-0.10392
U_P	0.13070	-0.0516
μ	-0.2632×10^{-4}	-0.13×10^{-6}
ρ	0.3984×10^{-2}	0.486×10^{-3}
T^N	-0.17555	-1.768
T^E	--	0.33764
T^O	--	0.07711
k^*	-0.17358	-0.12665
m^*	-0.41884	-0.34217
n^*	-0.71860	-0.63865

*Based on the rate equation: $r_{CH_4} = ke^{-E/RT} P_{H_2}^m P_{CO}^n$

the high CO case. This implies that a more extensive study of the reaction kinetics as well as further development of improved catalyst is necessary for methanation reaction. The dependency of the rate of reaction on the concentration and temperature should be more firmly established.

In addition, the maximum allowable temperature, T^N, for the high CO case is also a very sensitive factor. This means that if the maximum allowable temperature could be higher than 850°F, a considerable saving in the total equipment cost is possible, provided of course that the equilibrium hindrance is avoided by cooling the gas near the exit of the reactor. From the heat removal point of view the maximum temperature at which the catalyst can be operated without deactivation due to local sintering or carbon deposition, should be as high as possible. However, high temperatures also limit the materials of construction of the reactor and the equilibrium concentration for methane. Therefore, further study of catalyst reactivity, durability and regenerability are required. Other factors studied gave negligible sensitivities on the total equipment cost.

8. CONCLUSION

As a part of studies on optimization of coal gasification processes, an optimization of methanation processes has been performed. Three different systems employing fixed bed downflow, catalytic reactors are examined. They are the heat extraction system, the cold quench system and the recycle system. The most economical design of each of the systems are found under various operating conditions. The following conclusions are drawn from the results of the study.

i Owing to the extremely large heat of reaction, the removal of heat from the reacting gas is the major problem associated with methanation process. The cost of equipment involved in heat removal such as heat exchangers, etc., occupies a major portion of the total equipment cost. The problem of heat removal becomes more complicated when the feed gas contains a large amount of CO.

ii When CO concentration in the feed gas is less than 6.4 percent an adiabatic reactor without internal or intermediate cooling is sufficient to achieve a product gas equivalent to the pipeline gas quality. This concentration is obtained based on a design in which the feed gas temperature of 100°F and the maximum reactor temperature of 850°F are assumed.

iii The total equipment cost is largely affected by the concentration of CO in the feed gas. When CO concentration in the feed gas is larger than 6.4 percent, the cold quench system offers the least total equipment cost followed by the heat extraction system. The recycle system is by far the most expensive system among the three systems studied.

iv. The total equipment cost is also affected by the feed gas temperature and pressure. There is an optimum feed temperature for a given concentration. The optimum feed gas temperature for the low CO case is 200°F, for the intermediate CO case is 250°F and for the high CO case is 300°F. Since it is required to produce gas at 1000 psig to meet the pipeline gas specification, the feed gas pressure should be 1050 psig so that no compressor may be needed. This is because the compressors of the size required are extremely expensive in comparison to other equipment costs.

v. Although the equipment cost for the heat extraction system is not too much different from the cold quench system, from the maintenance and operational point of view, the heat extraction system is not easily controllable and may become unstable when small disturbances in the operating conditions are present.

vi. The recycle system on the other hand is the most costly among the three systems. However, the system is the easiest to control, particularly when the concentration of CO in the feed gas is high and when the distribution of gas through the catalyst bed may not be uniform.

vii Sensitivity analyses of the design parameters indicate that the maximum allowable temperature affects the equipment cost considerably. If a higher maximum temperature can be allowed, the cost of the equipment would reduce significantly. Also the accuracy of the kinetic rate constants and the orders of reaction would have some effect on the total equipment cost.

viii The minimum total equipment costs for the methanation processes are found to be $\$373.6 \times 10^3$ for the low CO case employing an adiabatic fixed bed reactor, $\$517.6 \times 10^3$ for the intermediate CO case, and $\$781.9 \times 10^3$ for the high CO case. The last two cases employ the cold quench system.

9. RECOMMENDATION

It is recommended that in the methanation process associated with the coal gasification for pipeline gas production, an adiabatic fixed bed reactor system should be selected for the low CO case and the cold quench system should be selected when the feed gas CO concentration is between 4.6 percent to 15 percent.

When CO concentration is higher than 15 percent, reactors with better heat removal devices will be needed. Therefore, systems such as those proposed by the Bureau of Mines utilizing sprayed catalyst on heat transfer surface to facilitate quick removal of heat should be investigated. In addition, more accurate kinetic information pertaining to the rates of methane formation and water-gas shift reaction on a given catalyst should be obtained. Particularly the maximum allowable temperature of the catalyst without deactivation or carbon deposition must be more accurately established. Furthermore, the durability and regenerability of the Harshaw catalyst must be more carefully investigated.

Notation

A_o	heat transfer area	($ft.^2$)
A_t^n	total heat transfer area of fin tube in n-th cell	($ft.^2$)
A^I, A^{II}, A^{III}	heat transfer area of first, second and third product gas cooler, respectively	($ft.^2$)
B	brake horse power	(HP)
B_r	brake horse power of recycle compressor	(HP)
B'	baffle spacing	(ft.)
C_{AO}	installed cost of heat exchanger per unit heat transfer area based on outside	($/$ft.^2$)
C_b	concentration of product gas in bulk of gas phase	(lb.mole/$ft.^3$)
C_i	cost for supplying one ft.-lb.force to pump fluid flowing through inside of tubes	($/ft.-lb.force)
C_L'	height of a unit cell	(ft.)
C_o	cost for supplying 1 ft.-lb.force to pump fluid flowing through shell side	($/ft.lb.force)
C_P	heat capacity of gases	(B.t.u./lb.°F)
$C_{P_i}^{(I)}$	molar heat capacity of i-th component at temperature $T^{(I)}$	(B.t.u./ lb.mole°F)
$\bar{C}_P^{(I)}$	heat capacity of product gas at temperature $T^{(I)}$	(B.t.u./lb.°F)
C_{pw}	heat capacity of water	(B.t.u./lb.°F)
C_R	cost per pound of material used for construction of reactor-shell	($/lb.)
C_S	concentration of product gas at surface of catalyst	(lb.mole/$ft.^3$)
C_T	total annual variable cost	($/years)
C_Y	cost year index	(--)
D	inside diameter of reactor	(ft.)
De	equivalent diameter for heat transfer tube	(ft.)
D_i	inside diameter of tube	(ft.)

D_S	inside shell diameter of heat exchanger	(ft.)
d_p	diameter of catalyst particle	(ft.)
E	efficiency of longitudinal joints or mechanical efficiency	(--)
E_C	catalyst cost	($)
E_{CP}	compressor cost	($)
E_{CR}	recycle compressor cost	($)
E_F	embedded fin tube cost	($)
E_H	heat exchanger cost	($)
E_i	power loss inside tube per unit of outside tube area	(ft.-lb.force/ hr.ft.^{2})
E_o	power loss outside tube per unit of outside tube area	(ft.-lb.force/ hr.ft.^{2})
E_R	reactor cost	($)
E_S	cost of unit tray	($/unit tray)
E_T	total equipment cost	($)
F_1^n	molar flow rate of CH_4 at n-th cell	(lb.mole/hr.)
F_2^n	molar flow rate of CO at n-th cell	(lb.mole/hr.)
F_3^n	molar flow rate of H_2 at n-th cell	(lb.mole/hr.)
F_4^n	molar flow rate of CO_2 at n-th cell	(lb.mole/hr.)
F_5^n	molar flow rate of H_2O at n-th cell	(lb.mole/hr.)
F_6^n	molar flow rate of N_2 at n-th cell	(lb.mole/hr.)
F^0	total molar flow rate of feed gas	(lb.mole/hr.)
F_i^0, F_i^n, F_i^r	molar flow rate of i-th component in feed, product and recycle gas, respectively	(lb.mole/hr.)
$F_i^{(2)}, F_i^{(3)}$	molar flow rate of i-th component at inlet of second and third reactor, respectively	(lb.mole/hr.)
F_d	flat blank diameter of top and bottom of domes of reactor	(ft.)

F_T	correction factor on Δt_m	(--)
G	superficial mass velocity	(lb./ft.^{2}hr.)
G_i	mass velocity inside tube	(lb./ft.^{2}hr.)
G_S	shellside mass velocity	(lb./ft.^{2}hr.)
ΔH	heat of reaction	(B.t.u./lb.mole CH_4)
H_y	hours of operation per year	(hr./year)
Δh	hydraulic head	(ft.H_2O)
h_i	inside film heat transfer coefficient of tube	(B.t.u./ft.^{2}hr.°F)
h_o	outside film heat transfer coefficient of tube	(B.t.u./ft.^{2}hr.°F)
h_p	fluid-particles heat transfer coefficient	(B.t.u./ft.^{2}hr.°F)
I_f	cost factor	(--)
J_H	heat transfer factor	(--)
J_M	mass-transfer factor	(--)
K	thermal conductivity of fluid	(B.t.u./ft.hr.°F)
K_d	diffusion coefficient	(ft.^{2}/hr.)
K_F	annual fixed charges	(--)
K_G	mass transfer coefficient	(lb.mole/hr.ft.^{2}atm.)
$K^*_{X_1}$	equilibrium constant of methanation reaction	(--)
$K^*_{X_2}$	equilibrium constant of shift reaction	(--)
K_{X_1}	mass action law ratio of product gas in methanation reaction	(--)
ke	effective thermal conductivity of catalyst particles	(B.t.u./ft.hr.°F)
k_f	fluid-particle mass transfer coefficient	(ft./hr.)
kg	thermal conductivity of gas	(B.t.u./ft.hr.°F)
k_s	thermal conductivity of catalyst	(B.t.u./ft.hr.°F)
L	length of reactor	(ft.)
L_H	length of heat exchanger	(ft.)

$\bar{M}$	average molecular weight of product gas	(lb./lb.mole)
M_m	mean molecular weight of fluid	(lb./lb.mole)
M_v	molecular weight of steam	(lb./lb.mole)
N	number of trays	(--)
N_{Pr}	Prandtl number	(--)
P	design pressure	(psig)
ΔP	pressure drop per unit cell	(lb./ft.^{2})
P_a	pressure at suction to compressor	(atm.)
P_b	pressure at discharge from compressor	(atm.)
P_c	partial pressure of steam at surface of tube	(atm.)
P_{gf}	logarithmic-mean pressure difference of non-condensing gas	(atm.)
P^N	outlet pressure of reactor	(atm.)
P^O	inlet pressure of reactor	(atm.)
ΔP_S	shell side pressure drop in heat exchanger	(psi)
P_v	partial pressure of steam at bulk fluid	(atm.)
P_v^{II}	vapor pressure of water at temperature T^{II}	(atm.)
P_w	partial pressure of steam in product gas	(atm.)
P_{CO}	partial pressure of CO	(atm.)
P_{H_2}	partial pressure of H_2	(atm.)
Q_c	total amount of heat generated in reactor	(B.t.u./hr.)
Q^n	amount of heat removed from n-th cell	(B.t.u./hr.)
q	total heat transfer rate in heat exchangers	(B.t.u./hr.)
q^I, q^{II}, q^{III}	heat duties of first, second and third product gas coolers, respectively	(B.t.u./hr.)
q'	volumetric flow rate	(gal./min.)
q_c	heat flux accompanied with condensation	(B.t.u./hr.ft.^{2})

q_p	volume of gas compressed	(S.C.F./min.)
q_r	recycle gas flow rate	(S.C.F./min.)
R	inside radius of cylinder	(in.)
R_{dw}	resistance to heat flow due to scaling	($ft.^2 hr.°F/B.t.u.$)
r	distance from center of catalyst particle	(ft.)
r_s	reaction rate per unit catalyst particle	(lb.mole CH_4/ hr.unit catalyst)
r_{CH_4}	reaction rate	(lb.mole CH_4/ hr.lb.catalyst)
S	maximum allowable stress	(psig)
s	specific gravity	(--)
T	temperature	(°F)
$T^{(1)}, T^{(2)}, T^{(3)}$	inlet temperatures of first, second and third reactor, respectively	(°F)
T^I, T^{II}	outlet gas temperature from first and second product gas cooler, respectively	(°F)
T^A	outlet gas temperature from intermediate cooler	(°F)
T^E	exit temperature of final reactor for high CO case	(°F)
T^F	feed gas temperature	(°F)
T^N	exit gas temperature of reactor	(°F)
T^{NP}	gas temperature leaving recycle gas cooler	(°F)
T^n	temperature at n-th cell	(°F)
T^o	gas temperature after quenching	(°F)
T^P	outlet product gas temperature from preheater	(°F)
$T^{(PF)}$	outlet feed gas temperature from preheater for recycle system	(°F)
T_a	temperature at suction to compressor	(°F)
T_b	bulk gas temperature in reactor	(°F)
T_h	thickness of reactor	(in.)

T_s	surface temperature of catalyst particles	(°F)
t_{C1}, t_{C2}, t_{C3}	outlet coolant temperature of first, second and third product gas coolers, respectively	(°F)
t'_c	inlet water temperature of first product gas cooler	(°F)
t_c	temperature of treated or spent water	(°F)
Δt_m	logarithmic-mean temperature difference	(°F)
U^I, U^{II}, U^{III}	overall heat transfer coefficients of first, second and third product gas coolers, respectively	(°F)
U_o	overall heat transfer coefficient of fin tubes	(B.t.u./ft.^{2}hr.°F)
U_P	overall heat transfer coefficient of preheater	(B.t.u./ft.^{2}hr.°F)
V_c^n	catalyst volume per unit cell	(ft.^{3})
W^N	molar flow rate of product gas	(lb.mole/hr.)
W_1, W_2	flow rate of treated and spend water in product gas coolers, respectively	(lb./hr.)
W_C	catalyst weight	(lb.)
W_O	mass flow rate of feed gas	(lb./hr.)
W_R	weight of reactor tube	(lb.)
W_{S1}, W_{S2}	flow rate of 400 psia steam and 35 psia steam in product gas cooler, respectively	(lb./hr.)
$X^*_{CH_4}$	equilibrium mole fraction of CH_4	(--)
$X^*_{H_2O}$	equilibrium mole fraction of H_2O	(--)
X^*_{CO}	equilibrium mole fraction of CO	(--)
$X^*_{H_2}$	equilibrium mole fraction of H_2	(--)
$X^*_{CO_2}$	equilibrium mole fraction of CO_2	(--)
X_{CH_4}	mole fraction of CH_4 in product gas	(--)
X_{H_2}	mole fraction of H_2O in product gas	(--)
X_{CO}	mole fraction of CO in product gas	(--)
X_{H_2}	mole fraction of H_2 in product gas	(--)
$Y^{(2)}, Y^{(3)}$	conversion of CO to CH_4 at inlet of second and third reactor	(--)
Y^N	total conversion of CO to CH_4	(--)

Greek Letters

α, $\bar{\alpha}$	objective function and that at optimum, respectively	
β, $\bar{\beta}$	system parameter subject to variation and a specific value of system parameters, respectively	
ϵ	void fraction of reactor	(--)
θ	internal porosity of catalyst	(--)
λ'	Lagrange multiplier	(--)
λ_1'	fraction of feed gas passing through preheater	(--)
λ_c	heat of condensation for steam	(B.t.u./lb.)
μ	gas viscosity	(lb./ft.hr)
ρ	gas density	(lb./ft.^{3})
ρ_c	catalyst density	(lb./ft.^{3})
ρ_m	density of reactor shell	(lb./ft.^{3})
ρ_w	density of cooling water	(lb./ft.^{3})
σ	sensitivity defined as $[\alpha - \bar{\alpha}/\alpha] / [\beta - \bar{\beta}/\beta]$	(--)
ϕ	cost factor	(--)

LITERATURE

1. Akers, W. W. and White, R. R., Chem. Eng. Progr. 44, 553-566 (1948).

2. ASME Boiler and Pressure Vessel Code, Section VIII, Unfired Pressure Vessels, The American Society of Mechanical Engineers, New York, 1956.

3. Bauman, H. C., "Fundamentals of Cost Engineering in the Chemical Industry," Reinhold, New York, 1964.

4. Chilton, C. "Cost Engineering in the Process Industries," McGraw Hill, New York, p. 50, 1960.

5. Communication, Harshaw Chemical Co., Cleveland, Ohio, July, 1967.

6. Ergun, S., Chem. Eng. Progr., 48, 89 (1952).

7. Fan, L. T., Lee, E. S. and Erickson, L. E., "Proceedings of the MASUA Conference on Modern Optimization Techniques and their Application in Engineering Design," Part II, The Mid-America State Universities Association, 1966.

8. Gamson, B. W., Chem. Eng. Progr., 47, 19 (1951).

9. Jones, P. R. and Katell, S., "Computer Usage for Evaluation of Design Parameters and Cost of Heat Exchangers with No Change in Phase and Pumping Costs of Both Fluids as Prime Parameters," IC Bureau of Mines Information Circular 8334, 1967.

10. Kern, D. Q., "Process Heat Transfer," McGraw Hill, New York, 1950.

11. McCabe, W. L. and Smith, J. C., "Unit Operations of Chemical Engineering," McGraw Hill, New York, 1956.

12. Page, J. S., "Estimator's Manual of Equipment and Installation Costs," Gulf, Houston, 1963.

13. Peters, M. W., "Plant Design and Economics for Chemical Engineers," McGraw Hill, New York, 1958.

14. Tajbl, D. G., Feldkirchner, H. L. and Lee, A. L., "Fuel Gasification," Ed. R. F. Gould, ACS, Washington, D. C., p. 166, 1967.

15. Rossini, F. D., et al., "Selected Values of Properties of Hydrocarbons," U.S. Department of Commerce, National Bureau of Standards, Washington, D. C., 1947.

16. Wen, C. Y. and Chang, T. M., Ind. Eng. Chem. Process Design Develop. 7, 49 (1968).

17. Wilke, C. R. and Hougen, O. C., Trans. A. I. Ch. E. 41, 445 (1949).

10. Supplement: Study of super high CO case by cold quench-recycle system

As a result of the previous study it is reasonable to expect that by combining the low cost cold quench system and the most flexible recycle system a better methanation process system may be obtained.

10.1 Process Analysis

A schematic flow diagram is presented in Figure VII-38. A fraction of feed gas is mixed prior to the entering of the reactor with a portion of product gas which has been partially cooled by a recycle cooler and pressurized by a centrifugal compressor to 1050 psig. The ratio of these two streams is adjusted so that the temperature of the mixed gas at the inlet point of the reactor is 550°F. The remainder of the feed gas is introduced at intervals along the reactor for the cold quench purpose. Because of the heat generation during the formation of methane the temperature of the reactant gas increases gradually along the reactor. When the temperature reaches a maximum of 850°F where it is believed that carbon deposition reaction might start to take place, a certain amount of fresh cold feed gas is introduced into the hot reactant gas at the quenching section of the reactor. Therefore, the temperature of the gas mixture is brought down to a minimum of 550°F. After the gas is cooled and the composition is readjusted the mixed gas then enters into the next stage of the reactor. The same procedures can be repeated until the concentration of methane in the gas stream reaches or exceeds the specified concentration. The temperature of gas coming out of the last stage should be less than 810°F to avoid equilibrium hindrance. The

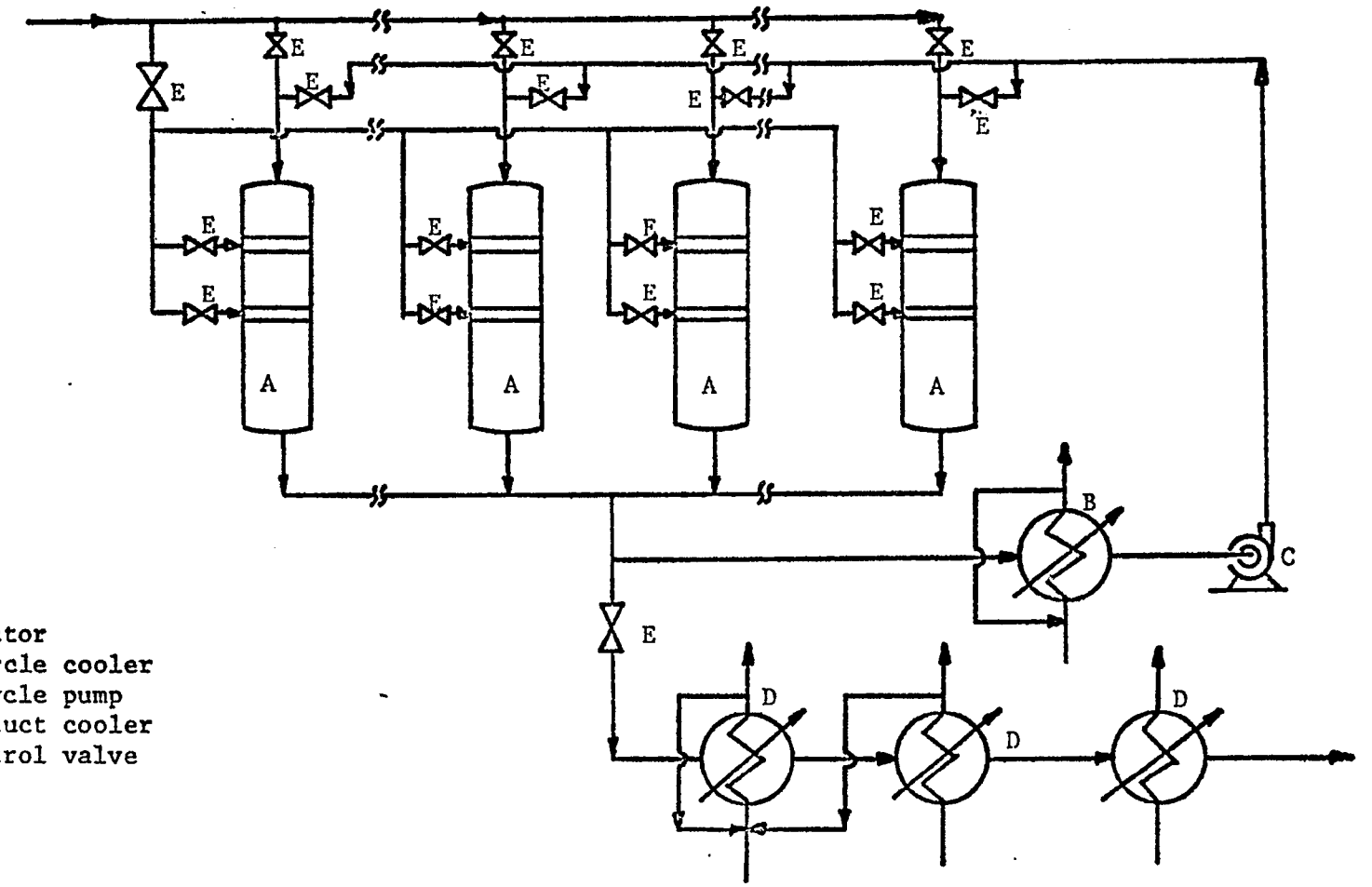

A Reactor
B Recycle cooler
C Recycle pump
D Product cooler
E Control valve

VII-

FIGURE 38 SCHEMATIC FLOW DIAGRAM IN HIGH CO CASE FOR COLD QUENCH-RECYCLE SYSTEM

product gas coming out of the last stage is split into two streams. One of the streams goes to recycle cooler via recycle pump and is used for recycle purpose. The other stream goes into a series of product coolers through which the product gas is cooled to 100°F. The same type of reactors can be arranged in parallel with manifolds at the inlet and outlet of the reactors. Thus one recycle cooler, one recycle pump and one set of product coolers can be used for the whole process.

10.3 Calculation Procedures

The technique of dynamic programming is based on Bellman's principle of optimality which states "that in staged systems with NO FEED BACK the optimal policy has the property that whatever the first state or decision may be, the remaining decisions must constitute an optimal policy with respect to the state resulting from the first decision" [1]. In other words, the state of the stream has been transformed at every stage of the process, but whatever the operating policy up to the last stage, the complete policy will not be optimal unless the last stage is operating with optimal policy with respect to its feed.

In methanation processes, a large amount of heat is generated during the formation of methane. This is especially true in high CO feed case. Therefore, it is impossible to achieve the desired conversion without any heat removing device. This has been thoroughly discussed in the previous study. In order to remove the heat generated from the reaction of carbon monoxide and hydrogen in the cold quench-recycle system, both cold shot quench and cooled product gas dilution methods are used.

Bellman's optimum policy is formulated such that it can not be directly applied to a system with recycle streams. This is because in a recycle system the decisions made in the last stage affect the optimal policy of the previous stage. In order to make it possible to use the dynamic programming technique in this study, a slightly modified technique is necessary.

For the purpose of simplification a three-stage reactor is being considered. The end conditions of the methanation process are fixed. That is, both the inlet and outlet composition, flow rate and temperature are given. The calculation is started by assuming a set of grid points for the fractions of the feed gas introduced directly into the top of the reactor. The above assumption corresponds to setting up a set of grid points of recycle ratio. Once a recycle ratio is assumed the optimal policy for the whole reactor can be determined by a regular backward dynamic programming method. After this optimal policy is determined another new recycle ratio selected from the grid points is used for calculation. The same calculation procedure is repeated until all the possible recycle rates are examined. The over all optimal policy is finally obtained from the above calculations. The procedure for the determination of the optimal policy at a particular recycle rate is described as follows.

In the first stage (numbered backward), the exit conditions, i.e. flow rate, temperature and conversion are given, and the objective function is the total equipment cost only. Hence there is no way to make any optimum decision from an assigned possible state variables at the inlet of the first stage. This means for any set of state variables picked from a pre-formulated grid points there is only one possible path to achieve the fixed end point. Here the state variables chosen are the conversion of the outlet stream of the second stage and the amount of fresh cold feed gas

introduced at the second quenching section (Figure VII-39). Since in the quenching section the calculation deals only with material and energy balances, the selection of such state variables can be justified.

In a three-stage reactor there are only two quenching points located between each pair of stages. Once the amount of the quenching gas used in the second quenching point is decided the amount of gas to be used in the first quenching section is automatically determined. Therefore, it is not necessary to consider the amount of quenching gas to be used in the first quenching section as a decision variable. For the second stage calculation the state variables are the conversion and the temperature of outlet stream from the third stage. The decision variables are the conversion and the temperature of the reactant gas at the end point of the second stage. By setting up sets of grid points of admissible state variables and decision variables, the combined optimal policy for the last two stages is determined. Here the grid points of the decision variable are calculated from the total energy and material balances around the reactor.

In the third stage the inlet temperature is fixed at 550°F as mentioned in the Process Analysis section. The conversion, or the composition of the inlet stream is also fixed by the recycle ratio. Since both of the state variables, i.e. temperature and conversion of the inlet stream are fixed already, the third stage calculation can be considered as a one end fixed optimization problem. In this case either the conversion or the temperature of the exit stream of the third stage can be used as a decision variable. The optimal policy for the third stage can then be determined.

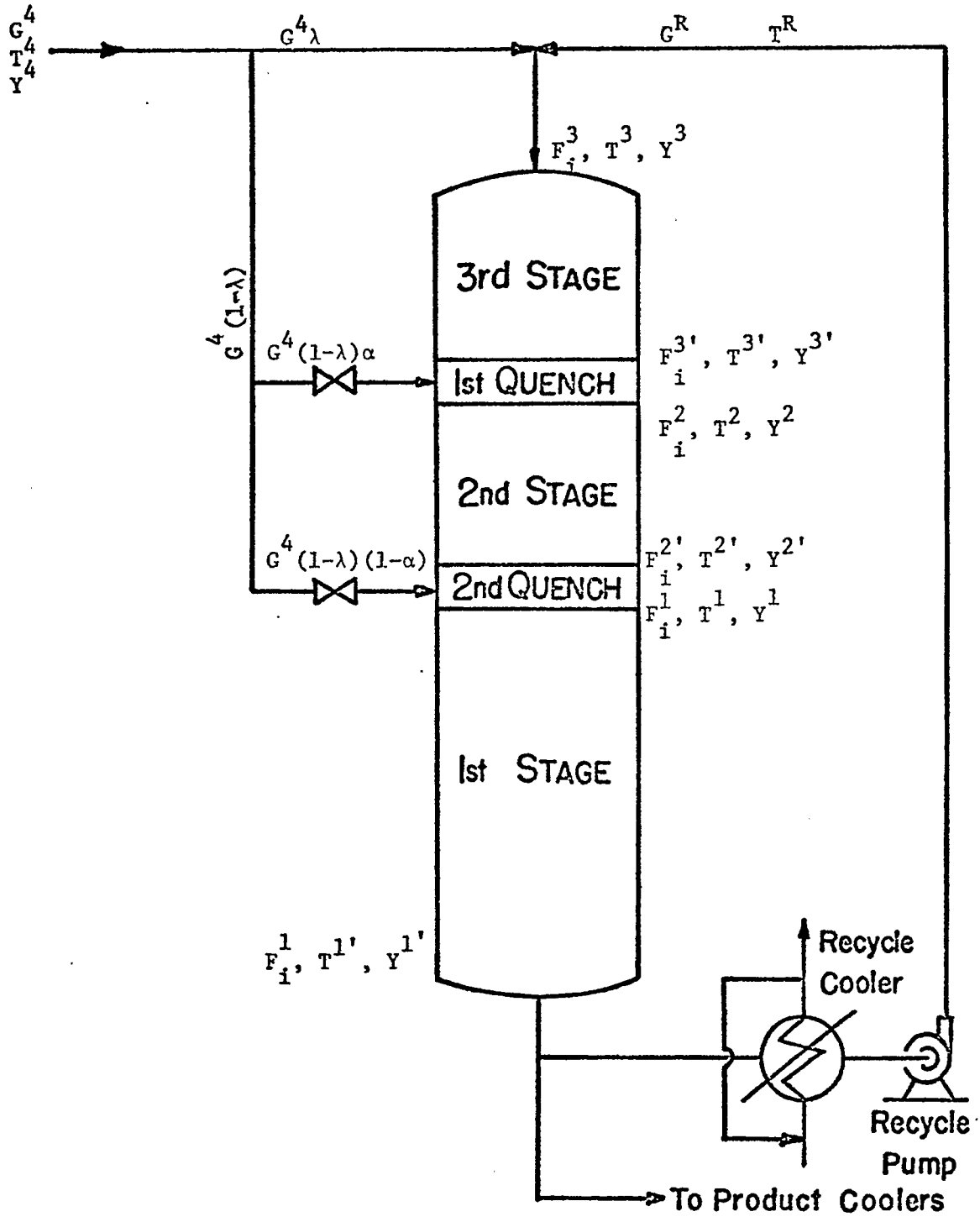

FIGURE VII-39 DETAIL OF THE SINGLE REACTOR ARRANGEMENT AND NOMENCLATURES USED IN THIS REPORT

Thus from the above calculations the total cost of the reactor shell, catalyst, catalyst support trays, control valves, recycle cooler, recycle pump and product gas coolers can be obtained.

The question whether the reactor diameter at each stage be treated as a decision variable for the calculation has been considered. Since we are interested in the cold quench-recycle system rather than the reactors-in-series with intermediate external cooling system, changing diameter from reactor to reactor not only causes difficulties in reactor fabrication and consequently increases the reactor cost, but also introduces difficulty in the overall calculation procedures. This problem is solved by the following method. In the primary calculation a single reactor is considered. The reactor diameter is so determined that the overall pressure drop in the reactor is no more than 10 psi, the same constraint assumed in the previous report[1]. After the optimum design conditions for a single reactor are determined, the optimum number of parallel reactors with total cross-sectional area same as a single reactor is searched. Since the a single reactor and the multiple reactors have the same total cross-sectional area, the mass flow rate and the perssure drop are the same. Thus the amount of catalyst, feed gas for quenching, the quench points and other operating conditions in a multiple reactors do not change from the optimum conditions already determined for the single reactor.

The total equipment cost is the summation of the costs of reactors, catalyst, catalyst support trays, control valves, recycle cooler, recycle pump and product coolers. The cost of the product coolers is essentially the same as the systems studied previously[1]. Therefore, in this study the same cost for the product coolers is used.

Some of the material and energy balances at the key points are listed below. The cell by cell calculations are basically the same as those appeared in the previous report[1] and will not be repeated here.

Recycle Rate And Recycle Gas Temperature Calculations

$$T^{1'} \sum_{i=1}^{6} C_{P_i}^{1'} F_i^{1'} = T^{3} \sum_{i=1}^{6} C_{P_i}^{3} (\lambda F_i^{4'} + F_i^{R}) + (1 - \lambda)\, T^{4'} \sum_{i=1}^{6} C_{P_i}^{4'} F_i^{4'} + Q^1 + Q^2 + Q^3$$

$$\gamma = \sum_{i=1}^{6} F_i^R M_i / \sum_{i=1}^{6} F_i^4 M_i$$

$$\lambda\, T^{4'} \sum_{i=1}^{6} C_{P_i}^{4'} F_i^{4'} + T^{R} \sum_{i=1}^{6} C_{P_i}^{R} F_i^{R} = T^{3} \sum_{i=1}^{6} C_{P_i}^{3} (\lambda F_i^4 + F_i^R)$$

Quenching Point Energy Balance

a). Energy Balance at the First Quenching Point:

$$T^{1'} \sum_{i=1}^{6} C_{P_i}^{1'} F_i^{1'} = T^{3'} \sum_{i=1}^{6} C_{P_i}^{3'} F_i^{3'} + (1 - \lambda)\, T^{4'} \sum_{i=1}^{6} C_{P_i}^{4'} + Q^1 + Q^2$$

$$T^{3'} \sum_{i=1}^{6} C_{P_i}^{3'} F_i^{3'} + (1 - \lambda)\, \alpha\, T^{4'} \sum_{i=1}^{6} C_{P_i}^{4'} F_i^{4'} = T^{2} \sum_{i=1}^{6} C_{P_i}^{2} F_i^{2}$$

b). Energy Balance at the Second Quenching Point:

$$T^{1'} \sum_{i=1}^{6} C_{P_i}^{1'} F_i^{1'} = T^{2'} \sum_{i=1}^{6} C_{P_i}^{2'} F_i^{2'} + (1 - \lambda)\,(1 - \alpha) T^{4'} \sum_{i=1}^{6} C_{P_i}^{4'} F_i^{4'} + Q^1$$

$$T^{2'} \sum_{i=1}^{6} C_{P_i}^{2'} F_i^{2'} + (1 - \lambda)\,(1 - \alpha) T^{4'} \sum_{i=1}^{6} C_{P_j}^{4'} F_i^{4'} = T^{1} \sum_{i=1}^{6} C_{P_i}^{1} F_i^{1}$$

Where

T	is temperature, (°F).
C_{P_i}	is the heat capacity of the i-th component, (BTU/lb.mole°F)
M_i	is the molecular weight of the i-th component, (lb/lb mole)
Q^1, Q^2, Q^3	are the heat of generation in the 1st, 2nd, and 3rd stage respectively, (BTU/hr)
F_i	is the molar flow rate of the i-th component, (lb mole/hr)

α is the fraction of the total quenching gas entering the 1st quenching point

γ is the recycle rate, (weight of recycle gas/weight of feed gas)

λ is the fraction of feed gas which directly enters into the top of the reactor

The superscript without prime on T, C and F denotes the inlet properties of flow rate of the specified stage. The superscript with prime denotes the outlet properties or flow rate of the specified stage.

10.4 Results

Figure VII-40 shows the effect of the reactor diameter on the total equipment cost. Fig. VII-40 shows the total equipment cost versus the number of reactor in parallel arrangement. The results are calculated from the optimum design for a single reactor. From these figures the optimum number of reactors in parallel is seen to be 4, the optimum reactor diameter to be 7 ft., and the reactor height to be 8.91 ft. The latter includes the height of the three quenching chambers, each of which is 6 inches high. The difference between the optimum equipment cost for one reactor and that with optimum number of reactors in parallel is $65,000.

Figures VII-42 to VII-45 show the temperature profile, reaction rate, concentration profiles, and conversion along the reactor height in high CO case for cold quench-recycle system respectively. Figure VII-46 shows the conversion versus temperature for an adiabatic reactor with recycle.

Tables VII-12 and VII-13 list the optimum operating conditions and the optimum equipment cost for the cold quench-recycle system. For the purpose of comparison the optimum equipment cost for the recycle system based on a cost factor $I_f = 3$ and cost year index $C_y = 1.2$ was also calculated and listed in the same tables. The cost factor and the cost year index used in the previous report [1] were 4 and 1.4 respectively.

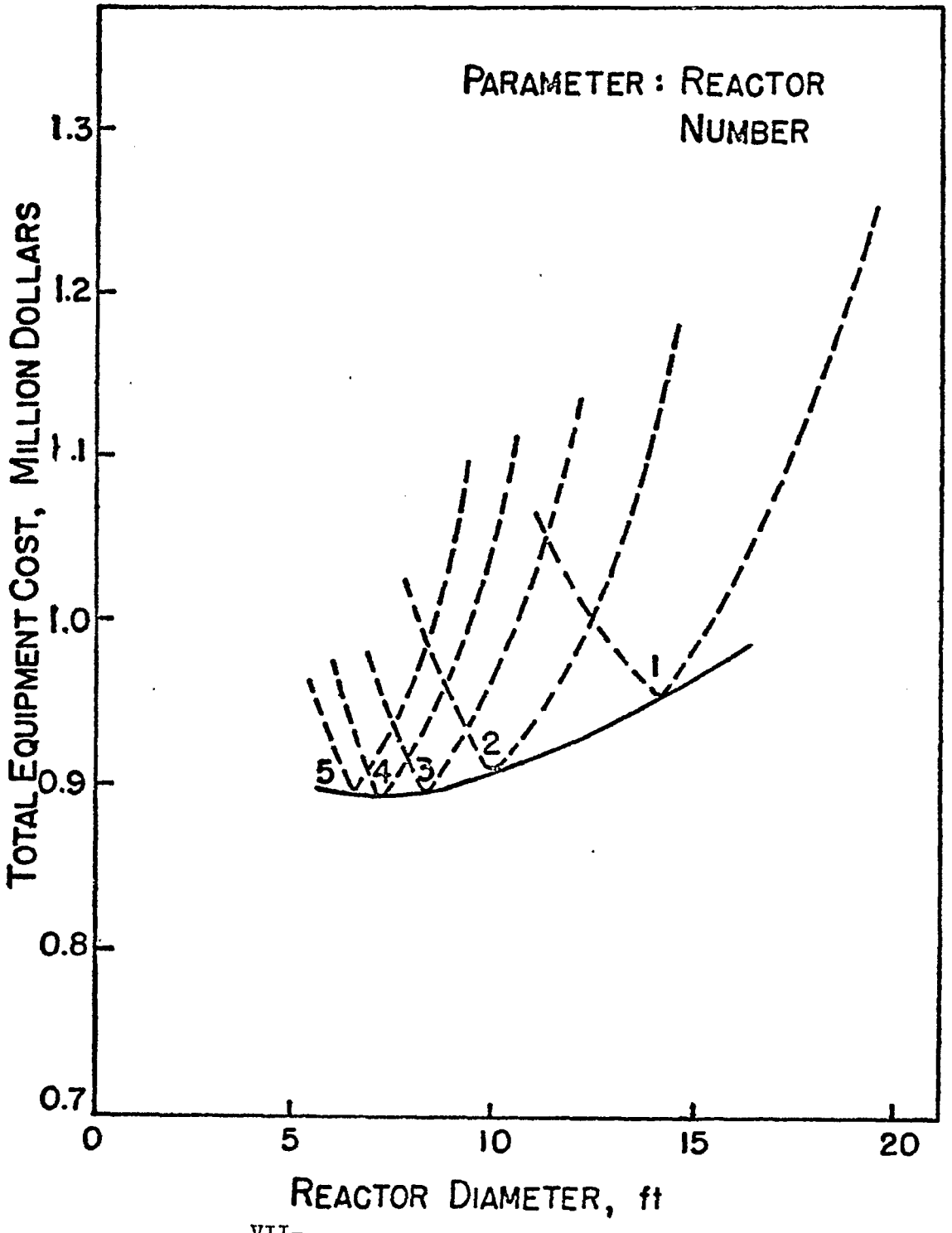

FIGURE VII-40 TOTAL EQUIPMENT COST VERSUS REACTOR DIAMETER IN HIGH CO CASE FOR COLD QUENCH-RECYCLE SYSTEM

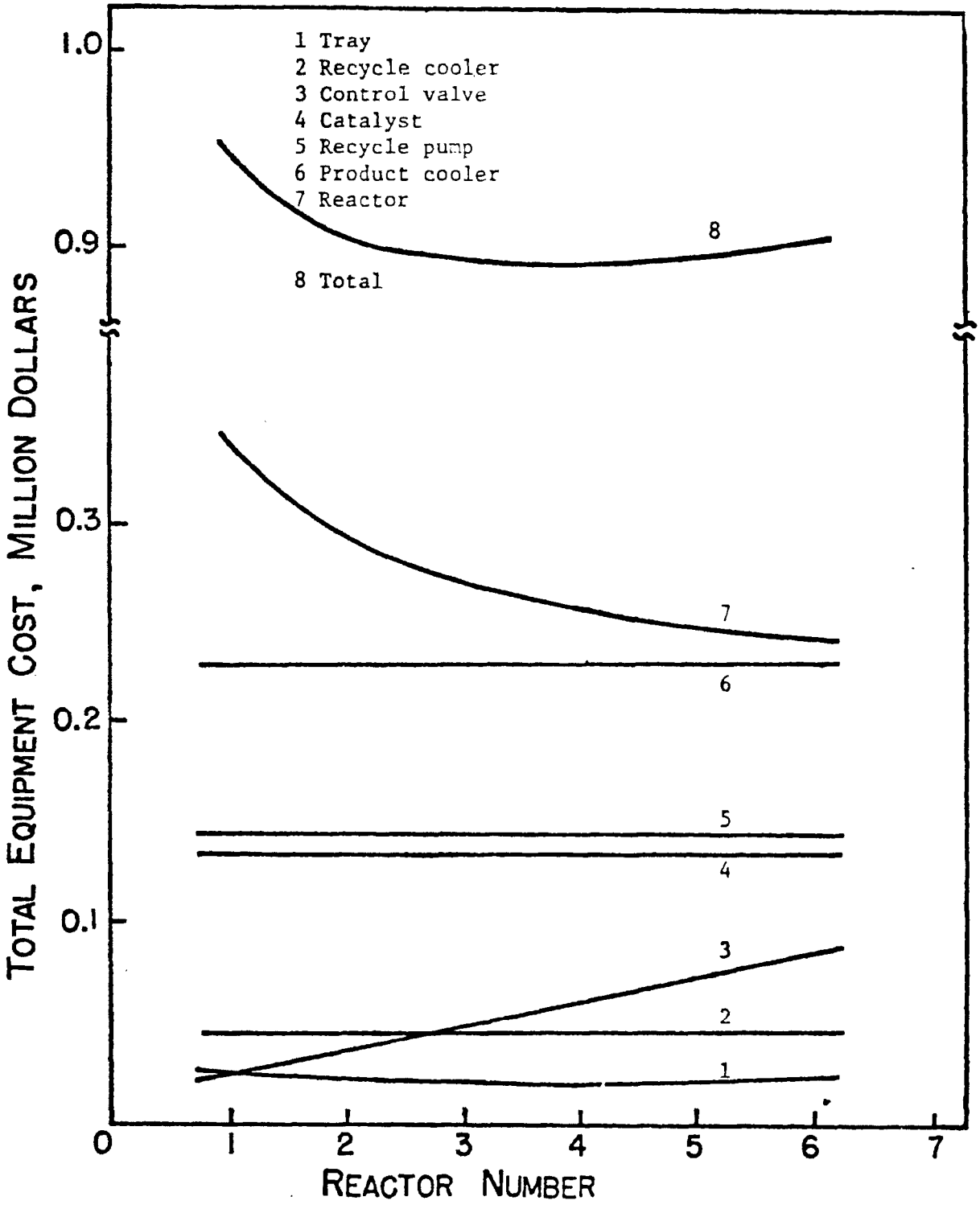

FIGURE VII-41 TOTAL EQUIPMENT COST VERSUS THE NUMBER OF REACTOR IN PARALLEL ARRANGMENT

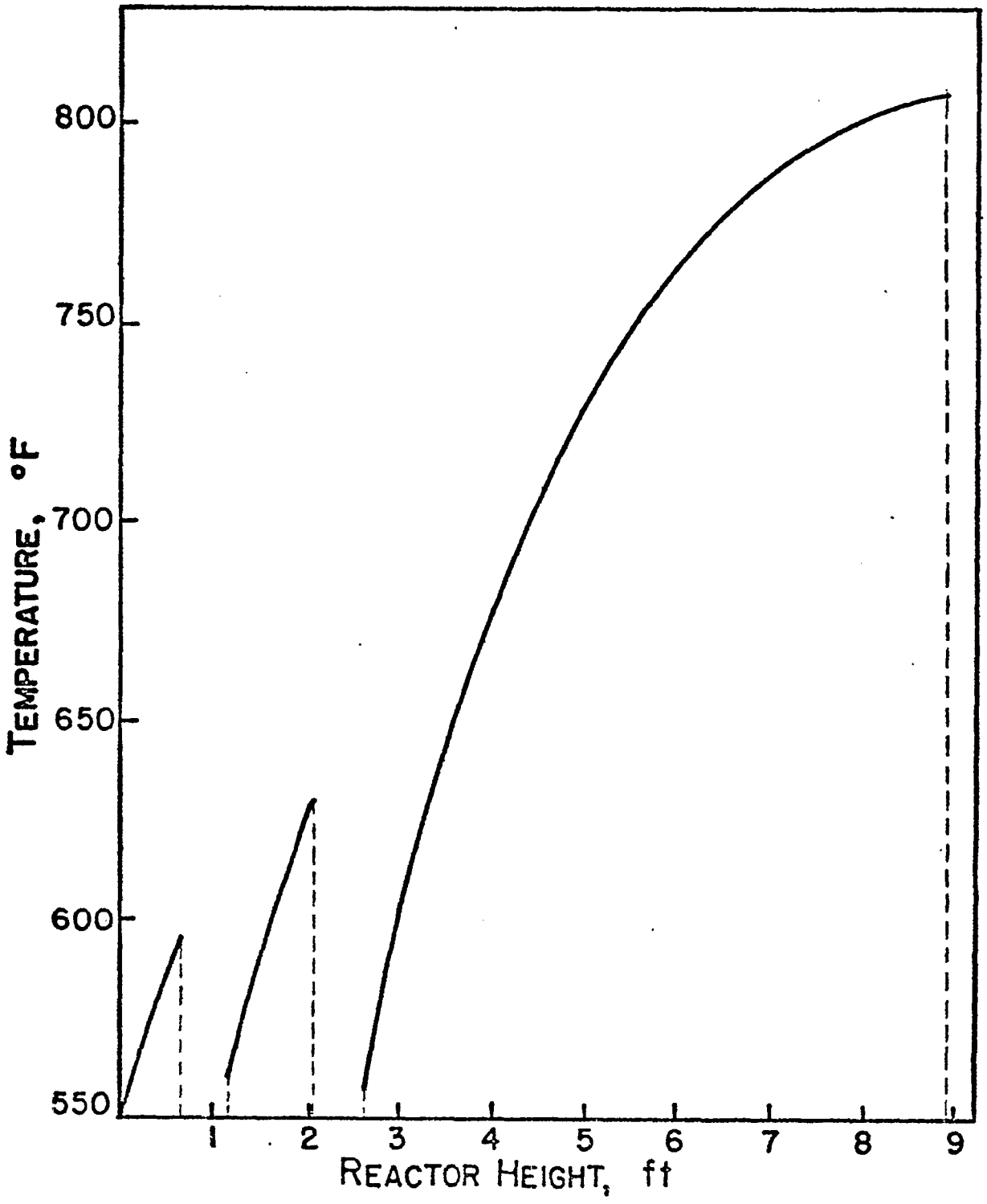

FIGURE VII-42 TEMPERATURE PROFILE ALONG THE REACTOR HEIGHT IN HIGH CO CASE FOR COLD QUENCH-RECYCLE SYSTEM

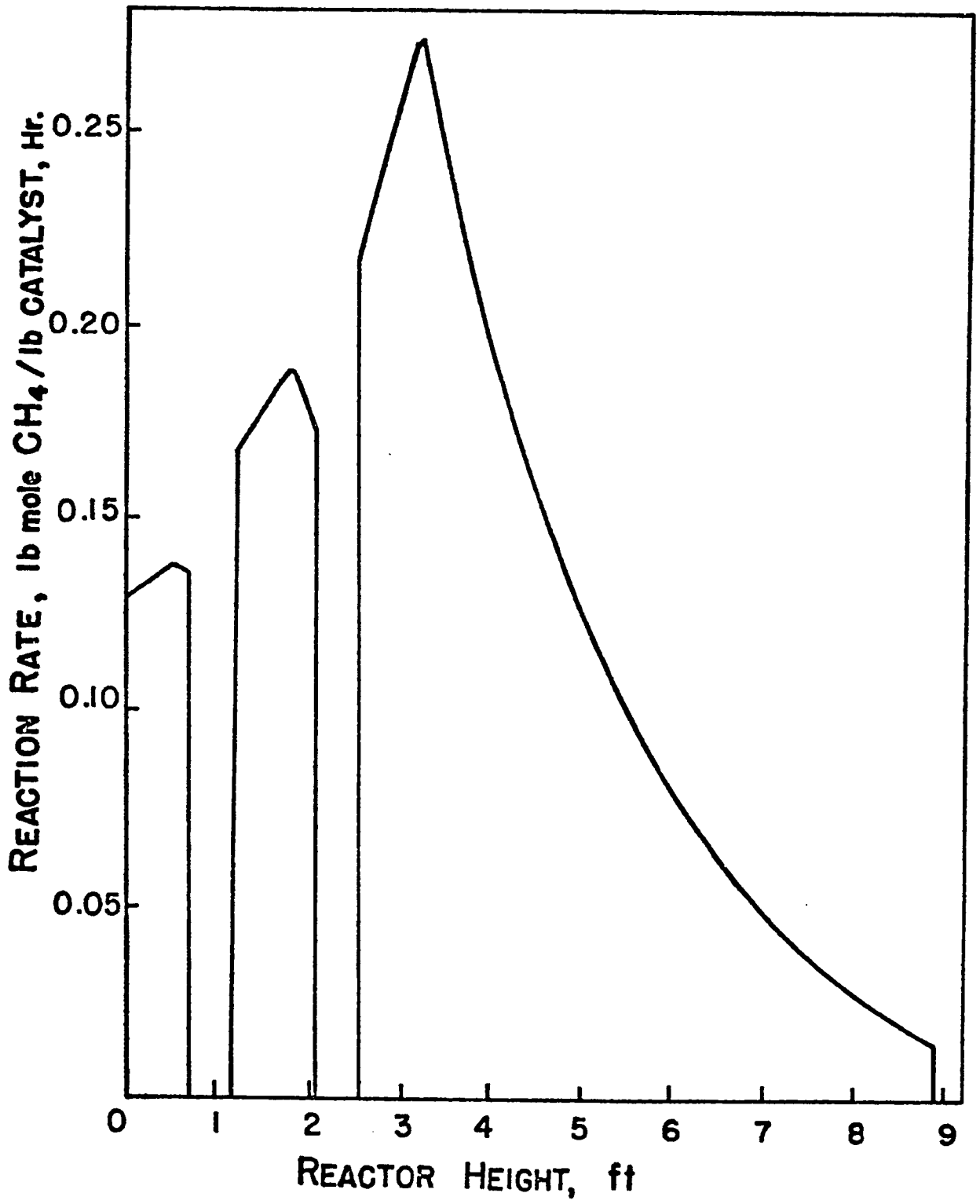

FIGURE VII-43 REACTION RATE ALONG THE REACTOR HEIGHT IN HIGH CO CASE FOR COLD QUENCH-RECYCLE SYSTEM

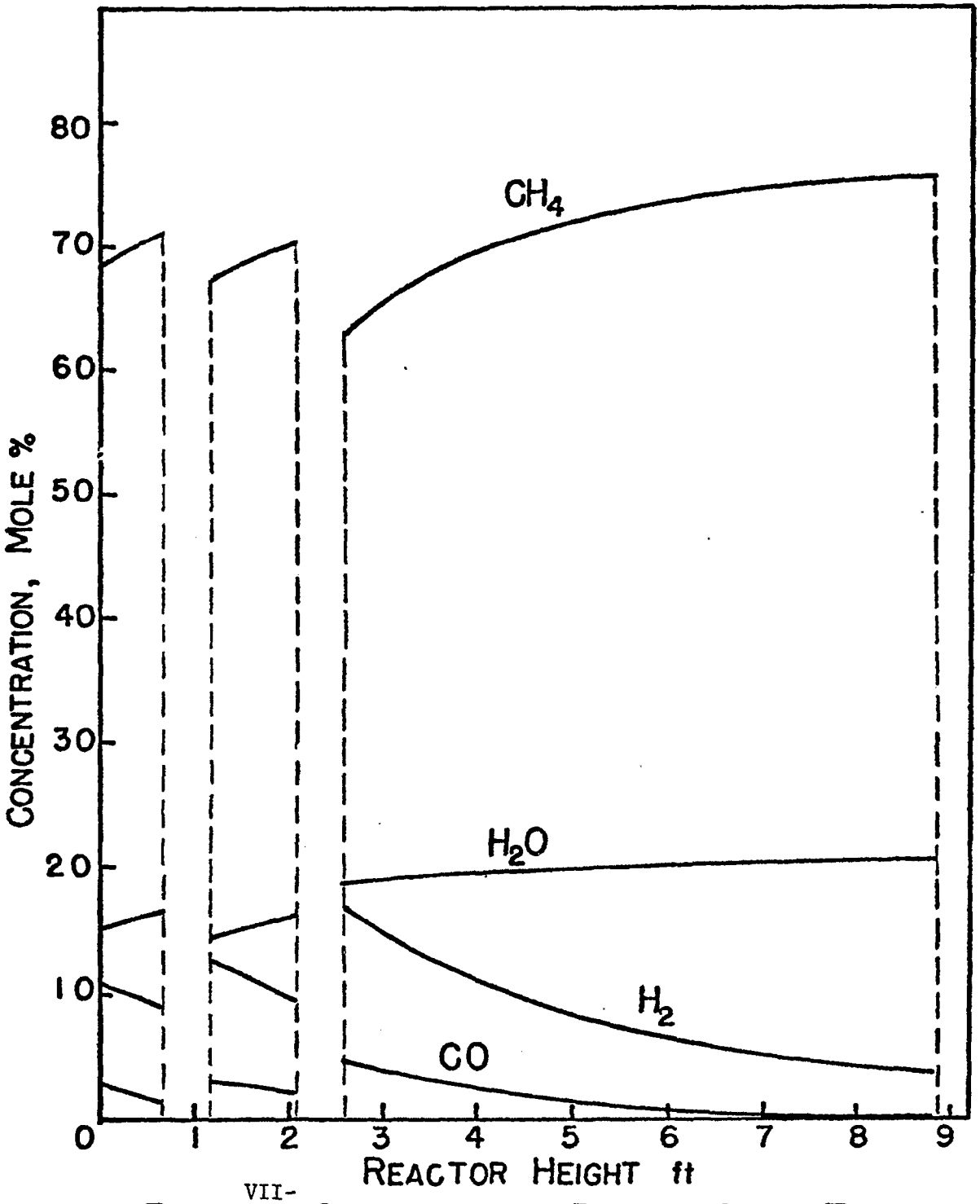

VII-44 FIGURE CONCENTRATION PROFILE ALONG THE REACTOR HEIGHT IN HIGH CO CASE FOR COLD QUENCH-RECYCLE SYSTEM

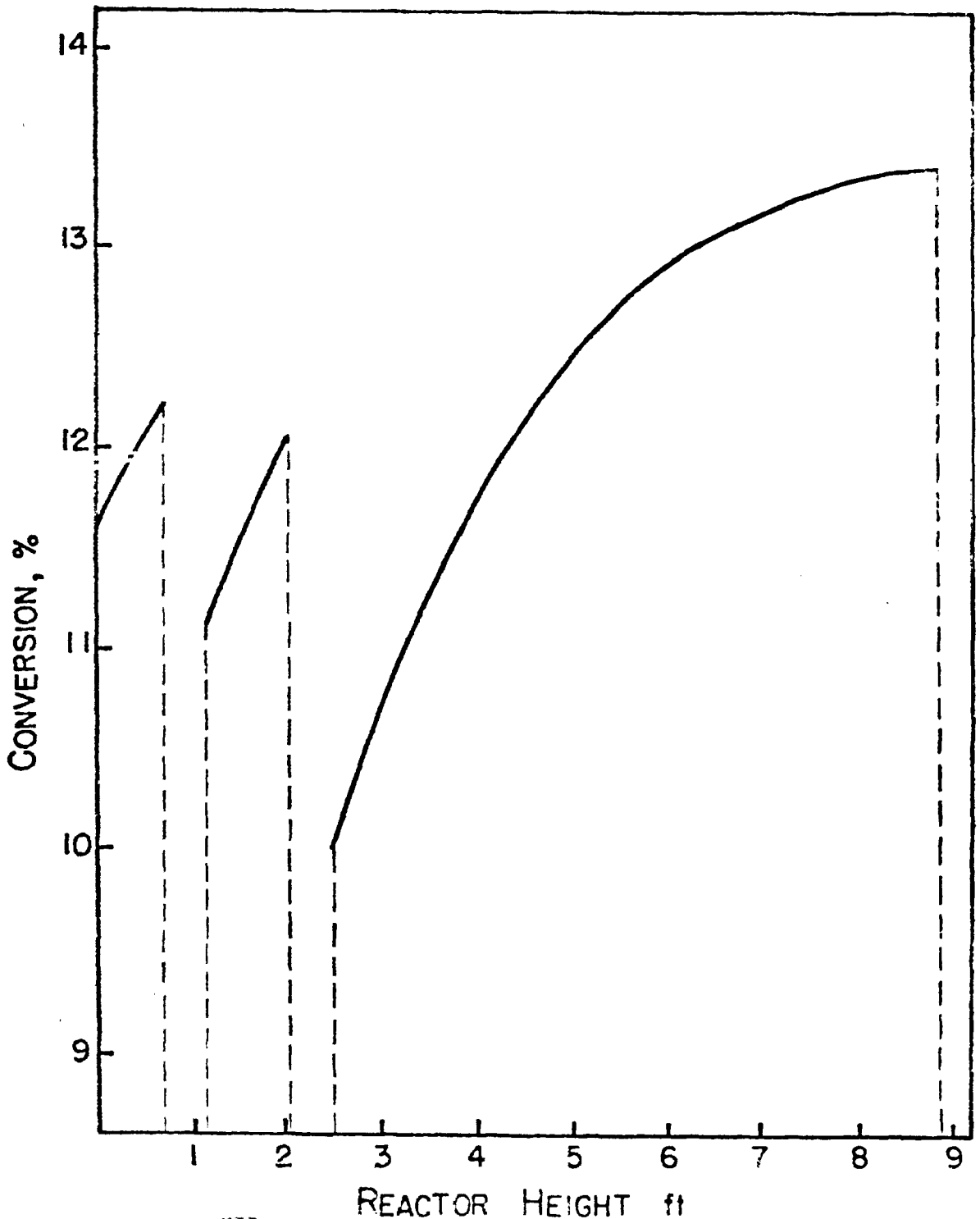

VII-45 FIGURE CONVERSION ALONG THE REACTOR HEIGHT IN HIGH CO CASE FOR COLD QUENCH-RECYCL SYSTEM

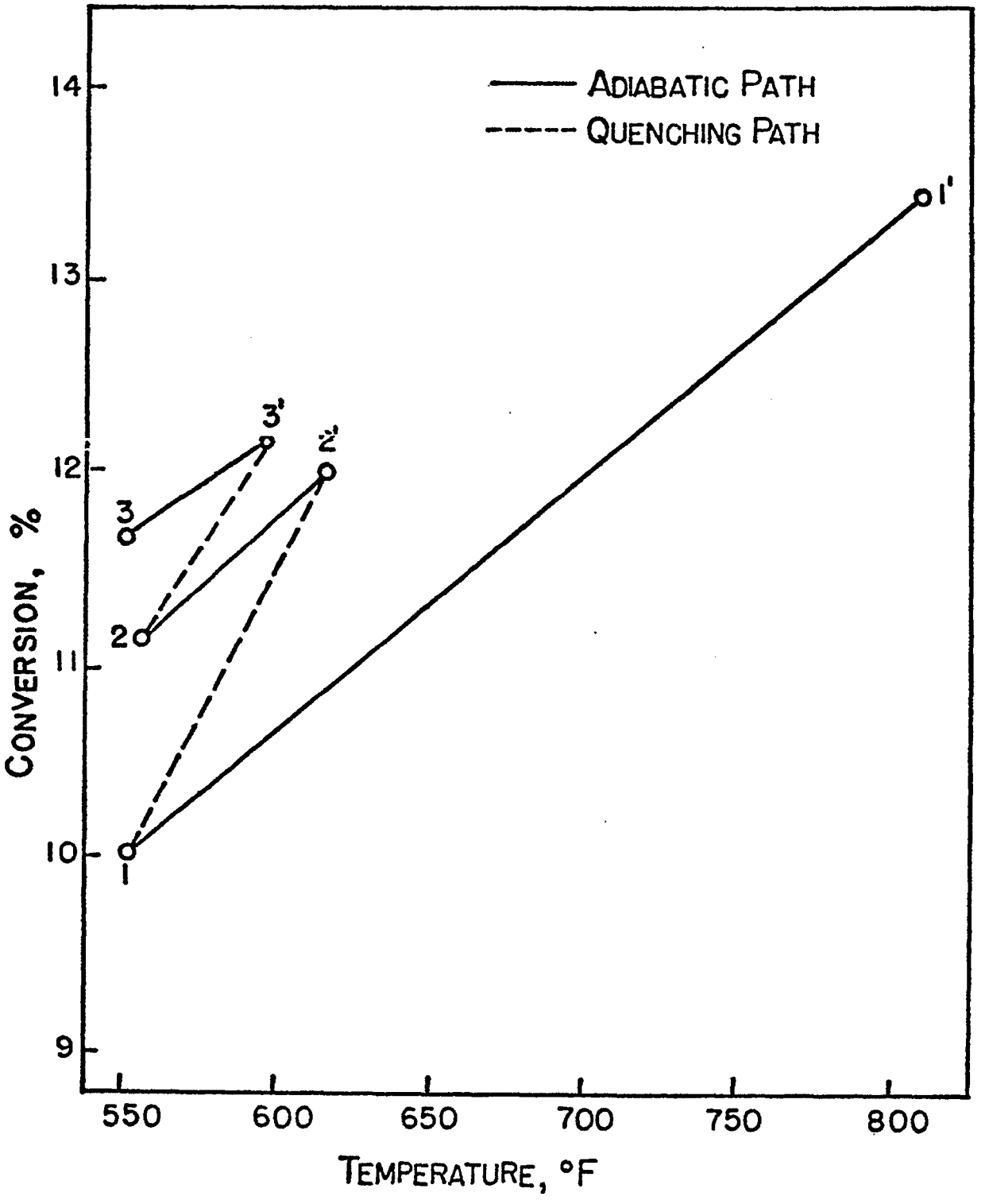

FIGURE VII-46 THE ADIABATIC PATH & THE QUENCHING PATH OF A REACTOR IN THE COLD QUENCH-RECYCLE SYSTEM

TABLE VII-12

OPTIMUM OPERATING CONDITION IN RECYCLE SYSTEM AND

COLD QUENCH-RECYCLE SYSTEM

	Recycle System	Cold quench-recycle System
Feed gas temperature, °F	100	100
Product gas temperature, °F	100	100
Feed gas pressure, psig	1,050	1,050
Product gas pressure, psig	1,000	1,000
Number of reactors	7	4
Reactor diameter, ft.	6.4	7.0
Catalyst weight, lbs.	57,880	53,630
Heat transfer surface area of product gas cooler I, ft^2.	6,140	6,140
Heat transfer surface area of product gas cooler II, ft^2.	15,630	15,630
Heat transfer surface area of product gas cooler III, ft^2.	21,200	21,200
Recycle ratio	2.91	1.93
Amount of gas recycled, lbs.	1,637,160	1,091,100
Temperature of recycle gas, °F	681	611
3rd stage inlet temperature, °F	---	550
3rd stage inlet gas conversion,%	---	11.646
3rd stage outlet gas temperature,°F	---	593
3rd stage outlet gas conversion,%	---	12.177
Amount of gas used in 1st quenching,lbs.	---	118,530
2nd stage inlet gas temperature,°F	---	556
2nd stage inlet gas conversion,%	---	11.13
2nd stage outlet gas temperature,°F	---	629

TABLE VII-12 (Cont'd.)

OPTIMUM OPERATING CONDITION IN RECYCLE SYSTEM AND

COLD-QUENCH RECYCLE SYSTEM

	Recycle System	Cold quench recycle System
2nd stage outlet gas conversion, %	---	12.059
Amount of gas used in 2nd quenching, lbs	---	276,560
1st stage inlet gas temperature, °F	550	551.5
1st stage inlet gas conversion,%	10.04	10.045
1st stage outlet gas temperature, °F	810	810
1st stage outlet gas conversion, %	13.453	13.453
Height of 3rd stage, in.	---	8
Height of 2nd stage, in.	---	11
Height of 1st stage, in.	69	76
Height of reactor, ft.	5.75	8.91

TABLE VII-13

OPTIMUM EQUIPMENT COSTS IN HIGH CO FEED FOR RECYCLE SYSTEM AND FOR COLD QUENCH-RECYCLE SYSTEM

	Recycle System	Cold quench-recycle System
Catalyst, $	143,130	134,120
Reactor, $	278,970	257,000
Tray, $	35,320	23,600
Control Valve, $	72,000	60,000
Recycle gas cooler, $	45,540	48,130
Product cooler I, $	60,620	60,620
Product cooler II, $	77,270	77,270
Product cooler III, $	91,670	91,670
Recycle pump, $	169,190	144,890
Total equipment, $	973,610	897,300

10.5 Discussion

It was found that the total equipment cost of the cold quench-recycle system is about 92.15% of the recycle system. The reactor cost, catalyst cost, recycle pump cost and product cooler cost are the four dominant items of the total equipment cost. They are about 28.1%, 14.9%, 16.3%, and 25.7% of the total cost, respectively. As to the cost estimation in the parallel reactor arrangement, for each additional reactor four control valves, each costing $3,000 are added. Also for the whole system two main control valves, each costing $6,000 are included. The cost of reactors decreases with the increase in the number of reactors up to a certain limit. The cost then increases because the number of the control valve increases rapidly with the number of reactors. The optimum number of parallel reactors is found to be four.

When a reactor is operated under an ideal plug flow condition, the amount of catalyst and the size of the reactor are smaller as compared to the reactor having a complete mixing flow. The cold-quench system is closer to the plug flow pattern while the recycle system is closer to the complete mixing flow. This is the reason why the total equipment cost of the cold quench system is much less than that of the recycle system as reported in the previous study[1]. In the cold quench-recycle system as it can be expected, the lowering the recycle ratio decreases the catalyst cost and the reactor cost. The lowest admissible recycle ratio in a high CO feed case for the cold quench-recycle system is found to be 1.795. This corresponds to the λ value of 0.2. The optimum operating conditions are searched around this lowest reycle ratio. The actual optimum recycle ratio is found to be 1.933.

The ratio of the amount of the quenching gas used at the first quenching point to the amount of the quenching gas used at the second quenching point plays an important role in the optimization calculation. One might expect that within the limit of the admissible operating conditions, a larger amount of quenching gas intorduced at the first quenching point will increase the average residence time of the reactants, thus enhancing the overall conversion and reducing the catalyst and reactor costs. This is not true in the present study. The introduction of a large amount of quenching gas at the early stage of the reaction will increase the pressure drop in the reactor. The pressure drop, according to the Ergun's equation, is roughly proportional to the square of the average mass flow rate in the catalyst packed reactor. In the cold quench-recycle system the cost of the recycle pump which is very sensitive to the pressure drop is considered as one of the major cost items. Therefore, in optimizing the processes, one should keep in mind that the catalyst cost and recycle pump cost are closely related. In this study it is found that the ratio of the amount of the quenching gas used at the first quenching point to the amount of the quenching gas used at the second quenching point is 3:7.

The tail effect is also very important in determining the optimum operating conditions. When the driving force becomes very low, the reaction rate becomes very slow and the reactor height increases considerably. In the cold quench-recycle system the specification of the product gas has already been given, therefore the tail effect at the end of the first stage is unavoidable. However, in the case of the second and the third stages at which the quenching gases are introduced the conversions should be so chosen that the tail effect can be reduced as much as possible.

In other words, the ideal quenching point should not be located too close to the equilibrium point nor too far away from the point where the reaction rate reaches its maximum. This implies that the quenching point should be located either before or after the reaction rate reaches its peak provided that the overall energy and material balances of the system are still held. The optimum quenching points for the second and the third stage found in this study are at the conversion of 12.1% and 12.2% respectively.

It has been reported in the previous study[1] that the reaction rate increases gradually with temperature up to approximately 600°F. From 600°F to 850°F, the rate remains substantially constant. From the theoretical point of view the temperature of the reactants after quenching should not be below 600°F. To operate a reactor at a temperature higher than this temperature the portion of the fresh feed gas entered at the top of the reactor should be higher compared to a reactor operated without this temperature restriction. If the portion of the fresh gas entered at the top of the reactor is small, the amount of heat generated in the third stage is not enough to raise the temperature of reactants to 600°F at the end of the third stage. Since the temperature at the top of the reactor has already been fixed at 550°F an increase in the amount of the fresh feed entering at the top of the reactor also means an increase in the recycle ratio. For example, if the lowest allowable operating temperature after the quenching is chosen at 600°F, the corresponding lowest recycle ratio calculated from overall energy balance is 1.933, whereas at 550°F, the ratio is 1.795. As has been discussed, the higher recycle ratio means the higher total equipment cost. Therefore, when the reaction rate does not change substantially

in the temperature range of 500° to 600°F, selection of a lower temperature as the temperature limit helps to reduce the total equipment cost. In the high CO case, using the temperature of 550°F as the lowest allowable operating temperature the total equipment cost is found to be less than that when 600°F is used as the lowest allowable temperature.

10.6 Conclusion

A cold quench-recycle system for the high CO feed gas methanation process has been studied. The optimum total equipment cost has been found to be $897,300, which is about $76,310 less than that for the recycle system. The optimum number of reactors is 4, the reactor diameter is 7 ft., and the reactor height is 8.91 feet.

10.7 B.C.R. Two Stage High Pressure System (Case III)

A case with CO concentration of 18.5%. which is roughly equivalent to the gas from B.C.R. Two Stage High Pressure Gasification System, has also been studied. The gas composition is shown in Table VII-1. The same calculation procedure as in the cold quench-recycle system are used and the results are reported in Table VII-14 and VII-15. The revenue requirement for this case is also included in Table VII-15.

TABLE VII-14

OPTIMUM OPERATING CONDITION IN COLD QUENCH-RECYCLE SYSTEM FOR B. C. R. CASE (CASE III)

	Cold quench-recycle System
Feed gas temperature, °F	100
Product gas temperature, °F	100
Feed gas pressure, psig	1,050
Product gas pressure, psig	1,000
Number of reactors	12
Reactor diameter, ft.	7.2
Catalyst weight, lbs.	113,450
Heat transfer surface area of product gas cooler I, $ft.^2$	15,450
Heat transfer surface area for product gas cooler II, $ft.^2$	21,000
Heat transfer surface area of product gas cooler III, $ft.^2$	21,650
Recycle ratio	4.4
Amount of gas recycled, lbs.	3,032,200
Temperature of recycle gas, °F	577
3rd stage inlet temperature, °F	550
3rd stage inlet gas conversion, %	17.39
3rd stage outlet gas temperature, °F	573
3rd stage outlet gas conversion, %	17.63
Amount of gas used in 1st quenching, lbs.	180,500
2nd stage inlet gas temperature, °F	551
2nd stage inlet gas temperature, %	16.69

TABLE VII-14 (Cont'd)

OPTIMUM OPERATING CONDITION IN COLD QUENCH-RECYCLE SYSTEM FOR B. C. R. CASE (CASE III)

	Cold quench-recycle System
2nd stage outlet gas temperature	586
2nd stage outlet gas conversion, %	17.07
Amount of gas used in 2nd quenching, lb.	300,800
1st stage inlet gas temperature, °F	551
1st stage inlet gas conversion, %	15.7
1st stage outlet gas temperature, °F	810
1st stage outlet gas conversion, %	21.18
Height of 3rd stage, in.	4
Height of 2nd stage, in.	5
Height of 1st stage, in.	63
Height of reactor, ft.	7

TABLE VII-15

OPTIMUM EQUIPMENT COSTS AND REVENUE REQUIREMENT

FOR B. C. R. CASE (CASE III)

	Cold quench-recycle System
Catalyst, $	283,600
Reactor, $	689,480
Tray, $	74,880
Control value, $	156,000
Recycle gas cooler, $	93,070
Product cooler I, $	76,740
Product cooler II, $	91,100
Product cooler III, $	92,800
Recycle pump, $	199,150
Total equipment, $	1,756,820
Revenue requirement, $/Yr.	1,139,400

REFERENCE

1. Bellman, R., "Dynamic Programming", Princeton University Press, Princeton, New Jersey, 1957.

U.S. DEPARTMENT OF COMMERCE
Technology Administration
National Technical Information Service
Springfield, VA 22161 (703) 605-6000